University of Glasgow

Aboorh, Ahmed (2026) *Decoupled electrolysis strategies for direct hydrogenation reactions under mild conditions.* PhD thesis.

https://theses.gla.ac.uk/86338/

Copyright and moral rights for this work are retained by the author

A copy can be downloaded for personal non-commercial research or study, without prior permission or charge

This work cannot be reproduced or quoted extensively from without first obtaining permission from the author

The content must not be changed in any way or sold commercially in any format or medium without the formal permission of the author

When referring to this work, full bibliographic details including the author, title, awarding institution and date of the thesis must be given

Enlighten: Theses
https://theses.gla.ac.uk
research-enlighten@glasgow.ac.uk

Decoupled Electrolysis Strategies for Direct Hydrogenation Reactions under Mild Conditions



Ahmed Aboorh

Submitted in fulfilment of the requirements for the

Degree of Doctor of Philosophy

School of Chemistry

College of Science and Engineering

University of Glasgow

March, 2026

Abstract

Electrochemistry is an increasingly important field within the physical sciences, offering sustainable alternatives to conventional chemical processes. In particular, the use of redox mediators in electrochemical systems provides a means of controlling electron transfer and improving selectivity under mild conditions. Polyoxometalates have attracted significant attention as redox active species due to their well defined structures and reversible redox behaviour.

The work presented in this thesis focuses on the investigation of silicotungstic acid as redox mediator for the electrochemical reduction of organic substrates. The aim of this study was to examine the electrochemical behaviour of the mediator, evaluate its reversibility, and assess its effectiveness in facilitating reduction reactions under controlled conditions.

Chapter 1 provides an overview of electrochemical processes and introduces the role of redox mediators, with particular emphasis on polyoxometalates and their application in organic electrosynthesis. Chapter 2 describes the experimental techniques employed throughout this work, including electrochemical methods such as cyclic voltammetry and bulk electrolysis, as well as analytical techniques including gas chromatography (GC), nuclear magnetic resonance (NMR), ultraviolet-visible (UV-Vis) spectroscopy, and Fourier transform infrared (FT-IR) spectroscopy.

Chapter 3, the electrochemical properties of silicotungstic acid are examined, including its redox behaviour and stability during repeated cycling. The reversibility of the mediator system is evaluated using cyclic voltammetry, and conditions for controlled electrolysis are established. Chapter 4 investigates application of the reduced mediator in the chemical reduction of organic substrates, including nitriles, ketones, and aldehydes. Product formation is confirmed using GC, GC-MS, NMR, and FT-IR analysis. The efficiency and selectivity of the process are assessed under different experimental conditions.

Chapter 5 explores further applications and optimisation of the system, including variations in electrolysis conditions and assessment of competing side reactions such as hydrogen evolution. The

role of electrochemical parameters in influencing reaction outcomes is discussed. Finally, Chapter 6 summarises the key findings of this work and outlines potential directions for future research.

Overall, this study demonstrates that silicotungstic acid is an effective redox mediator for electrochemical reduction processes. The results highlight its stability, reversibility, and applicability in facilitating selective transformations, contributing to the development of more sustainable electrochemical methodologies.

Table of Contents

Abstract ii
Table of Contents iv
List of Conferences and Courses viii
Acknowledgment ix
Author's Declaration x
List of Abbreviations xi
Chapter 1: Introduction and Background to Polyoxometalate Mediated Electrochemical Reduction 1
1. Introduction 2
1.1 Electrochemistry and Sustainable Chemical Synthesis 2
1.1.1 Basic principles of Electrochemical Cells 5
1.2 Polyoxometalates as Multi-Electron Redox Mediators 7
1.2.1 Structural Types of Polyoxometalates 8
1.2.2 Redox Behaviour of Polyoxometalates 10
1.3 Silicotungstic Acid 11
1.3.1 Physicochemical Properties 12
1.3.2 Applications in Redox Mediation 13
1.3.3 Relevance to This Thesis 14
1.4 Electrochemical Redox Behaviour of Silicotungstic Acid 14
1.4.1 Multi-Electron Redox Properties of Polyoxometalates 14
1.4.2 Electrochemical Reduction of Silicotungstic Acid 15
1.4.3 Polyoxometalates as Redox Mediators 16
1.4.4 Cyclic Voltammetry of Silicotungstic Acid 17
1.4.5 Stability and Reversibility of Reduced Species 18
1.5 Polyoxometalate-Mediated Electrochemical Reduction of Organic Compounds 19
1.5.1 Polyoxometalates as Redox Mediators 20
1.5.2 Relevance to the Present Study 21
1.6 Carbon Monoxide Reduction and the Potential Role of Polyoxometalate Mediators 22
1.6.1 Importance of Carbon Monoxide 22
1.6.2 Challenges in Electrochemical Carbon Monoxide Reduction 23
1.6.3 Catalysts for Carbon Monoxide Reduction 24
1.6.4 Potential Role of Redox Mediators 26
1.6.5 Summary 27
1.7 Aims and Scope of this Thesis 27
1.8 References 30

Chapter 2: Overview of the Techniques Used **33**
2.1 Electrochemical Techniques 34
2.2 Electrode setup 34
2.2.1 Single cell configuration 34
2.2.2 H-cell configuration 36
2.3 Cyclic voltammetry 37
2.4 Reversibility of the Mediator System 38
2.5 Electrolysis 39
2.5.1 Chronoamperometry 39
2.5.2 Chronopotentiometry 40
2.6 Characterisation techniques: 41
2.6.1 Gas Chromatography (GC) 41
2.6.2 Gas chromatography-mass spectrometry (GC-MS) 42
2.6.3 Ultraviolet–Visible (UV–Vis) Spectroscopy 44
2.6.4 Fourier Transform Infrared Spectroscopy (FT–IR) 45
2.6.5 Thermogravimetric Analysis (TGA) 46
2.6.6 X-ray Diffraction (XRD) 47
2.6.6.1 Single Crystal X-ray Diffraction (SCXRD) 49
2.6.7 Nuclear Magnetic Resonance (NMR) Spectroscopy 50
2.7 References 55
Chapter 3: Controlled Multi-Electron Reduction and Redox Stability of Silicotungstic Acid **57**
3.1 Introduction 60
3.2 Experimental Methods 62
3.2.1 Materials and Reagents 62
3.2.2 Electrochemical Setup and Procedures 63
3.2.3 Spectroscopic and Structural Characterisation 64
3.2.4 Reoxidation Experiments 65
3.3 Results and Discussion 65
3.3.1 Electrochemical reduction of silicotungstic acid 65
3.3.2 Spectroscopic evidence of multi-electron reduction 81
3.3.3 Structural analysis by single-crystal X-ray diffraction 87
3.3.4 Structural Characterisation by Powder X-ray Diffraction 90
3.3.5 Thermal behaviour and hydration state (TGA) 91
3.4 Redox stability and reactivity 93
3.4.1 Re-oxidation behaviour and stability 93
3.4.1.1 Practical limitations during deep electrochemical reduction 96
3.4.2 Practical Electron Storage Capacity 97

3.5 Conclusions 98
3.6 Appendix 100
3.7 References 104
Chapter 4: Application of Electrochemically Reduced Silicotungstic Acid in Indirect Organic Reduction 105
4.1 Introduction 108
4.2 Experimental 110
4.2.1 Materials 110
4.2.2 Electrochemical Generation of Reduced STA 110
4.2.3 General Procedure for the Reduction of Organic Substrates 111
4.2.4 Product Analysis and Determination of Conversion, and Yield 111
4.3 Results and Discussion 112
4.3.1 Hydrogenation of 4-Cyanobenzaldehyde 112
4.3.2 Hydrogenation of 4-(Trifluoromethyl)benzaldehyde 119
4.3.3 Substrate Scope and Functional Group Tolerance 122
4.4 Conclusions 125
4.5 Appendix 127
4.6 References 137
Chapter 5: Electrochemical Investigation of Polyoxometalate Mediators for Carbon Monoxide Reduction 138
5.1 Introduction 141
5.2 Experimental 143
5.2.1 Materials 143
5.2.2 Electrochemical Generation of Reduced Mediators 143
5.2.3 Reaction of Reduced Mediator with Carbon Monoxide 145
5.3 Results and Discussion 146
5.3.1 Electrochemical behaviour of phosphomolybdic acid 146
5.3.2 Influence of electrode material 148
5.3.3 Reactivity of reduced silicotungstic acid with CO 149
5.3.4 Effect of deeper reduction of silicotungstic acid 150
5.3.5 Reactivity of reduced phosphomolybdic acid with CO 152
5.3.6 NMR analysis of reaction mixtures 153
5.3.7 Implications for CO reduction using polyoxometalate mediators 155
5.4 Mechanistic Considerations and Limitations 156
5.5 Conclusions and Future Outlook 157
5.6 References 159

Chapter 6: Overall Conclusions and Future Perspectives 160
6.1 Overall Conclusions 161
6.2 Mechanistic Insights 162
6.3 Limitations of the Mediator Based Approach 163
6.4 Future Perspectives 163
6.5 Final Remarks 164
6.6 References 166

List of Conferences and Courses

- Certificates for Electrochem, Manchester, UK, 2024. Poster presentation
- International Society of Electrochemistry, Manchester, UK, 2024, Oral presentation
- Functional Metal Oxide and Cluster Systems (FMOCS VIII), Mainz, Germany. Poster presentation
- X-Ray Awareness Course
- Gas Cylinder Safety Course, 2026
- Class & Tutor Introduction to Learning and Teaching in Higher Education
- Postgraduate Research Training
- CHEM Level 4/5 Special Topics (ST) Lectures, 2022-2023
- CHEM Level 4/5 Physical Chemistry Lectures, 2022-2023
- CHEM Level 4/5 Tutorials, 2022-2023
- CHEM Level 4/5 Organic Chemistry Lectures, 2022-2023
- Safety Committee Training
- Diversity in the Workplace
- Introduction to Research Data Management
- Information Security Awareness

Acknowledgment

I would like to begin by expressing my sincere gratitude to God Almighty for granting me the strength, patience, and perseverance to complete this work.

I would like to express my deepest appreciation to my supervisor, Professor Mark Symes, at the University of Glasgow, for his continuous guidance, support, and encouragement throughout my studies. His knowledge, patience, and dedication have been invaluable, and I am truly grateful for his mentorship.

I would also like to extend my sincere thanks to Dr. Zeliha Ertekin, with whom I had the pleasure of working during my research. Her guidance, support, and valuable insights have greatly contributed to this work. I truly appreciate the experience of working with her and look forward to future collaborations.

I would like to thank all members of the Symes research group for their support and collaboration, and for creating a positive and motivating research environment. It has been a pleasure to be part of such a supportive and inspiring team.

I am also grateful to the University of Jeddah for providing me with the academic foundation and support that enabled me to pursue my studies abroad.

I would like to express my gratitude to my home country, Saudi Arabia, for supporting my education. Coming from Jeddah to the United Kingdom has been a meaningful and life changing journey.

My deepest thanks go to my family for their endless love and support. I especially thank my parents for their sacrifices and encouragement, and my sister for always standing by me, listening with patience, and offering kindness and reassurance when I needed them most.

I am particularly grateful to my fiancée for her love, patience, and encouragement, which have been a source of comfort and strength.

Finally, I would like to thank my friends and colleagues for their support and for making my time in the UK more enjoyable and memorable.

Author's Declaration

I declare that, except where explicit reference is made to the contribution of other, this thesis is the result of my own work and has not been submitted for any other degree at the University of Glasgow or any other institution.

I confirm that this thesis has been completed in accordance with the University's regulations and the principles of good research practice.

I further declare that that all sources of information have been appropriately acknowledged, and any assistance received during the course of this work has been properly credited.

Printed Name: Ahmed Aboorh

Signature:

List of Addreviations

Ag/AgCl	Silver/silver chloride (reference electrode)
ASU	Asymmetric unit
ATR	Attenuated total reflectance
Au	Gold
BioLogic	BioLogic potentiostat system
BTL	Biomass-to-liquids
C1	One-carbon
C2+	Multicarbon
C≡O	Carbon-oxygen triple bond
CCDC	Cambridge Crystallographic Data Centre
$CDCl_3$	Deuterated chloroform
CO	Carbon monoxide
CO_2	Carbon dioxide
CTL	Coal-to-liquids
CV	Cyclic voltammetry
DCM	Dichloromethane
DET	Direct electron transfer
e^-	Electron
EWG	Electron-withdrawing group

FID	Free induction decay
FT	Fischer-Tropsch
FT-IR	Fourier transform infrared spectroscopy
GC	Gas chromatography
GC-MS	Gas chromatography-mass spectrometry
GTL	Gas-to-liquids
H-cell	Two-compartment electrochemical cell
H_2	Hydrogen
HER	Hydrogen evolution reaction
IET	Indirect electron transfer
iR	Ohmic drop correction
IVCT	Intervalence change transfer
MET	Mediator-based electron transfer
Nafion®	Perfluoro sulfonic acid membrane
NHE	Normal hydrogen electrode
NMR	Nuclear magnetic electrode
OER	Oxygen evolution reaction
PMA	Phosphomolybdic acid
POM	Polyoxometalate
Pt	Plantinum
PXRD	Powder X-ray diffraction

RF	Radiofrequency
SCXRD	Single-crystal X-ray diffraction
SHE	Standard hydrogen electron
STA	Silicotungstic acid
TCD	Thermal conductivity detector
TCI	Tokyo Chemical Industry
TGA	Thermogravimetric analysis
UV-Vis	Ultravuolet-Visible spectroscopy
WO_3	Tungsten trioxide
XRD	X-ray diffraction

Chapter 1: Introduction and Background to Polyoxometalate Mediated Electrochemical Reduction

Synopsis

Electrochemistry offers an attractive route to sustainable chemical synthesis because it enables redox transformations to be driven by electrical energy rather than by stoichiometric chemical reagents. In electrochemical systems, electrons supplied from an electrode act as clean reagents, reducing the formation of chemical waste and allowing precise control over reaction conditions. However, direct electrochemical reduction of many organic and small molecules substrates often suffers from slow electron transfer kinetics, poor selectivity, and competing side reactions at electrode surfaces. One strategy for overcoming these limitations is the use of soluble redox mediators, which act as electron shuttles between the electrode and substrate in solution. Among the various mediator systems investigated, polyoxometalates have attracted considerable attention because of their ability to undergo reversible multi-electron reduction while maintaining structural stability.

This chapter introduces the fundamental electrochemical principles relevant to the work presented in this thesis and reviews the chemistry of polyoxometalates as multi-electron redox mediators. Particular emphasis is placed on Keggin-type heteropolyacids such as silicotungstic acid, whose well defined structure, strong Brønsted acidity, and reversible multi-electron redox behaviour make it a useful model system for mediated electrochemical reactions. The chapter also discusses the role of polyoxometalates in mediated electrochemical reduction of organic compounds and considers the challenges associated with the electrochemical activation of carbon monoxide. Finally, the aims and scope of the thesis are outlined, focusing on the controlled multi-electron reduction of silicotungstic acid and the evaluation of its reduced forms as mediators for the reduction of organic substrates and small molecules.

1. Introduction

1.1 Electrochemistry and Sustainable Chemical Synthesis

The development of more sustainable chemical processes has become an important objective in modern chemistry. Conventional reduction reactions in organic and inorganic synthesis often rely on stoichiometric reducing agents such as lithium aluminium hydride ($LiAlH_4$), sodium borohydride ($NaBH_4$), or dissolving metals.[1,2] Although these reagents are highly effective, they frequently generate significant quantities of inorganic waste and may require hazardous reaction conditions during handling and disposal. As a result, considerable research has focused on developing alternative approaches that reduce chemical waste and improve the environmental sustainability of synthetic processes.[3–8]

Traditional chemical reductions involve the transfer of electrons from a chemical reducing agent to a substrate. While this approach is widely used in organic synthesis, it often produces inorganic by-products derived from the reagent. For example, reductions using $LiAlH_4$ produce aluminium hydroxide as a by-product, while $NaBH_4$ reductions typically generate borate-containing waste following hydrolysis during the reaction or work-up.[1,2] The formation of these stoichiometric by-products contributes to chemical waste and reduces the overall atom economy of the process.[1,2] In contrast, electrochemical synthesis uses electrical energy to drive oxidation and reduction reactions. In these systems, electrons required for reduction are supplied directly from the cathode rather than from a chemical reducing agent. As a result, electrons act as clean reagents that do not introduce additional chemical waste into the reaction mixture.[4,5,9] This feature makes electrochemical methods particularly attractive in the context of green chemistry.

In addition to direct electrolysis, in which the substrate undergoes electron transfer at the electrode surface, electrochemical transformations can proceed indirectly through the use of a soluble redox mediator. In an indirect electrochemical process, the mediator undergoes electron transfer at the electrode and subsequently transfers redox equivalents to a substrate or catalyst in solution. This

separates the heterogeneous electron-transfer process at the electrode from the subsequent homogeneous chemical reaction in solution, as illustrated in Figure 1.1.[10]

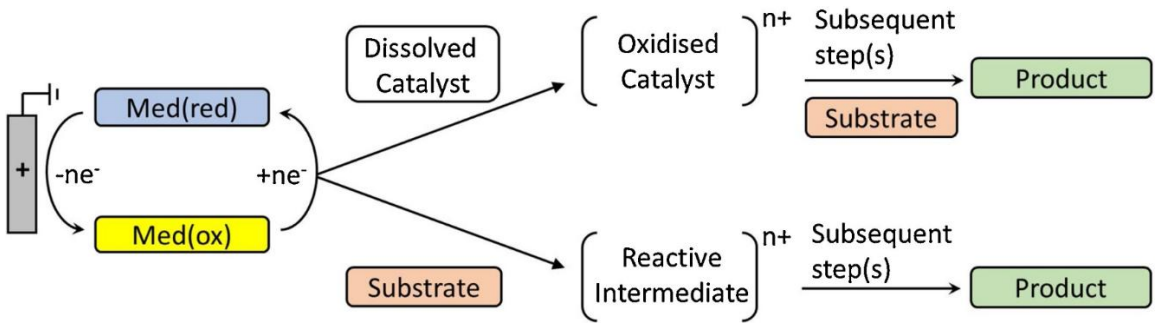


Figure 1.1. General representation of the possible modes of operation of a redox mediator in an indirect electrochemical process, using an organo-oxidation reaction.[10]

Electrochemical reactions occur at the interface between an electrode and an electrolyte solution. The electrode at which reduction occurs is defined as the cathode, while the electrode at which oxidation occurs is defined as the anode. When an external potential is applied across the electrodes, electrons flow through the external circuit while ions in the electrolyte move to maintain electrical neutrality within the solution.[8]

One of the major advantages of electrochemical methods is the ability to control the thermodynamic driving force of a reaction through the applied potential. The relationship between the Gibbs free energy change and the electrochemical potential is described by Equation 1.1.[8]

$$\Delta G = -nFE \qquad \text{(Equation 1.1)}$$

where ΔG is the Gibbs free energy change of the reaction, while n represents the number of electrons transferred, F is the Faraday constant (96485 C mol^{-1}), and E denotes the cell potential. The relationship shows that the energy required for an electrochemical transformation can be supplied through the applied potential. As a result, specific redox processes can be selectively activated while suppressing competing reactions.[8]

The potential of an electrochemical reaction also depends on the concentration of the oxidised and reduced species present in solution. This relationship is described by the Nernst equation, given in Equation 1.2.[8]

$$E = E^0 + \frac{RT}{nF} In \frac{[O_x]}{[Red]} \quad \text{(Equation 1.2)}$$

where E is the electrode potential under non-standard conditions. E^0 is the standard reduction potential, R is the universal gas constant, T is the absolute temperature, n is the number of electrons transferred, F is the Faraday constant, and the terms [Ox] and [Red] represent the concentrations of the oxidised and reduced species, respectively.

Despite these advantages, direct electrochemical reduction of organic molecules can sometimes present practical challenges. In many cases, electron transfer between the electrode surface and the substrate is slow. To achieve a practical reaction rate, an electrode potential different from the thermodynamic equilibrium potential may therefore need to be applied. The difference between the applied electrode potential and the equilibrium potential is known as the overpotential (η). Increasing the magnitude of the overpotential generally increases the driving force for electron transfer and, consequently, the rate of the electrode reaction. For electrochemical reduction, this typically requires the application of potentials more negative than the equilibrium potential.[7,8,11]

Large overpotentials can lead to competing reactions or reduced selectivity. In aqueous media, strongly negative potentials can result in the hydrogen evolution reaction (HER), where protons are reduced to hydrogen gas. In addition, reactive intermediates formed during electrochemical reactions may adsorb onto the electrode surface, leading to electrode fouling and decreased reaction efficiency.[12,13]

To address these limitations, considerable interest has developed in mediated electrochemical systems, in which a soluble redox mediator transfers electrons between the electrode and the substrate. In these systems, the mediator is first reduced at the electrode surface and subsequently transfers electrons to the substrate in solution. If the mediator is reduced at a less negative potential than that required for direct substrate reduction, it can provide an alternative electron-transfer pathway that avoids the need for the more negative potential required for direct reduction. After transferring electrons to the substrate,

the oxidised form of the mediator is reduced again at the electrode, allowing the process to proceed through a catalytic cycle.[13]

Among the various mediator systems that have been investigated, polyoxometalates represent an important class of redox mediators because of their ability to undergo reversible multi-electron reductions while maintaining structural stability. These properties make polyoxometalates promising candidates for mediated electrochemical transformations. The structure and properties of polyoxometalates are therefore discussed in the following section.

1.1.1 Basic Principles of Electrochemical Cells

Electrochemical reactions occur in systems known as electrochemical cells, where oxidation and reduction reactions take place at separate electrodes. In a typical electrochemical cell, two electrodes are immersed in an electrolyte solution and connected through an external electrical circuit. The electrode at which reduction occurs is called the cathode, while oxidation takes place at the anode. When an external potential is applied across the electrodes, electrons flow through the external circuit, while ions in the electrolyte move to maintain electrical neutrality within the solution.[8]

Electrochemical reactions proceed through two complementary half reactions occurring at the electrode surfaces. A well known example that illustrates these principles is the electrolysis of water, where water is split into hydrogen and oxygen gases.[8,14] In acidic electrolyte, hydrogen is produced at the cathode through the hydrogen evolution reaction (HER), while oxygen is formed at the anode through the oxygen evolution reaction (OER). These half reactions can be written as follows:[8,15]

Cathode (hydrogen evolution reaction):

$$2H^+ + 2e^- \rightarrow H_2 \qquad \text{(Equation 1.3)}$$

Anode (oxygen evolution reaction):

$$2H_2O \rightarrow O_2 + 4H^+ + 4e^- \qquad \text{(Equation 1.4)}$$

The overall reaction therefore corresponds to the splitting of water into hydrogen and oxygen:

$$2H_2O_{(l)} \rightarrow 2H_{2(g)} + O_{2(g)} \qquad \text{(Equation 1.5)}$$

Under standard conditions, the equilibrium potential for oxygen evolution is approximately +1.23 V versus the standard hydrogen electrode (SHE), corresponding to a thermodynamic cell voltage of approximately 1.23 V for overall water splitting.[8,14] However, in practice, an applied cell voltage greater than the thermodynamic value is generally required to achieve practical rates because of kinetic limitations at the electrodes.[8,15] These kinetic limitations give rise to electrode overpotentials, which contribute to the additional voltage required for practical water electrolysis.[8,15]

The stability of water in electrochemical systems depends strongly on both the electrode potential and the pH of the electrolyte.[8,15] This relationship is commonly represented using a potential-pH diagram, also known as a Pourbaix diagram.[8,15] Such diagrams define the thermodynamic region in which water is stable and indicate the potentials at which hydrogen evolution or oxygen evolution occurs.[8,15]

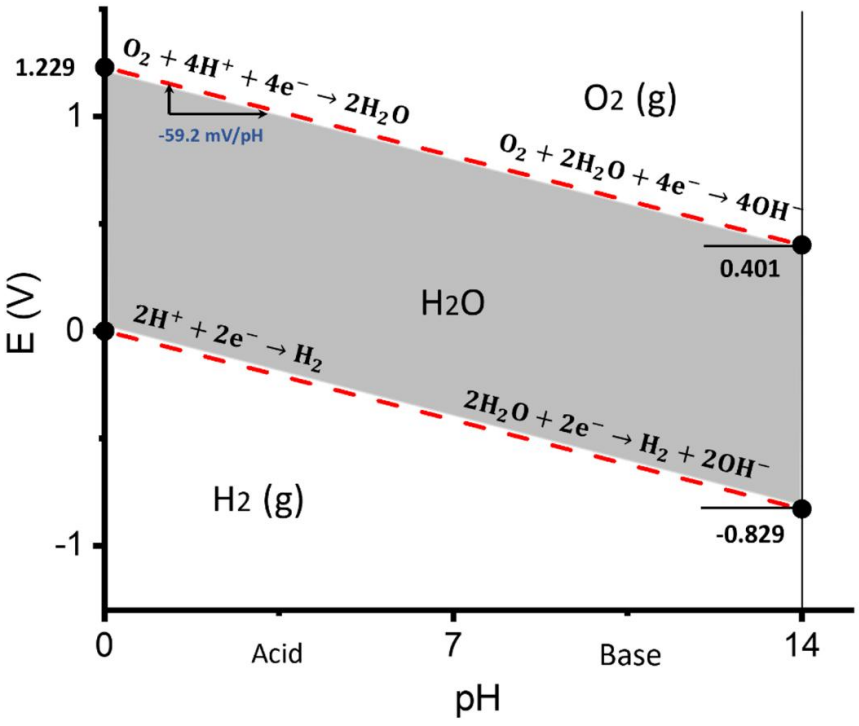


Figure 1.2. Potential pH (Pourbaix) diagram for water showing the thermodynamic stability region of water and the boundaries for the hydrogen evolution and oxygen evolution reactions.[8]

As Shown in Figure 1.2, water remains thermodynamically stable only within a specific potential window that varies with pH. At potentials more negative than the lower boundary, hydrogen evolution

becomes favourable, whereas at more positive potentials oxygen evolution occurs.[8] The slopes of the lines in the diagram arise from the pH dependence of the reactions described by the Nernst equation.[8] Understanding these limits is important when designing electrochemical reactions in aqueous media because competing hydrogen or oxygen evolution reactions may occur when sufficiently negative or positive potentials are applied.[8] For electrochemical reduction processes carried out in acidic media, the hydrogen evolution reaction often represents the main competing reaction.

In mediated electrochemical systems, however, the presence of a redox mediator can help control electron transfer between the electrode and the substrate, allowing the reaction to occur at potentials where direct reduction would otherwise be inefficient. These principles are particularly relevant for the polyoxometalate mediated electrochemical reactions investigated in this thesis.

1.2 Polyoxometalates as Multi-Electron Redox Mediators

Polyoxometalates (POMs) are a large family of discrete metal oxygen clusters composed mainly of early transition metals such as tungsten, molybdenum, or vanadium in high oxidation states. These compounds are typically formed through the condensation of metal-oxygen polyhedral units, commonly MO_6 octahedra, in acidic aqueous solution. The resulting structures contain multiple metal centres linked by bridging oxygen atoms, producing stable molecular clusters with well-defined architectures.[16,17]

Because of their structural diversity, high stability, and tunable electronic properties, polyoxometalates have attracted considerable attention in several areas of chemistry, including catalysis, materials science, and electrochemistry.[16–18] In particular, their ability to undergo reversible multi-electron redox processes makes them attractive candidates for use as redox mediators in electrochemical reactions.

In contrast to many organic molecules that typically participate in single electron transfer reactions, polyoxometalates contain multiple metal centres that can accept electrons in a stepwise manner. This property allows them to act as molecular electron reservoirs, storing several electrons within the metal-oxide framework while maintaining their structural integrity.[17,18] As a result, polyoxometalates can

transfer these stored electrons to substrates in solution, making them useful mediators in electrochemical transformations.

1.2.1 Structural Types of Polyoxometalates

Polyoxometalates can generally be classified into two main groups: isopolyoxometalates, which consist only of metal-oxygen atoms, and heteropolyoxometalates, which incorporate a central heteroatom such as phosphorus, silicon, or germanium within the metal-oxygen framework.[17]

Several structural archetypes of polyoxometalates have been identified, among which the Lindqvist, Keggin, and Wells-Dawson structures are the most widely studied. Representative examples of these structures are shown in Figures 1.3.[19]

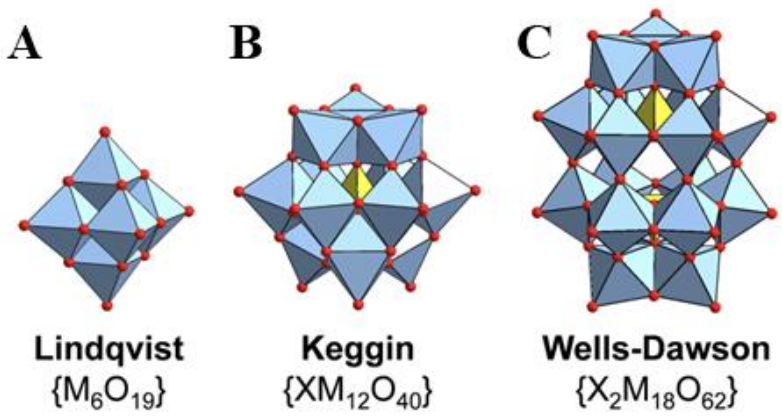


Figure 1.3. Representative structural types of polyoxometalates: (A) Lindqvist $[M_6O_{19}]^{n-}$, (B) Keggin $[XM_{12}O_{40}]^{n-}$, and (C) Wells-Dawson $[X_2M_{18}O_{62}]^{n-}$ clusters, where M represents the addenda metal (e.g., W, Mo, or V) and X represents the central heteroatom (e.g., P or Si).[19]

The Lindqvist structure is one of the simplest polyoxometalate architectures and typically has the general formula $[M_6O_{19}]^{n-}$. In this structure, six metal-oxygen octahedra are arranged around a central oxygen atom to form a compact octahedral cluster. Lindqvist type clusters are often considered fundamental building blocks in polyoxometalate chemistry.[17]

The Wells-Dawson structure is larger and more complex, generally represented by the formula $[X_2M_{18}O_{62}]^{n-}$, where X represents the heteroatom and M represents the addenda metal. These clusters contain two heteroatom centred units surrounded by eighteen metal-oxygen octahedra, resulting in an elongated structure. The α-Wells-Dawson structure exhibits D_3h symmetry.[16]

Among the various polyoxometalate structures, the Keggin structure is one of the most widely studied because of its high symmetry and remarkable stability. Keggin type polyoxometalates have the general formula $[XM_{12}O_{40}]^{n-}$, where X represents a central heteroatom and M is typically tungsten or molybdenum. In this structure, a central tetrahedral XO_4 unit is surrounded by twelve MO_6 octahedra arranged into four M_3O_{13} units connected through bridging oxygen atoms. This arrangement forms a compact and highly symmetrical cluster framework with approximately tetrahedral symmetry, as illustrated in Figure 1.4.[17,20]

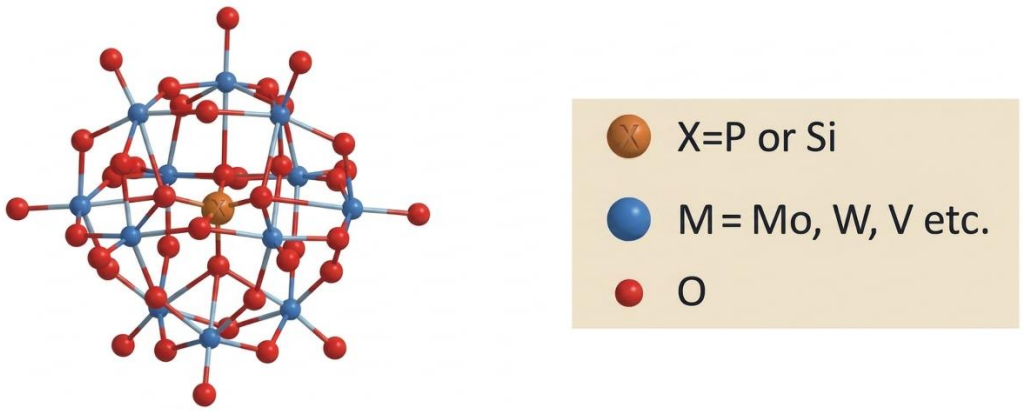


Figure 1.3. Schematic representation of the Keggin-type polyoxometalate structure $[XM_{12}O_{40}]^{n-}$, where X represents the central heteroatom (e.g., P or Si) and M represents the addenda metal (e.g., Mo, W, or V). The structure consists of a central tetrahedral heteroatom surrounded by twelve metal-oxygen octahedra connected through bridging oxygen atoms.[21]

Within the Keggin structure, several distinct types of oxygen atoms are present, including terminal oxygen atoms (M=O), bridging oxygen atoms linking adjacent metal centres (M–O–M), and internal oxygen atoms connecting the heteroatom to the surrounding metal-oxide framework. These different

oxygen environments influence both the chemical reactivity and the electron-transfer properties of the cluster.[20,22]

1.2.2 Redox Behaviour of Polyoxometalates

One of the most important characteristics of polyoxometalates is their ability to undergo multiple reversible reduction processes. In many tungsten- and molybdenum-based clusters, electrons can be added sequentially to the metal centres while the overall structure remains largely unchanged. These reductions often appear as a series of redox waves in cyclic voltammetry experiments.[18]

When electrons are introduced into the cluster framework, they are frequently delocalised across several metal centres. This delocalisation stabilises the reduced species and allows polyoxometalates to accommodate multiple electrons without significant structural distortion. As a result, reduced polyoxometalates often exist as mixed valence systems, where oxidised and reduced metal centres coexist within the same cluster.[16,18]

In tungsten-based polyoxometalate, partial reduction commonly produces intensely coloured species known as heteropoly blues. These species arise from intervalence charge transfer transitions between metal centres in different oxidation states within the cluster framework.[18]

Because of their reversible redox behaviour and structural stability, polyoxometalates have been widely investigated as redox mediators in electrochemical reactions. In mediated electrochemical systems, the polyoxometalate is first reduced at the electrode surface and then transfers electrons to a substrate in solution. After these electron transfer step, the oxidised mediator is regenerated at the electrode, allowing the reaction to proceed through a catalytic cycle.[18]

Among the many polyoxometalates that have been studied, silicotungstic acid $H_4[SiW_{12}O_{40}]$ is a Keggin-type heteropolyacid with high solubility in aqueous media, strong Brønsted acidity, and well-defined electrochemical properties. The structure and properties of silicotungstic acid are discussed in the following section.

1.3 Silicotungstic Acid

Silicotungstic acid $H_4[SiW_{12}O_{40}]$ is one of the most widely studied members of the polyoxometalate family and belongs to the class of Keggin type heteropolyacids. The compound contains the heteropolyanion $[SiW_{12}O_{40}]^{4-}$, which adopts the classical Keggin structure described in Section 1.2. Structure,[15,17,19] a central tetrahedral SiO_4 unit surrounded by twelve WO_6 octahedra. These octahedra arranged into four groups of three octahedra, commonly referred to as W_3O_{13} units, which surround the central heteroatom. [15,17,19]

These units are connected through bridging oxygen atoms to form a highly symmetrical metal-oxide cluster framework. The strong tungsten-oxygen bonding within the cluster provides significant structural stability, allowing the framework to undergo electron transfer processes without major structural rearrangement. This structural arrangement is illustrated in Figure 1.5.[18,23,24]

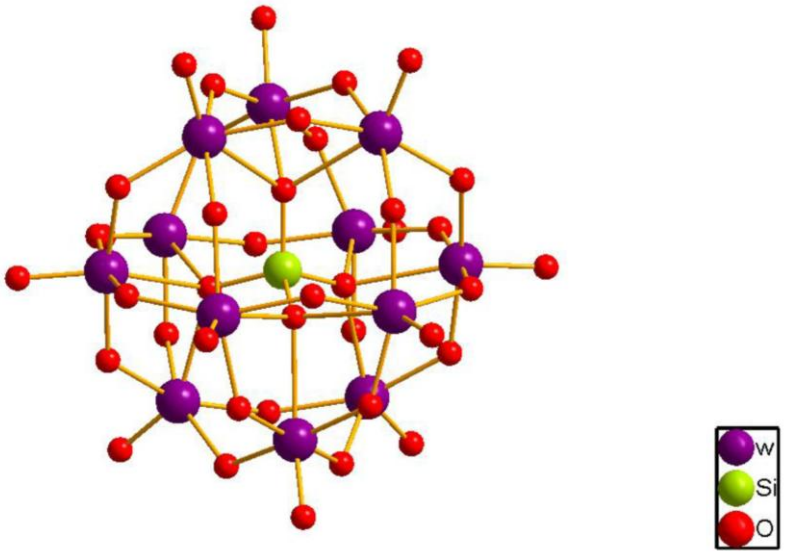


Figure 1.5. Molecular structure of the Keggin-type silicotungstate anion $[SiW_{12}O_{40}]^{4-}$. The structure consists of a central tetrahedral SiO_4 unit surrounded by twelve WO_6 octahedra arranged in four W_3O_{13} groups, each comprising three edge-sharing WO_6 octahedra. The W_3O_{13} groups are connected to one another through shared oxygen atoms to form the Keggin framework.[18]

1.3.1 Physicochemical Properties

Silicotungstic acid is characterised by its strong Brønsted acidity and high solubility in aqueous media. Brønsted acidity refers to the ability to donate protons (H^+), and high solubility in aqueous media. In water, the compound readily dissociates to release protons, producing highly acidic solutions. This strong acidity arises from the stabilisation of the conjugate base through delocalisation of negative charge across the extended metal-oxygen framework of the Keggin anion. This charge delocalisation stabilises the deprotonated form, thereby facilitating proton dissociation. Because of these properties, silicotungstic acid and other heteropolyacids are frequently employed as homogeneous catalysts in organic reactions such as hydration, esterification, and oxidation.[20,25]

In addition to its acidic properties, silicotungstic acid exhibits well defined redox electrochemical behaviour associated with the reduction of tungsten centres within the cluster framework. When electrons are introduced into the polyoxometalate structure, mixed valence tungsten species can be generated while the overall cluster structure remains intact. These reduced mixed valence species often exhibit a characteristic blue colouration and are commonly referred to as heteropoly blues, as illustrated in Figure 1.6.[17,19,26]

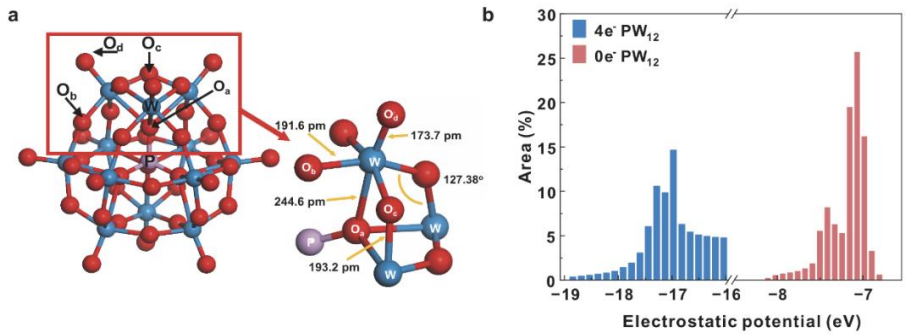


Figure 1.6. Schematic illustration of electronic changes in reduced Keggin type polyoxometalates. (A) Structure of the reduced PW_{12} cluster showing the coordination environment within the Keggin framework. (B) Electrostatic potential distribution on the surface of oxidised ($0e^-$) and reduced ($4e^-$) PW_{12} clusters, illustrating the increase in negative charge upon electron addition.[26]

Recent studies have further demonstrated the multi-electron redox behaviour of tungsten polyoxometalates under electrochemical conditions. For example, Li et al. reported that sodium-substituted phosphotungstate ($3Na\text{-}PW_{12}$) can reversibly accept and release up to five electrons during charge-discharge cycling. During deep reduction, the increase in electrolyte pH suppresses hydrogen evolution and enables potentials as negative as −1.1 V vs. SHE. Under these conditions, PW_{12} partially converts to a lacunary PW_{11} structure, with the PW_{12} structure being recovered upon discharge.[26]

1.3.2 Applications in Redox Mediation

The redox properties of silicotungstic acid make it particularly useful as a mediator in electrochemical and catalytic transformations. In mediated electrochemical systems, the polyoxometalate is first reduced at the electrode surface and subsequently transfers stored electrons to substrates in solution before being regenerated electrochemically at the electrode. This process allows the reaction to proceed through a catalytic cycle while separating the electrochemical generation of reducing equivalents from the chemical transformation of the substrate.[27]

Several studies have highlighted the role of silicotungstic acid in mediated reduction processes. For example, MacDonald et al. reported that the two-electron reduced form of silicotungstic acid can act as an efficient reducing agent for nitroarenes, producing the corresponding aniline derivatives in aqueous solution under mild conditions and without the need for additional catalysts.[27] Notably, halogenated substrates were found to retain their halogen substituents during the reaction, representing a significant advantage compared with conventional catalytic hydrogenation methods that often lead to dehalogenation.

More recently, Stergiou and Symes demonstrated that phosphotungstic acid, a closely related Keggin type polyoxometalate, can mediate the electrochemical reduction of substituted nitroarenes with very high selectivity. In their work, mediated electrochemical reduction produced aniline derivatives in aqueous solution at room temperature with selectivities exceeding 99%.[28]

Polyoxometalates have also been investigated as mediators in oxidative transformations. Early work by Sadakane and Steckhan examined manganese substituted polyoxometalates for alcohol oxidation reactions, while later studies by Neumann and co-workers demonstrated that phosphovanadomolybdate clusters can mediate the selective oxidation of methylarenes to benzaldehyde derivatives with high conversion and selectivity.[17,29] These examples highlight the versatility of polyoxometalate mediators in both reductive and oxidative electrochemical reactions.

1.3.3 Relevance to This Thesis

Although the electrochemical behaviour of silicotungstic acid has been widely investigated, the formation and stability of more deeply reduced states remain important topics of study. Understanding how these reduced species are generated and stabilised is essential for evaluating their potential as soluble redox mediators in electrochemical transformations.

In this thesis, silicotungstic acid was selected as the primary polyoxometalate mediator because of its well defined structure, strong acidity, and reversible redox behaviour. The electrochemical reduction of silicotungstic acid and the stability of its reduced species are examined in detail in Chapter 3, where cyclic voltammetry and controlled potential electrolysis are used to investigate multi-electron reduction processes within the Keggin framework.

1.4 Electrochemical Redox Behaviour of Silicotungstic Acid

1.4.1 Multi-Electron Redox Properties of Polyoxometalates

Polyoxometalates are widely recognised for their characteristic electrochemical behaviour, which arise from the presence of multiple transition-metal centres within metal-oxygen cluster framework. In these compounds, the metal ions, typically tungsten or molybdenum, exist in high oxidation states and can undergo reduction under electrochemical conditions. Because the metal-oxygen framework remains largely intact during these processes, polyoxometalates are able to accept and store several electrons in

a stepwise manner. [16–18] This behaviour makes them attractive systems for studying multi-electron redox reactions in aqueous solution.[16–18]

The electrochemical properties of polyoxometalates are commonly investigated using cyclic voltammetry, where the potential applied to an electrode is varied cyclically and the resulting current response is recorded. In many polyoxometalates, reduction occurs through a series of reversible or quasi reversible electron transfer processes. Each of these processes corresponds to the addition of electrons to the cluster framework and appears as distinct redox waves in cyclic voltammogram.[8,17]

1.4.2 Electrochemical Reduction of Silicotungstic Acid

Among the various polyoxometalates studied electrochemically, silicotungstic acid $H_4[SiW_{12}O_{40}]$ exhibits particularly well defined redox behaviour. In acidic aqueous solution, cyclic voltammetry of the silicotungstic acid anion typically reveals several sequential reduction waves associated with the stepwise reduction of tungsten centres within the Keggin cluster.[8,30,31]

The first reduction processes generally correspond to reversible one-electron transfer reactions, resulting in the partial reduction of W(VI) centres to W(V) and the formation of mixed-valence W(VI)/W(V) species. At more negative potentials, additional reductions may occur, often involving proton-coupled electron-transfer processes. These deeper reductions produce more highly reduced forms of the polyoxometalate cluster while the overall structure of the Keggin framework remains preserved under appropriate experimental conditions.[31,32]

The positions and reversibility of these reduction waves depend strongly on experimental parameters such as pH of the solution, electrolyte composition, electrode material, and scan rate. Understanding these electrochemical properties is therefore important when evaluating the potential of silicotungstic acid as a mediator in electrochemical reactions.[31,32]

1.4.3 Polyoxometalates as Redox Mediators

Reduced tungsten polyoxometalates can form intensely coloured mixed-valence species known as heteropoly blues.[17,18,32] In Keggin type tungstates, initial reduction involves the partial reduction of W^{6+} centres to W^{5+}, producing mixed-valence species containing both W^{5+} and W^{6+} centres. With increasing levels of reduction, the distribution and localisation of the added electrons within the polyoxometalate framework can change, as illustrated in Figure 1.7.[19]

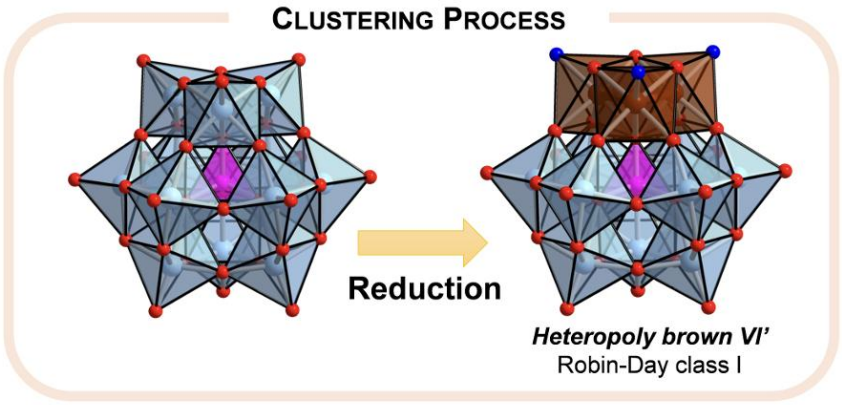


Figure 1.7. Schematic representation of changes in electron distribution associated with progressive reduction of a keggin-type polyoxometalate, illustrating the transition from delocalised reduced states to more localised states at higher levels of reduction.[19]

In mixed-valence reduced states, intervalence charge transfer (IVCT) transitions, involving electron transfer between tungsten centres in different oxidation states, such as W^{5+} and W^{6+}, can give rise to strong absorption bands in the visible region of the spectrum, resulting in the characteristic colouration of reduced polyoxometalates. [17,18]

The ability of polyoxometalates to undergo reversible reduction and accommodate multiple electrons makes them attractive redox mediators. In mediated electrochemical systems, the polyoxometalate is first reduced at the electrode surface and subsequently transfers electrons to a substrate in solution. Following electron transfer, the oxidised polyoxometalate can be reduced again at the electrode, allowing it to participate in repeated redox cycles. [17,18] This approach has been investigated in a range

of electro-organic transformations, with polyoxometalates acting as soluble electron-transfer mediators between the electrode and organic substrates.[17,18,33]

1.4.4 Cyclic Voltammetry of Silicotungstic Acid

The electrochemical behaviour of silicotungstic acid can be examined experimentally using cyclic voltammetry. During this measurement, the potential applied to the working electrode is scanned over a defined range while the resulting current is recorded. The appearance of oxidation and reduction peaks in the cyclic voltammogram provides information about the redox properties of the system.[8,31] A representative cyclic voltammogram of silicotungstic acid obtained in acidic aqueous solution is shown in Figure 1.8.[34]

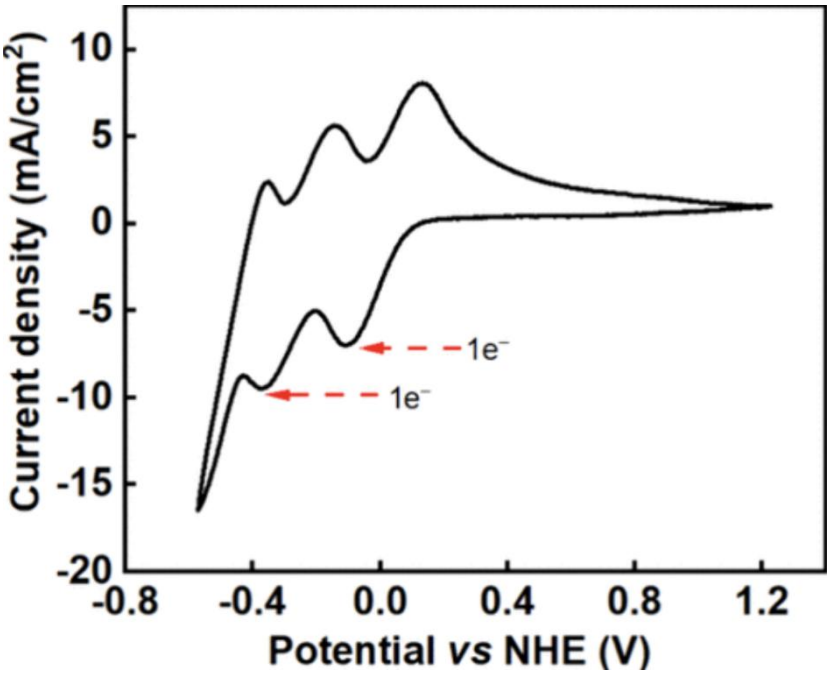


Figure 1.8. Representative cyclic voltammogram of silicotungstic acid (0.5 M) in acidic aqueous solution recorded at a scan rate of 10 mV s^{-1} using a glassy carbon working electrode. The first two waves correspond to reversible one-electron transfer processes within the Keggin cluster, producing the one-electro and two-.[34]

The cyclic voltammogram displays several well-defined reduction waves corresponding to successive electron-transfer processes within the Keggin cluster. The first two waves correspond to reversible one-

electron transfer reactions, leading sequentially to the formation of one-electron-reduced and two-electron-reduced silicotungstate species.[34] These successive reductions involve the stepwise reduction of W(VI) centres to W(V). The detailed reduction reactions are discussed in Chapter 3.

Analysis of cyclic voltammetric data provides information about the number of electrons involved in a reaction, the reversibility of the redox processes, and the stability of the species formed during electrochemical reduction.

1.4.5 Stability and Reversibility of Reduced Species

Although silicotungstic acid exhibits good stability under moderate reduction conditions, deeper reduction can sometimes lead to irreversible structural changes. Prolonged electrolysis at highly negative potentials may result in decomposition processes such as the formation of reduced tungsten oxide species or partial degradation of the Keggin framework.[32] As recently discussed by Falaise (2025), maintaining structural integrity in super-reduced polyoxometalates remains a significant challenge for their application in aqueous media.[19]

Understanding the conditions under which reversible electron storage transitions to irreversible degradation is therefore important for practical use of silicotungstic acid as a redox mediator. The stability of its reduced forms is a key factor determining its effectiveness in systems.[17,32]

The detailed electrochemical behaviour of silicotungstic acid, including the formation and stability of its reduced species under controlled experimental conditions, is examined in Chapter 3. These investigations help to clarify the extent to which reversible multi-electron reduction can occur within the Keggin framework and provide the foundation for the mediated reduction reactions explored in later chapters of this thesis.

1.5 Polyoxometalate-Mediated Electrochemical Reduction of Organic Compounds

Electrochemical methods provide an attractive alternative to conventional reduction reactions because electrons supplied from an electrode can replace stoichiometric chemical reducing agents.[5,35–37] In principle this allows reduction reactions to proceed without generating reagent-derived waste products. However, the direct electrochemical reduction of many organic substrates can be difficult in practice. Many organic molecules exhibit slow electron transfer kinetics at electrode surfaces and therefore require the application of strongly negative potentials in order to undergo reduction. Under such conditions poor selectivity may occur, together with competing side reactions or electrode fouling caused by absorption of reaction intermediates on the electrode surface.[7,11]

One approach that can overcome these limitations is the use of mediated electrochemical reduction. In mediated systems, a soluble redox mediator transfers electrons between the electrode and the substrate. As illustrated in Figure 1.9, silicotungstic acid is first reduced electrochemically through successive electron-transfer and proton-coupled electron-transfer processes, generating reduced species capable of storing multiple electrons. The successive reduction reaction leading to the $1e^-$, $2e^-$, and $4e^-$ reduced silicotungstate acid species are described in detail in Chapter 3 (Equations 3.1–3.3). These reduced forms can then transfer the stored electrons to an organic substrate (Ar–EWG, where Ar represents an aromatic ring and EWG represents an electron-withdrawing group, such as CN, COR, or CHO) in solution in an ex situ reduction step, producing the reduced product while regenerating the oxidised mediator. The mediator is subsequently reduced again at the electrode, allowing the process to proceed through a catalytic cycle.

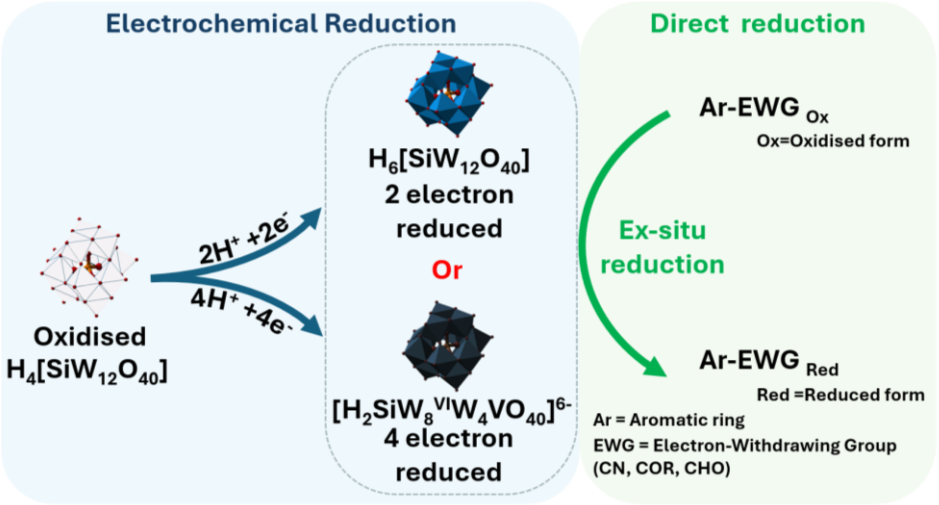


Figure 1.9. Polyoxometalate mediated electrochemical reduction using silicotungstic acid. The oxidised species is reduced via proton coupled electron transfer to form multi-electron reduced states, which transfer electrons to the substrate in solution and are regenerated electrochemically. **Ar** represents an aromatic ring and **EWG** represents an electron-withdrawing group (e.g., CN, COR or CHO).

This separation of the heterogeneous electron transfer step at the electrode from the homogeneous reaction occurring in solution enables electrochemical reductions to proceed under mild conditions and with improved selectivity compared with direct electrolysis. [7,11]

1.5.1 Polyoxometalates as Redox Mediators

The application of polyoxometalates as redox mediators in organic transformations has been discussed in Section 1.3.2. In addition to the mediated reduction of nitroarenes, Wu et al. reported that reduced silicotungstic acid can be used in combination with heterogeneous metal catalysts such as Pd/C to promote hydrogenation reactions, further demonstrating the applicability of reduced polyoxometalates to organic reductions.[38] Selected examples of polyoxometalate-mediated reductions reported in the literature are summarised in Table 1.1.

Table 1.1. Selected examples of polyoxometalate-mediated organic reduction reported in the literature.

Mediator (reduction state)	Substrate	Product	Conditions	Yield	Reference
$H_6[SiW_{12}O_{40}]$ ($2e^-$ reduced)	Nitrobenzene	Aniline	Aqueous, RT, 12h	99%	MacDonald et al.[27]
$H_6[SiW_{12}O_{40}]$ ($2e^-$ reduced)	4-Bromonitrobenzene	4-Bromoaniline	Aqueous, RT, 12h	63 %	Stergiou et al.[28]
$H_6[SiW_{12}O_{40}]$ ($2e^-$ reduced)	4-Nitrobenzonitrile	4-Aminobenzonitrile	Aqueous, RT, 12h	95 %	Stergiou et al.[28]
$H_6[SiW_{12}O_{40}]$ ($2e^-$ reduced)	Phenylacetylene	Ethylbenzene	EtOH/H_2O, Pd/C	100 %	Wu et al.[38]

More recently, polyoxometalate-mediated nitroarene reduction has been extended to flow electrochemical systems, demonstrating the continued development of this approach beyond batch-mediated reductions. The use of phosphotungstic acid as a redox mediator enabled chemoselective reduction of nitroaromatics under mild conditions, with product selectivity influenced by the reaction medium.[39] These examples demonstrate the ability of reduced polyoxometalates to convert organic substrates into synthetically useful products, including aniline derivatives and hydrogenated products. Such transformations can provide access to value-added products that may serve as useful intermediates for further chemical synthesis.[27,28,38]

1.5.2 Relevance to the Present Study

Although polyoxometalate mediated reductions of organic substrates have been demonstrated, reductive applications remain relatively underexplored compared with oxidative transformations.[10,33] In particular, systematic studies examining how the degree of reduction of silicotungstic acid influences reactivity and chemoselectivity remain limited.[10,27,28] Understanding how multi-electron reduced forms of silicotungstic acid behave in mediated reduction systems is therefore important for evaluating the potential of polyoxometalates as tunable redox mediators. This question is addressed in Chapter 4, where the 2-electron, 4-electron, and 6-electron reduced forms of silicotungstic acid are evaluated as soluble redox mediators for the reduction of electron deficient aromatic compounds.

To investigate chemoselectivity in these systems, 4-cyanobenzaldehyde was selected as a model substrate because it contains two potentially reducible functional groups: an aldehyde and a nitrile group. The strongly electron withdrawing nitrile substituent activates the aldehyde group toward reduction while itself remaining relatively resistant to reduction under mild conditions. This system therefore provides a useful platform for examining the selectivity of polyoxometalate mediated reduction processes. By comparing the reactivity of different reduced states of silicotungstic acid, the influence of electron storage capacity on reaction efficiency and selectivity can be systematically evaluated.

1.6 Carbon Monoxide Reduction and the Potential Role of Polyoxometalate Mediators

1.6.1 Importance of Carbon Monoxide

Carbon monoxide (CO) is an important one-carbon (C1) feedstock in industrial chemistry and a key component of synthetic gas (syngas), a mixture of carbon monoxide and hydrogen that serves as the starting material for numerous large scale chemical processes.[40] Through catalytic transformation, CO can be converted into a variety of valuable products including hydrocarbons, alcohols, and oxygenated compounds.[41] Consequently, the activation and conversion of carbon monoxide have attracted considerable scientific and industrial interest.[42]

One of the most established industrial processes involving carbon monoxide is the Fischer–Tropsch (FT) synthesis, in which syngas is catalytically converted into hydrocarbons over transition metal catalysts such as iron or cobalt.[43] This process forms the basis of several industrial technologies including gas to liquids (GTL), coal to liquids (CTL), and biomass to liquids (BTL) systems used for the production of synthetic fuels and chemical feedstocks. A simplified process flow diagram of a laboratory scale Fischer–Tropsch system is shown in Figure 1.10,[41] illustrating the main steps of gas purification, compression, catalytic conversion in a slurry reactor, and subsequent separation of the resulting hydrocarbon products. [38]

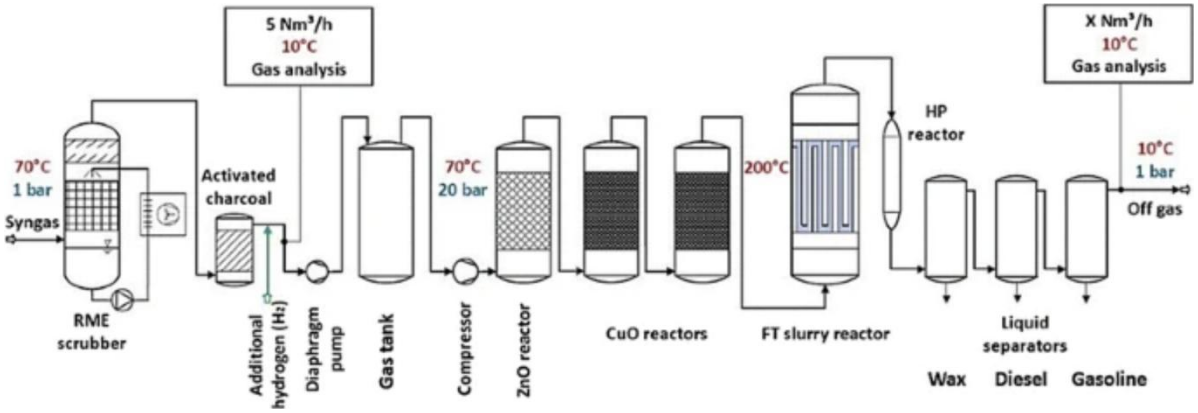


Figure 1.10. Simplified process flow diagram of a laboratory scale Fischer–Tropsch synthesis system for converting synthesis gas into hydrocarbon products.[41]

Although Fischer–Tropsch synthesis demonstrated the potential of CO as a carbon source for fuel production, the process typically operates at elevated temperatures (200-350 °C) and pressures (10-60 bar), requiring complex industrial infrastructure and significant energy input.[43] These demanding conditions motivate the search for alternative strategies for carbon monoxide conversion under milder conditions, including electrochemical approaches.[42]

1.6.2 Challenges in Electrochemical Carbon Monoxide Reduction

Electrochemical methods offer an alternative strategy for activating and transforming carbon monoxide. In electrochemical systems, electrons supplied by an electrode can drive reduction reactions that convert small molecules into more reduced products. When coupled with renewable electricity sources, such processes offer the possibility of more sustainable chemical synthesis.[42]

However, the electrochemical reduction of carbon monoxide presents several fundamental challenges. One major obstacle is the exceptional stability of the CO molecule. The C≡O triple bond has a bond dissociation energy of approximately 1076 kJ mol^{-1}.[44] The C≡O bond consists of one σ and two π bonding interactions, which contribute to the high bond strength and stability of the molecule. Interaction of CO with suitable metal centres can facilitate activation of the molecule through σ-

donation from CO to the metal and π-back-donation from the metal to CO, with the latter weakening the C–O bond.[45]

In addition to this molecular stability, electrochemical CO reduction presents challenges associated with reaction kinetics and product selectivity. Multiple reaction pathways are possible, leading to a range of products including methane, ethylene, ethanol, and higher hydrocarbons.[44,46] Controlling selectivity toward a desired product therefore represents a major challenge. Furthermore, in aqueous electrochemical systems, the hydrogen evolution reaction (HER) can compete with CO reduction, reducing the efficiency of the process.[46] The thermodynamic potentials for selected CO and CO_2 reduction reactions are summarised in Table 1.2.

Table 1.2. Thermodynamic potentials for selected CO/CO_2 electroreduction reactions vs SHE in acidic media.[42,47]

Reaction	E° (V vs SHE)
$CO_2 + 8H^+ + 8e^- \rightarrow CH_4 + 2H_2O$	+ 0.17
$CO_2 + 2H^+ + 2e^- \rightarrow CO + H_2O$	−0.11
$2CO + 8H^+ + 8e^- \rightarrow C_2H_4 + 2H_2O$	+0.28
$3CO + 8H^+ + 8e^- \rightarrow C_3H_5OH + 2H_2O$	+0.19
$3CO + 12H^+ + 12e^- \rightarrow C_3H_7OH + 2H_2O$	+0.21

Although these thermodynamic potentials are relatively modest, substantial kinetic overpotentials are typically required to achieve practical reaction rates.[48] As a result, the development of efficient catalysts capable of activating CO under electrochemical conditions has been an important area of research.

1.6.3 Catalysts for Carbon Monoxide Reduction

Among the various catalysts investigated for electrochemical carbon monoxide reduction, copper-based materials have attracted particular attention. Since the pioneering work of Hori and co-workers, copper

has been recognised as the only monometallic catalyst capable of converting CO into multicarbon (C_2^+) products with appreciable efficiency.[49]

Copper surfaces provide an environment in which adsorbed CO intermediates can undergo further reduction and carbon–carbon (C–C) coupling, enabling the formation of both C1 and multicarbon ($C2^+$) products. The resulting product distribution depends strongly on factors including the applied potential, electrolyte composition, catalyst surface structure, and reaction conditions.[50] As a result, copper catalysts can produce a variety of products including methane, ethylene, ethanol, and propanol depending on the applied potential, electrolyte composition, and catalyst morphology.

The reaction network involved in CO electroreduction on copper is complex and involves multiple proton-coupled electron-transfer steps as well as C–C coupling pathways leading to C1 and C_2^+ products. The proposed pathways for CO reduction on copper are illustrated in Figure 1.11.[49,51]

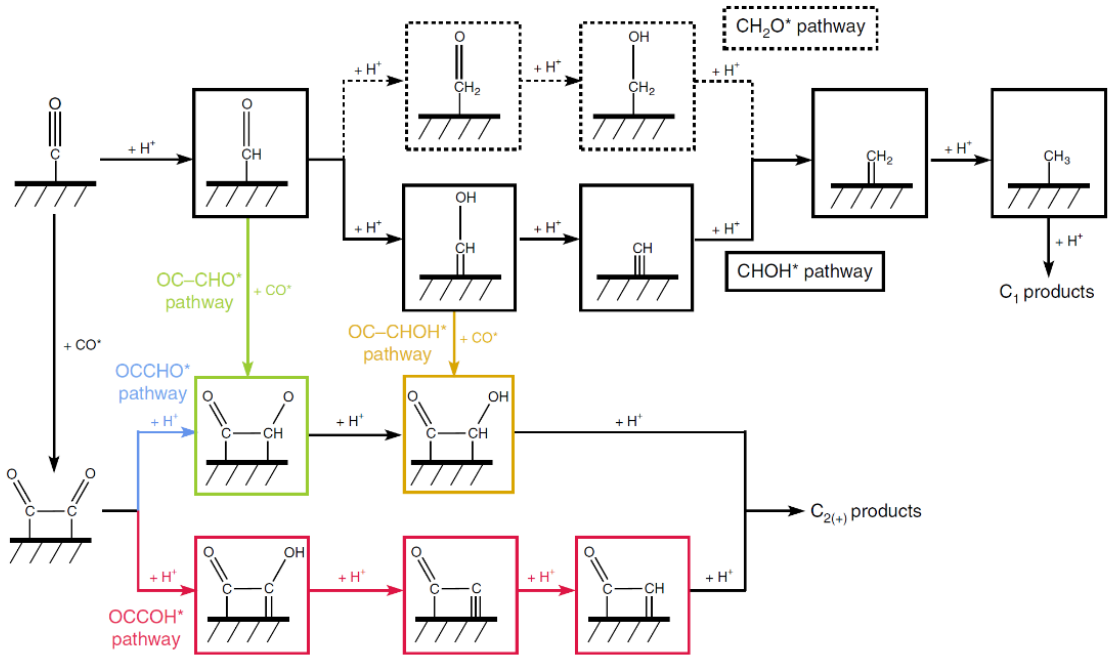


Figure 1.11. Proposed reaction pathways for electrochemical reduction of CO on copper catalysts leading to C_1 and C_2^+ products. The black pathway represents a proposed route to C_1 products through proton-coupled electron-transfer steps, while the coloured pathways illustrate proposed C–C coupling routes leading to multicarbon products.[51]

The proposed pathways for CO reduction on copper have been investigated using a combination of experimental and computational approaches. Experimental electrolysis and electrochemical measurements provide information on the formation and distribution of reaction products and possible intermediates, while density functional theory (DFT) calculations can be used to evaluate the relative energetics of proposed surface intermediates and elementary reaction steps.[49,51] Together, these approaches provide evidence for the proposed reaction pathways, although individual elementary steps and intermediates may remain the subject of mechanistic investigation.

Considerable research has focused on controlling catalyst structure and the local reaction environment to improve the activity and selectivity of copper-based catalysts for CO electroreduction. Strategies including catalyst nanostructuring and control of surface structure have been investigated to influence reaction pathways and the formation of $C2^{+}$ products.[46,50] Nevertheless, achieving high activity, selectivity, and stability simultaneously remains an important challenge in CO electroreduction.[46,50]

1.6.4 Potential Role of Redox Mediators

Given the challenges associated with direct electrochemical CO reduction at electrode surfaces, including competing reactions and difficulties in controlling product selectivity, alternative strategies for facilitating electron transfer and substrate activation are of interest.[46,50] One such approach involves the use of redox mediators, which can transfer electrons between the electrode and the substrate in solution.

Whether reduced polyoxometalates possess sufficient reducing power to activate the strong C≡O bond of carbon monoxide remains an open question. More specifically, it is unclear whether these soluble multi-electron redox reservoirs can transfer stored electrons to CO in the absence of a catalytic surface capable of adsorbing and activating the molecule. Such electron transfer could, in principle, occur through an outer-sphere pathway, in which electrons are transferred from the reduced polyoxometalate to CO without direct coordination of CO to the mediator.[52] Alternatively, under acidic conditions, proton transfer may be coupled to electron transfer through a proton-coupled electron-transfer pathway.[31]

However, whether either pathway occurs during the interaction of reduced polyoxometalates with CO remains uncertain and is not established in this thesis. Investigating this possibility may therefore provide new insight into mediated electrochemical reduction mechanisms and the potential use of polyoxometalates for small-molecule activation.

Carbon monoxide is therefore an attractive but challenging target for mediated electrochemical reduction. This question is examined in Chapter 5, where the reactivity of electrochemically reduced silicotungstic acid and phosphomolybdic acid toward carbon monoxide is investigated under homogeneous and catalyst-assisted conditions.

1.6.5 Summary

Carbon monoxide represents an important C1 feedstock with significant industrial relevance. However, its activation and conversion remain challenging due to the strength of the C≡O bond, slow reaction kinetics, and competing reactions under electrochemical conditions. Although heterogeneous copper catalysts have demonstrated the ability to convert CO into multicarbon products, these systems still face limitations in efficiency and selectivity.

The use of soluble redox mediators such as polyoxometalates offers a potential alternative strategy for CO activation under milder conditions. The multi-electron storage capability of silicotungstic acid makes it a promising candidate for such mediated electrochemical transformations. The interaction between reduced silicotungstic acid and carbon monoxide is therefore investigated in Chapter 5 of this thesis.

1.7 Aims and Scope of this Thesis

Polyoxometalates represent a particularly promising class of redox mediators because of their ability to undergo reversible multi-electron redox processes and accommodate multiple electrons within their metal-oxide frameworks. Among these compounds, silicotungstic acid $H_4[SiW_{12}O_{40}]$ has attracted considerable attention due to its well-defined Keggin structure, strong Brønsted acidity, and capacity to

store multiple electrons within its metal-oxygen cluster framework. These properties make silicotungstic acid a suitable candidate for investigating mediated electrochemical reduction processes involving both organic molecules and small gaseous substrates.

The primary aim of this thesis is therefore to investigate the electrochemical behaviour of silicotungstic acid and to evaluate its potential as a multi-electron redox mediator. In particular, this work examines the electrochemical reduction of silicotungstic acid under strongly acidic conditions and investigates the formation, stability, and reversibility of the reduced polyoxometalate species generated during multi-electron reduction. The ability of these reduced species to transfer stored electrons to chemical substrates in solution is then explored in order to assess their potential as mediators for indirect electrochemical reduction reactions. This work also examines whether more deeply reduced forms of silicotungstic acid ($4e^-$ and $6e^-$ reduced) exhibit different reactivity or selectivity compared with the well-studied $2e^-$ reduced form, providing insight into the relationship between electron storage capacity and mediator performance.

To address these objectives, the research presented in this thesis investigates two principal applications of reduced silicotungstic acid. First, the reactivity of reduced polyoxometalate species toward organic substrates is examined, with particular emphasis on the reduction of electron-deficient aromatic carbonyl compounds. Secondly, the possibility of electron transfer from reduced polyoxometalate species to small molecules such as carbon monoxide is investigated in order to evaluate the feasibility of mediated electrochemical reduction of gaseous substrates.

The thesis is organised as follows. Chapter 2 describes the experimental methods and analytical techniques used throughout the study, including electrochemical instrumentation and procedures for the preparation and handling of polyoxometalate solutions. Chapter 3 investigates the electrochemical reduction behaviour of silicotungstic acid using cyclic voltammetry and controlled-potential electrolysis, with particular emphasis on the formation and stability of reduced polyoxometalate species. Chapter 4 examines the application of reduced silicotungstic acid as a mediator for the electrochemical reduction of selected aromatic aldehydes and related organic substrates. Chapter 5 explores the

interaction between reduced polyoxometalate mediators and carbon monoxide in order to assess the potential role of polyoxometalates in mediated small-molecule reduction. Finally, Chapter 6 summarises the main findings of the work and discusses possible directions for future research.

Through the systematic investigation of silicotungstic acid as a multi-electron redox mediator, this thesis aims to provide new insight into the use of polyoxometalates in electrochemical synthesis and to assess their potential for facilitating more sustainable reduction processes.

1.8 References

1 F. A. Carey and R. J. Sundberg, *Advanced organic chemistry. Part B, Reactions and synthesis*, Springer, 2007.

2 J. Clayden, N. Greeves and S. G. Warren, *Organic chemistry*, Oxford University Press, 2012.

3 A. Wiebe, T. Gieshoff, S. Möhle, E. Rodrigo, M. Zirbes and S. R. Waldvogel, *Angew. Chem. Int. Ed.*, 2018, **57**, 5594–5619.

4 M. Yan, Y. Kawamata and P. S. Baran, *Chem. Rev.*, 2017, **117**, 13230–13319.

5 B. A. Frontana-Uribe, R. D. Little, J. G. Ibanez, A. Palma and R. Vasquez-Medrano, *Green Chem.*, 2010, **12**, 2099–2119.

6 P. T. Anastas and J. C. Warner, *Green Chemistry: Theory and Practice*, Oxford University Press, 2000.

7 R. Francke and R. D. Little, *Chem. Soc. Rev.*, 2014, **43**, 2492–2521.

8 A. J. Bard and L. R. Faulkner, *Electrochemical methods: fundamentals and applications*, John Wiley & Sons, Inc., 2001.

9 A. Gemünde, B. Lai, L. Pause, J. Krömer and D. Holtmann, *ChemElectroChem*, 2022, **9**, e202200216.

10 A. D. Stergiou and M. D. Symes, *Catal. Today*, 2022, **384–386**, 146–155.

11 E. Steckhan, *Angew. Chem. Int. Ed. Engl.*, 1986, **25**, 683–701.

12 E. J. Horn, B. R. Rosen and P. S. Baran, *ACS Cent. Sci.*, 2016, **2**, 302–308.

13 J.-M. Savéant, *Elements of molecular and biomolecular electrochemistry: an electrochemical approach to electron transfer chemistry*, John Wiley & Sons, 2006.

14 P. Atkins, J. De Paula and R. Friedman, *Physical chemistry: quanta, matter, and change*, Oxford University Press, 2014.

15 J. M. Gonçalves, A. Kumar, M. I. da Silva, H. E. Toma, P. R. Martins, K. Araki, M. Bertotti and L. Angnes, *Energy Technol.*, 2021, **9**, 2000927.

16 M. T. Pope, Y. Jeannin and M. Fournier, *Heteropoly and isopoly oxometalates*, Springer, 1983, vol. 33.

17 M. Sadakane and E. Steckhan, *Chem. Rev.*, 1998, **98**, 219–238.

18 S.-S. Wang and G.-Y. Yang, *Chem. Rev.*, 2015, **115**, 4893–4962.

19 C. Falaise, *Eur. J. Inorg. Chem.*, 2025, **28**, e202400827.

20 A. Proust, R. Thouvenot and P. Gouzerh, *Chem. Commun.*, 2008, 1837–1852.

21 M. R. Horn, A. Singh, S. Alomari, S. Goberna-Ferrón, R. Benages-Vilau, N. Chodankar, N. Motta, K. (Ken) Ostrikov, J. MacLeod, P. Sonar, P. Gomez-Romero and D. Dubal, *Energy Environ. Sci.*, 2021, **14**, 1652–1700.

22 J. D. Kammert, G. Brezicki, N. Miyake, E. Stavitski and R. J. Davis, *ChemCatChem*, 2020, **12**, 314–325.

23 G. S. Girolami and A. P. Sattelberger, *Inorganic Syntheses, Volume 36*, John Wiley & Sons, 2014, vol. 36.

24 M. Saghi, K. Mahanpoor and H. Shafiei, *Iran. J. Chem. Chem. Eng.*, 2018, **37**, 1–10.

25 C. L. Hill, *Chem. Rev.*, 1998, **98**, 1–2.

26 W. Li, W. Xu, Z. Sun, L. Tang, G. Xu, X. He, Y. Deng, W. Sun, B. Zhou, J. Song and W. Liu, *Nat. Commun.*, 2025, **16**, 4654.

27 L. MacDonald, B. Rausch, M. D. Symes and L. Cronin, *Chem. Commun.*, 2018, **54**, 1093–1096.

28 A. D. Stergiou, D. H. Broadhurst and M. D. Symes, *ACS Org. Inorg. Au*, 2023, **3**, 51–58.

29 B. B. Sarma, I. Efremenko and R. Neumann, *J. Am. Chem. Soc.*, 2015, **137**, 5916–5922.

30 B. Keita and L. Nadjo, *J. Electroanal. Chem. Interfacial Electrochem.*, 1987, **227**, 77–98.

31 B. Keita and L. Nadjo, *J. Electroanal. Chem. Interfacial Electrochem.*, 1987, **217**, 287–304.

32 T. Ueda, *ChemElectroChem*, 2018, **5**, 823–838.

33 S. D. Mürtz, J.-C. Raabe, M. J. Poller, R. Palkovits, J. Albert and N. Kurig, *ChemCatChem*, 2024, **16**, e202301632.

34 O. Mbang Eze, Z. Ertekin and M. D. Symes, *Energy & Fuels*, 2025, **39**, 7129–7136.

35 O. Hammerich and B. Speiser, *Organic electrochemistry*, CRC Press, Taylor & Francis Group, 2015.

36 D. Pletcher and F. C. Walsh, in *Industrial Electrochemistry*, Springer, 1990, pp. 481–542.

37 M. B. Smith and J. March, *March's advanced organic chemistry: reactions, mechanisms, and structure*, Wiley-Interscience, 2007.

38 W. Wu, X.-Y. Wu, S.-S. Wang and C.-Z. Lu, *J. Catal.*, 2019, **378**, 376–381.

39 D. Wang, T.-Q. Wang and B. Li, *Chem. Eng. Sci.*, 2025, **310**, 121473.

40 P. M. Maitlis and A. de Klerk, in *Greener Fischer-Tropsch Processes for Fuels and Feedstocks*, 2013, pp. 337–358.

41 S. Müller, P. Groß, R. Rauch, R. Zweiler, C. Aichernig, M. Fuchs and H. Hofbauer, *Biomass Convers. Biorefin.*, 2018, **8**, 275–282.

42 R. Francke, B. Schille and M. Roemelt, *Chem. Rev.*, 2018, **118**, 4631–4701.

43 M. E. Dry, *Catal. Today*, 2002, **71**, 227–241.

44 M. Gattrell, N. Gupta and A. Co, *J. Electroanal. Chem.*, 2006, **594**, 1–19.

45 G. Frenking, I. Fernández, N. Holzmann, S. Pan, I. Krossing and M. Zhou, *JACS Au*, 2021, **1**, 623–645.

46 M. Jouny, G. S. Hutchings and F. Jiao, *Nat. Catal.*, 2019, **2**, 1062–1070.

47 A. A. Peterson and J. K. Nørskov, *J. Phys. Chem. Lett.*, 2012, **3**, 251–258.

48 K. P. Kuhl, E. R. Cave, D. N. Abram and T. F. Jaramillo, *Energy Environ. Sci.*, 2012, **5**, 7050–7059.

49 Y. Hori, A. Murata and R. Takahashi, *J. Chem. Soc., Faraday Trans. 1*, 1989, **85**, 2309–2326.

50 W. Ma, X. He, W. Wang, S. Xie, Q. Zhang and Y. Wang, *Chem. Soc. Rev.*, 2021, **50**, 12897–12914.

51 X. Liu, P. Schlexer, J. Xiao, Y. Ji, L. Wang, R. B. Sandberg, M. Tang, K. S. Brown, H. Peng, S. Ringe, C. Hahn, T. F. Jaramillo, J. K. Nørskov and K. Chan, *Nat. Commun.*, 2019, **10**, 32.

52 I. A. Weinstock, *Chem. Rev.*, 1998, **98**, 113–170.

Chapter 2: Overview of the Techniques Used

Synopsis

This chapter introduces the main electrochemical and analytical methods used in chapters 3-5. A brief theoretical background is also provided to help the reader understand these techniques before they are applied in the following chapters.

2.1 Electrochemical Techniques

Electrochemical methods played an important role in this work, as they allow the redox behaviour of chemical species to be studied directly at electrode surfaces.[1] These techniques make it possible to monitor changes in oxidation state, follow electron-transfer processes, and evaluate the stability of redox-active species under controlled conditions. The aim of this chapter is to describe the experimental approaches used to investigate the electrochemical reduction of the mediator. The methods were selected to determine the mediator's redox properties, to examine its behaviour during repeated electrochemical cycling, and to generate reduced forms under controlled conditions.

Two electrochemical techniques were employed in this study. Cyclic voltammetry (CV) was first used to obtain information about the redox activity of the mediator, including the identification of suitable reduction and oxidation potentials and the assessment of electrochemical reversibility.[2] Bulk electrolysis was then used to generate the reduced mediator on a larger scale, enabling further characterisation to be carried out outside the electrochemical cell.

The following sections describe the electrode arrangements, the electrochemical cell configurations, and instrumentation used in these experiments. Particular attention is given to the single-compartment cell used for cyclic voltammetry and to the H-cell configuration employed for bulk electrolysis.

2.2 Electrode setup

Electrochemical experiments in this study used two different cell configurations, depending on the type and purpose of the measurement. A single compartment cell was used for cyclic voltammetry (CV) experiments, while an H-cell configuration was employed for bulk electrolysis.[3]

2.2.1 Single cell configuration

A single-compartment electrochemical cell was used for cyclic voltammetry to study the redox behaviour of the mediator. A three-electrode setup was employed for these measurements (Figure 2.1).

The setup included a working electrode, a reference electrode, and a counter electrode. All electrodes were connected to a potentiostat, which controlled the applied potential while recording the current. The potential of the working electrode was measured relative to the reference electrode, which ideally carried negligible current, while the current flowed between the working and counter electrodes.

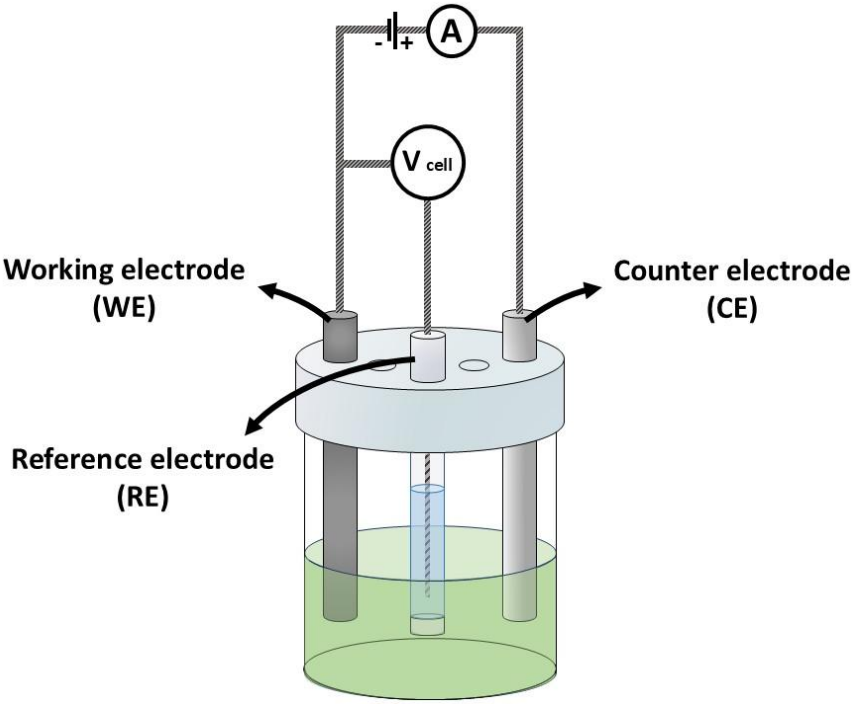


Figure 2.1. Schematic representation of a conventional three electrode single cell setup used for cyclic voltammetry measurements.

In this configuration, a glassy carbon electrode was used as the working electrode and served as the surface for the electrochemical reactions. Measurements were referenced against an Ag/AgCl electrode in the aqueous medium, while charge balance within the cell was maintained using a platinum wire as the counter electrode.[4,5] The use of glassy carbon ensured a wide usable potential range and reproducible behaviour, and the Ag/AgCl reference provided a stable and well-defined potential throughout the experiments.

This configuration was used for preliminary electrochemical characterisation of the mediator under well-defined conditions. Alternative cell configurations employed for other measurements are described in the following section.

2.2.2 H-cell configuration

For bulk electrolysis, the electrochemical setup comprised an H-type cell in which a proton exchange membrane separated two compartments (Figure 2.2).[3] One compartment contained the mediator solution together with the working and reference electrodes and served as the cathodic chamber, where the reduction reaction occurred. The counter electrode was confined to the second compartment, which functioned as the anodic chamber and was filled with 1 M phosphoric acid.[4,6]

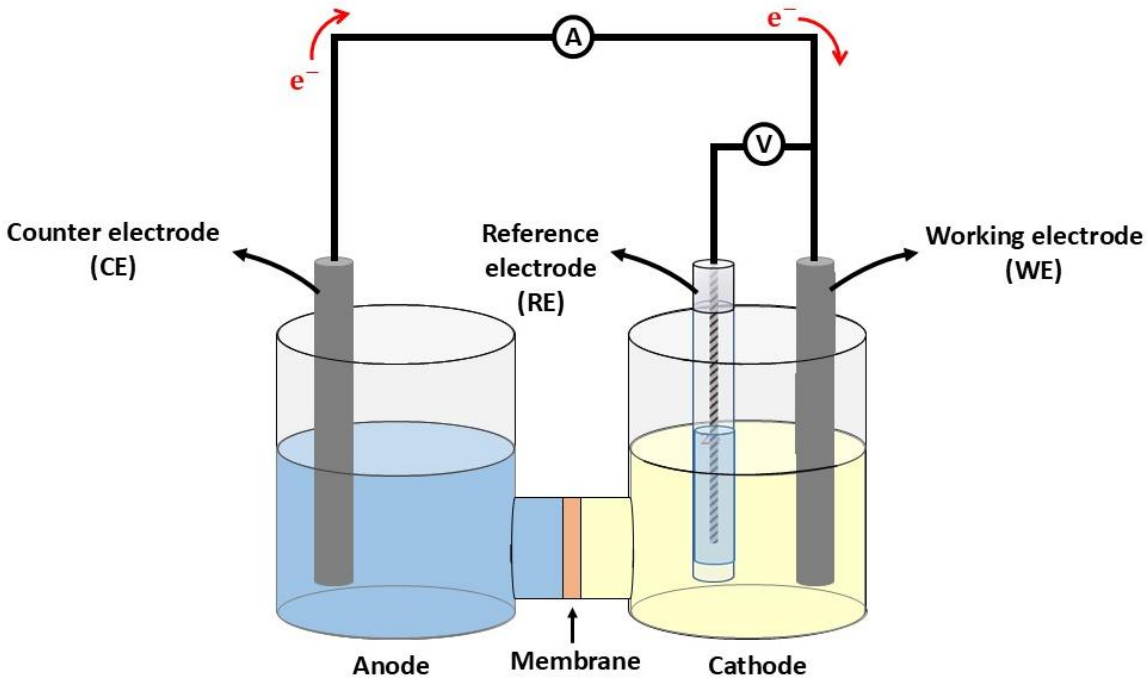


Figure 2.2. Schematic of the H-cell used for the bulk electrolysis. The cathodic chamber contained the mediator solution, while the anodic chamber was filled with 1 M phosphoric acid, H_3PO_4.

The acidic electrolyte supported the anodic reaction and helped maintain proton conductivity across the membrane during electrolysis.[7] Separation of the compartments limited the transfer of electroactive species of between them, while still allowing sufficient proton transport for sustained electrolysis.[8] This arrangement slowed the mixing of products generated at the electrodes and minimised re-oxidation processes at the counter electrode.[9]

2.3 Cyclic voltammetry

Cyclic voltammetry (CV) is an electrochemical technique used to study redox-active systems.[1] In this work, CV was used to examine the redox behaviour of the mediator. During a CV experiment, the potential at the working electrode is changed between two set limits at a fixed scan rate. The current response is recorded at the same time. Reversing the scan direction allows both reduction and oxidation processes to be observed in a single experiment.[10]

The potential-time profile of a typical CV experiment is shown in Figure 2.3. The scan starts at an initial potential (E_i), sweeps to a switching potential (E_1), then reverses back to E_i (or to E_i via a second switching potential E_2) to complete the cycle.

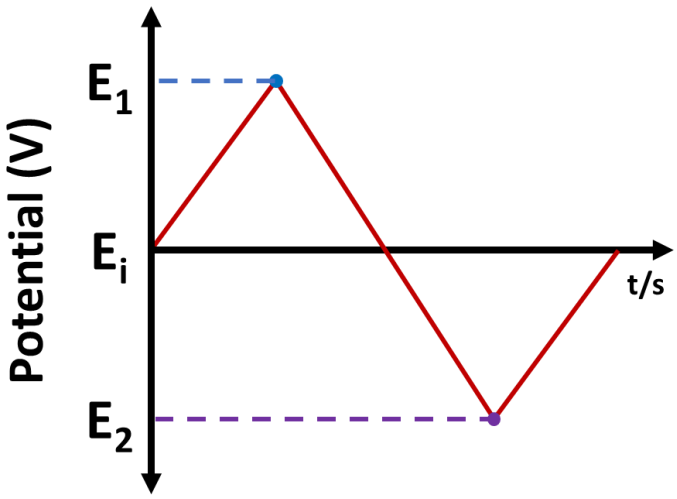


Figure 2.3. Potential-time waveform for cyclic voltammetry. The potential is swept linearly from E_i to E_1 (and potentially E_2) and then back to E_i, completing one or more cycles.

The shape of the voltammogram gives information about the redox behaviour of species in solution. From these responses, it is possible to assess whether the electrochemical process is reversible, quasi-reversible, or irreversible.[2] CV can also provide information about electron transfer behaviour and indicate whether chemical reactions occur during the electrochemical process.[11]

In this study, CV was used to identify the potential range where the mediator undergoes oxidation and reduction. The results were used to select suitable conditions for later bulk electrolysis experiments. Repeated scans were also carried out to examine the stability of the mediator during successive redox cycles.

2.4 Reversibility of the Mediator System

For effective use as a mediator, the material must undergo oxidation and reduction without losing activity. For this reason, the reversibility of silicotungstic acid was examined using cyclic voltammetry.[11] Attention was given to whether the voltammetric response remained consistent over repeated scans.

Reversible behaviour in CV is usually associated with paired oxidation and reduction peaks that are similar in size and shape. Reversibility was evaluated by comparing the positions of the oxidation and reduction peaks and by examining the relative sizes of their currents. For an ideal, reversible one-electron redox redox couple at room temperature, the theoretical peak-to-peak separation (ΔE_p) is approximately 59 mV and identical peak anodic and cathodic current values are expected. Larger separations or differences in relative currents indicate reduced reversibility or slower electron transfer.[2,12]

The redox behaviour of the mediator can be described by the simplified reaction shown in Equation 2.1:

$$Ox + ne^- \rightleftharpoons Red \qquad \text{(Equation 2.1)}$$

In a chemically reversible system, the oxidised and reduced forms interconvert without permanent change.[11] If side reactions or decomposition occur, changes in the voltammetric response may be observed, indicating a loss of reversibility.

In this study, cyclic voltammetry was used to monitor changes in peak shape, peak separation, and current magnitude. These features were used to assess the stability and reversibility of silicotungstic acid within the selected potential range (Figure 2.4).

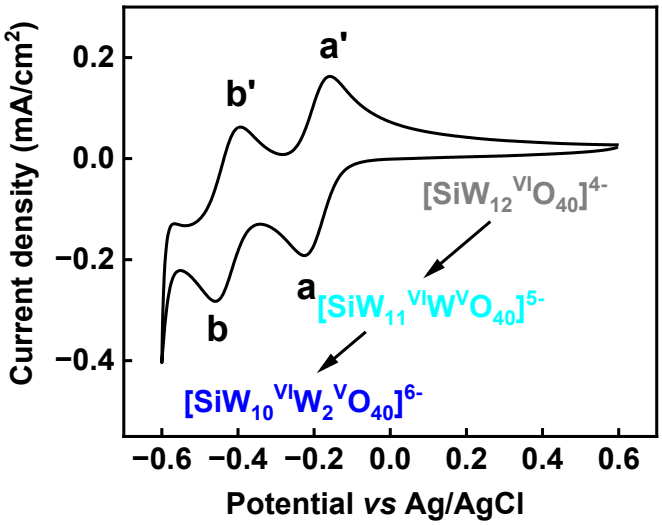


Figure 2.4. Cyclic voltammogram of silicotungstic acid showing anodic and cathodic peaks used to assess electrochemical reversibility.

2.5 Electrolysis

Electrolysis was carried out to convert silicotungstic acid between its oxidised and reduced forms under controlled conditions. This was achieved by applying either a fixed potential or a fixed current. Two electrochemical approaches were used: chronoamperometry, where the potential was kept constant, and chronopotentiometry, where a constant current was applied.[1] In both cases, changes during the conversion were followed over time.

2.5.1 Chronoamperometry

In chronoamperometry, a constant potential was applied during the experiment, and changes in current were followed with time. This method allows the redox state of the mediator to be controlled at a defined potential.[11] The potentials used in these experiments were chosen based on cyclic voltammetry measurements of silicotungstic acid.

As electrolysis progressed, the current decreased as the mediator was consumed at the electrode surface. The process was considered complete when the current reached a low and stable value.[5] In this work, chronoamperometry was used to follow the bulk reduction and reoxidation of silicotungstic acid.

2.5.2 Chronopotentiometry

Chronopotentiometry, also referred to as galvanostatic electrolysis, was carried out under fixed-current conditions. The electrode potential is the potential difference between the working electrode and the reference electrode. During the experiment, the potential changed as the reaction progressed.[11]

Since the potential is not directly controlled, it may move into regions where additional reactions can occur. For this reason, chronopotentiometry is less selective than chronoamperometry.[13] However, it remains useful for driving redox reactions under constant-current conditions. In this study, it was used to examine the behaviour of silicotungstic acid during fixed-current electrolysis.

Faraday's Law

The total charge passed during electrolysis was related to the amount of mediator undergoing redox transformation using Faraday's law.[14] This relationship was used to estimate the extent of mediator conversion, defined as the fraction of silicotungstic acid converted between its oxidised and reduced forms under the applied electrochemical conditions:

$$Q = nmF \qquad \text{(Equation 2.2)}$$

Where Q is the total charge (C), n is the number of electrons transferred per molecule, m is the number of moles of mediator undergoing redox conversion, and F is the Faraday constant (96,485 C mol^{-1}).[5]

2.6 Characterisation techniques:

2.6.1 Gas Chromatography (GC)

Gas chromatography served as the method for analysing gases present in the headspace of the H-cell during bulk electrolysis. The main aim was to determine whether hydrogen was produced under the applied electrochemical conditions, as this would indicate the occurrence of the hydrogen evolution reaction alongside the reduction of the mediator.[15] Headspace samples were withdrawn periodically during electrolysis and injected into the GC for analysis, allowing the detection and estimation of any hydrogen formed. A simplified layout of a gas chromatograph used in this work is presented in Figure 2.5.

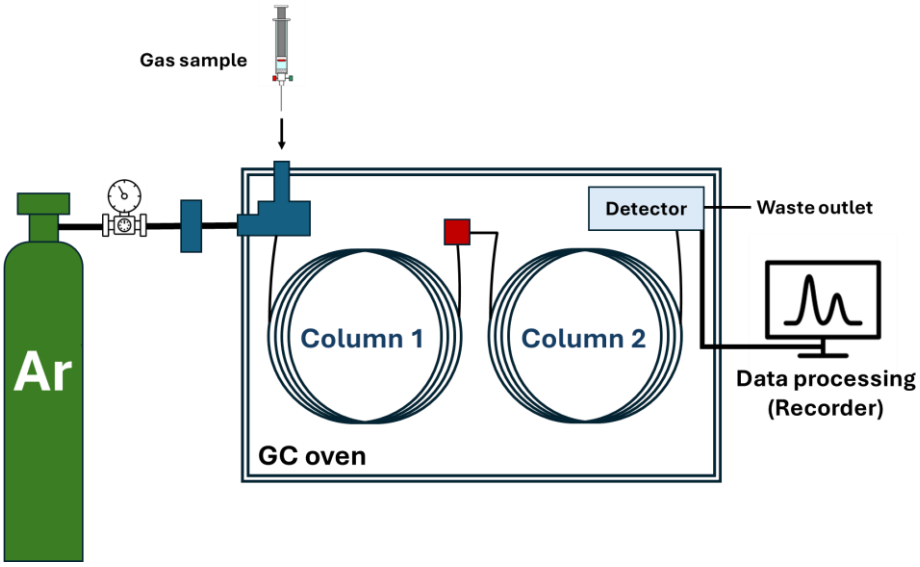


Figure 2.5. General layout of a gas chromatograph, showing the injection port, column oven, and detector, and two columns connected via a valve-switching system.

As illustrated in Figure 2.5, the injected gas sample is carried by argon through the two-column system, where its components are separated before passing to the detector for analysis. In gas chromatography, separation occurs because components of a gas mixture interact to different extents with the stationary phase inside the analytical column.[16] An inert carrier gas transports the sample through the column. In

this work, argon was selected as the carrier gas because its thermal conductivity is well suited to the detector employed.

GC analysis was performed using an Agilent 8890 instrument. A thermal conductivity detector (TCD) was used for detection. Changes in detector response were observed when gas leaving the column differed in thermal conductivity from the carrier gas.[17] Hydrogen produced a strong response because its thermal conductivity is much higher than that of argon, resulting in a distinct and easily recognisable signal.

The GC system was configured with two columns connected via a valve-switching arrangement to enable efficient separation of permanent gases and light hydrocarbons. Initially, the sample was directed through Column 1 for the analysis of hydrogen, which eluted within the first 1.8 minutes. The flow was then switched to Column 2 to allow separation of carbon dioxide, ethylene, and ethane. After 8 minutes, the system was switched back to Column 1 for the analysis of oxygen, nitrogen, methane, and carbon monoxide. This valve-switching configuration utilised the different selectivities of the two columns to improve the separation of the gas components.

As each component elutes, the detector response is recorded as a peak at a characteristic retention time. Calibration standards were analysed to confirm the retention time of hydrogen and to allow quantification when hydrogen was present in the headspace samples.[17]

In this study, GC-TCD enabled the monitoring of hydrogen formation during the reduction of silicotungstic acid and provided a way to assess whether hydrogen evolution occurred as a competing side reaction.

2.6.2 Gas chromatography-mass spectrometry (GC-MS)

Gas chromatography-mass spectrometry (GC-MS) enabled the analysis of organic products formed after chemical reduction with the reduced form of silicotungstic acid. The technique was applied to

confirm product identity. It was also used to check whether any starting material remained and to detect possible side products formed during the attempted reduction of aryl nitriles, ketones, and aldehydes.[13]

Separation of the sample occurred in the gas chromatograph, where components passed through the GC column and were separated according to volatility and interaction with the stationary phase.[16] After elution from the column, each component entered the mass spectrometer. Ionisation and fragmentation then occurred, producing a mass spectrum that was compared with reference data for compound identification.[18] A schematic representation of the GC-MS system is shown in Figure 2.6.

For analysis, organic products were dissolved in dichloromethane (DCM) and injected into the instrument. An Agilent 7890A gas chromatograph was used in conjunction with an Agilent 5975C inert mass selective detector. An Agilent J&W DB-35ms capillary column (30 m × 0.30 mm, 0.25 µm) was employed for separation.

GC-MS was therefore used to confirm product formation, check for remaining reactants, and identify additional species formed under the reduction conditions.

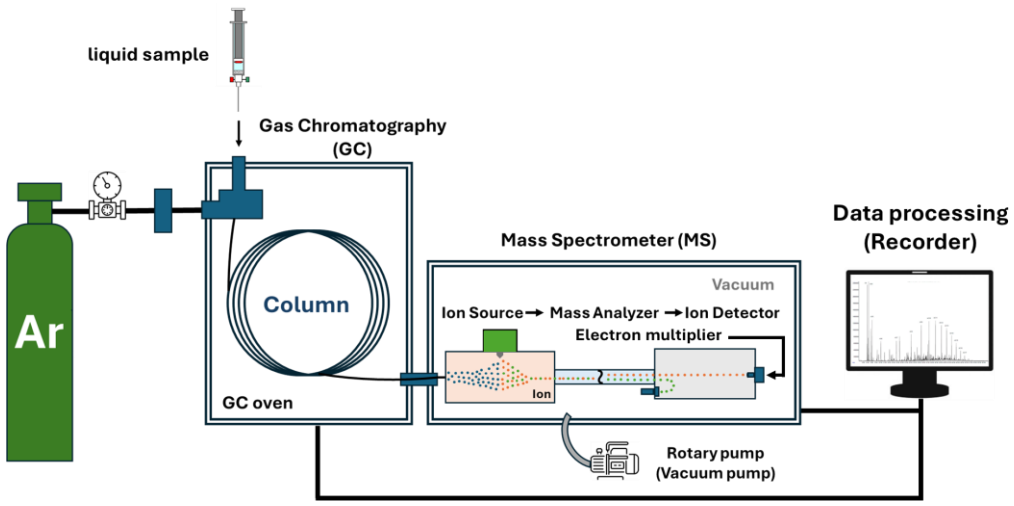


Figure 2.6. Schematic representation of a gas chromatography-mass spectrometry system, showing the injector, GC column, and mass spectrometer.

2.6.3 Ultraviolet–Visible (UV–Vis) Spectroscopy

Ultraviolet-Visible (UV–Vis) spectroscopy allowed characterisation of the electronic absorption properties of silicotungstic acid before and after reduction.[11] A schematic overview of a UV–Vis spectrophotometer is shown in Figure 2.7. By comparing spectra recorded for the oxidised and reduced forms, changes in electronic structure were monitored in both the solution and solid states. After reduction, additional absorption bands appeared in the visible region. These bands were associated with electronic transitions of the reduced tungsten centres.[11]

Absorbance data were interpreted in accordance with the Beer-Lambert relationship, with the measured intensity changes depending on both the concentration of the absorbing species and the path length of the sample cell:

$$A = \log_{10}\left(\frac{I_0}{I_t}\right) = \varepsilon c l \qquad \text{(Equation 2.3)}$$

Where A represents absorbance, I_0 and I_t correspond to the intensities of incident and transmitted light, respectively, ε is the molar absorptivity (L mol^{-1} cm^{-1}), c is the concentration of the absorbing species (mol L^{-1}), and l is path length (cm). Consequently, modifications in the UV-Vis spectrum provide direct insight into changes in the electronic environment and relative abundance of chromophoric centres within the sample.

UV–Vis spectra of the mediator in solution were recorded using an Agilent Cary 60 UV–Vis spectrophotometer operating between 190 and 1100 nm under controlled conditions. This allowed absorption features associated with the reduced species to be followed and compared directly with those of the fully oxidised material.[17]

Solid samples were analysed using a Shimadzu UV-2600 spectrophotometer (185–900 nm) fitted with an air-sensitive sample holder, preventing contact between the reduced material and air. Comparison of solution and solid-state spectra was used to assess whether the reduced electronic characteristics were retained after isolation.

Overall, UV–Vis spectroscopy provided a complementary method for confirming successful reduction of the mediator and for assessing the stability of the reduced mediator in both solution and solid form.

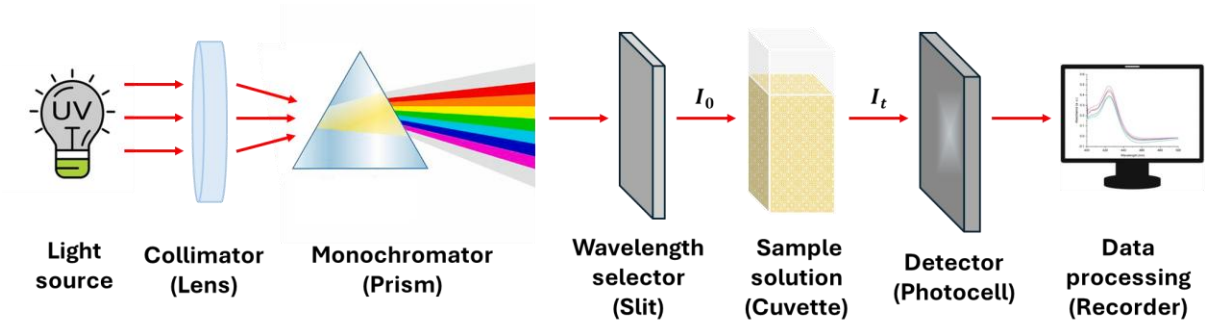


Figure 2.7. Schematic overview of a UV–Vis spectrophotometer, showing the light source, sample compartment, and detector.

2.6.4 Fourier Transform Infrared Spectroscopy (FT–IR)

Infrared Spectroscopy provided a means to examine functional-group changes during the reduction of organic substrates with the silicotungstic acid mediator.[19] A schematic representation of the FT-IR spectrometer equipped with an attenuated total reflectance (ATR) accessory is shown in Figure 2.8. Spectra recorded before and after reaction were compared to determine whether reduction had occurred and whether any starting material or additional products remained.

FT-IR spectra were recorded over a defined wavenumber range, and absorption bands corresponding to specific bond vibrations were analysed. In this work, particular attention was given to bands associated with nitrile (C≡N), carbonyl (C=O) and O–H stretching modes, as these functional groups are expected to change during the reduction of aryl nitriles, ketones, and aldehydes.[19]

The FT-IR data were obtained on a Shimadzu IRAffinity-1S FT-IR spectrometer using an attenuated total reflectance (ATR) accessory. The ATR setup allowed both solid and liquid samples to be analysed directly, without additional preparation such as pellet formation or solvent removal.[20] Measurements were recorded over the mid-infrared region from 4000 to 400 cm^{-1}, and multiple scans were averaged for each sample to improve signal quality.

Overall, FT-IR spectroscopy was employed to assess substrate conversion by comparing key absorption bands before and after reduction and by identifying the presence of any unreacted starting material or side products. Changes in band position and intensity were used as qualitative indicators of chemical transformation. FT-IR spectroscopy thus enabled rapid identification of functional group changes, such as the appearance or disappearance of characteristic bands. However, as the technique is not inherently quantitative, it was not suitable for determining product yields.

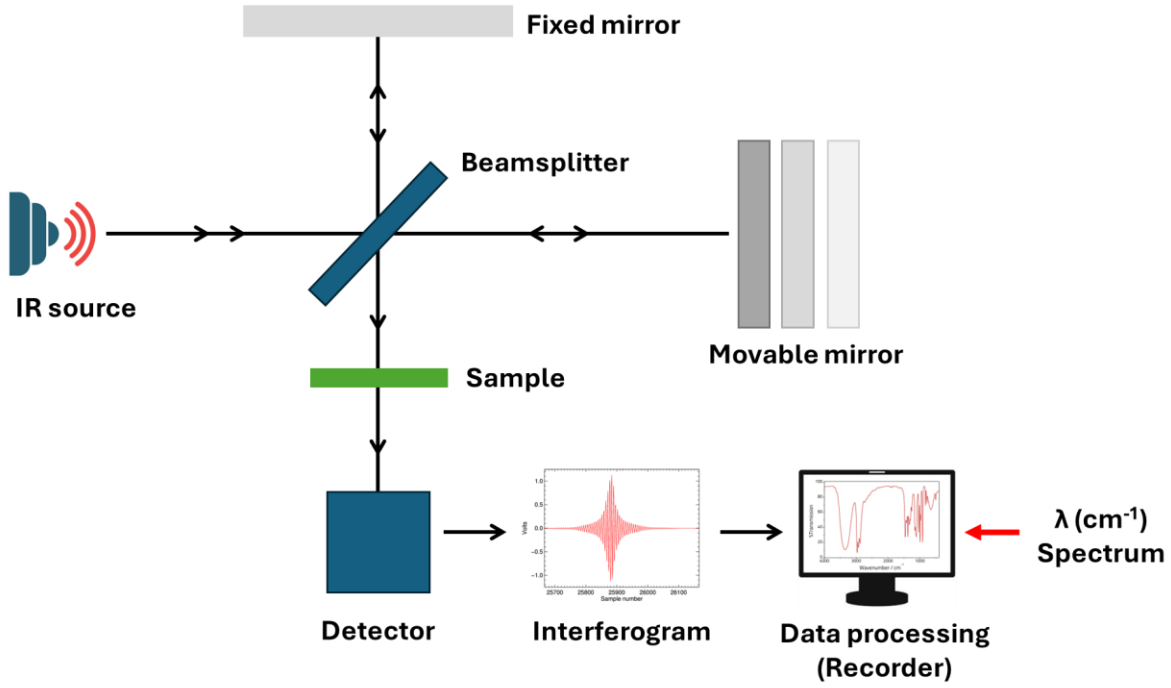


Figure 2.8. Schematic representation of an FT-IR spectrometer equipped with an ATR accessory.

2.6.5 Thermogravimetric Analysis (TGA)

Thermogravimetric analysis (TGA) provided information on the thermal behaviour and water content of the oxidised form of silicotungstic acid.[17] Changes in sample mass were followed as the temperature increased. These mass changes were used to identify processes such as the loss of adsorbed moisture, removal of more strongly bound water, and the onset of thermal decomposition.[21]

During the experiment, the sample was placed in a temperature-controlled furnace on a microbalance. Mass changes were recorded as heating progressed. The resulting thermogram showed different stages of mass loss, which were associated with distinct thermal processes in the material.

In this study, measurements were carried out using a TA Instruments Discovery TGA-550. The oxidised silicotungstic acid sample was heated from ambient temperature to 600 °C under a nitrogen atmosphere in order to minimise oxidative reactions. Heating was performed at a controlled rate, and changes in mass were monitored to assess the amount of water present in the solid material.

The TGA data thus enabled quantification of water loss from the oxidised mediator and provided insight into its hydration state and thermal stability (Figure 2.9).

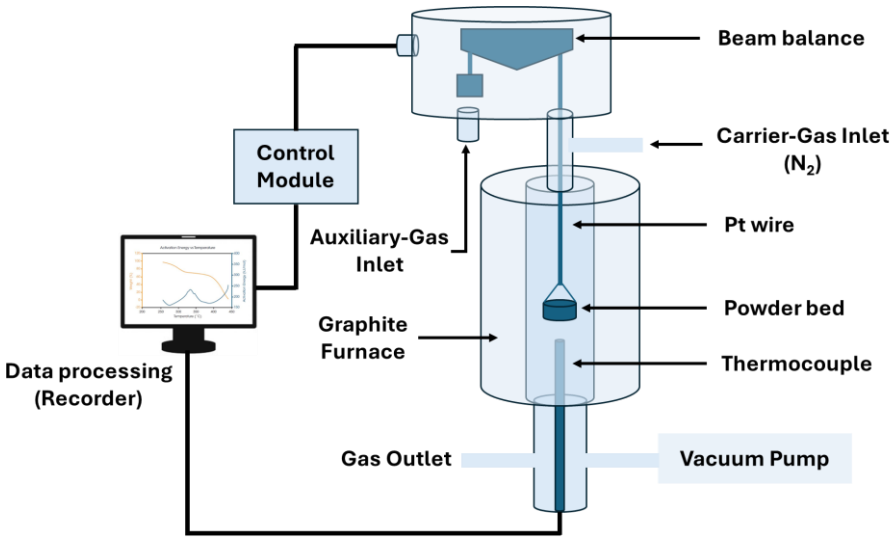


Figure 2.9. Schematic illustration of thermogravimetric analysis (TGA) system.

2.6.6 X-ray Diffraction (XRD)

X-ray diffraction provided structural information on silicotungstic acid and allowed comparison between its oxidised and reduced forms.[22] The technique is sensitive to long-range atomic order and can reveal changes in crystallinity caused by chemical modification.[22] A schematic representation of the X-ray diffraction process is shown In Figure 2.10, illustrating incident X-rays interacting with parallel lattice planes and producing constructive interference.

The positions of the diffraction peaks were analysed according to Bragg's Law:

$$n\lambda = 2d \sin\theta \qquad \text{(Equation 2.3)}$$

Where n is an integer representing the order of diffraction, λ is the wavelength of the incident X-ray radiation, d is the interplanar spacing between crystal lattice planes, and θ is the diffraction angle. As illustrated In Figure 2.10, constructive interference occurs when of X-rays reflected from adjacent lattice planes travel an additional distance equal to an integer multiple of the wavelength. This path difference is directly related to the interplanar spacing (d) and the angle of incidence (θ) giving rise to a characteristic peak.

Changes in crystal structure, reflected by variations in interplanar spacing (d), result in corresponding shifts in diffraction angle (θ) in the measured pattern. These shifts provide insight into structural modifications within the material.

Powder XRD patterns were collected for both oxidised and reduced samples in order to assess whether reduction led to changes in crystallinity or lattice arrangement. Before analysis, solvent was removed by rotary evaporation, followed by additional drying at room temperature. After drying, the materials were stored under a nitrogen atmosphere to minimise exposure to air and prevent re-oxidation.

Diffraction patterns obtained from the oxidised and reduced forms were compared to identify any shifts in peak position, changes in peak intensity, or loss of crystallinity. Such differences provide insight into structural modifications associated with the reduction of the polyoxometalate framework.

X-ray diffraction therefore served as a complementary technique for evaluating whether the reduction process affected the solid-state structure of silicotungstic acid.

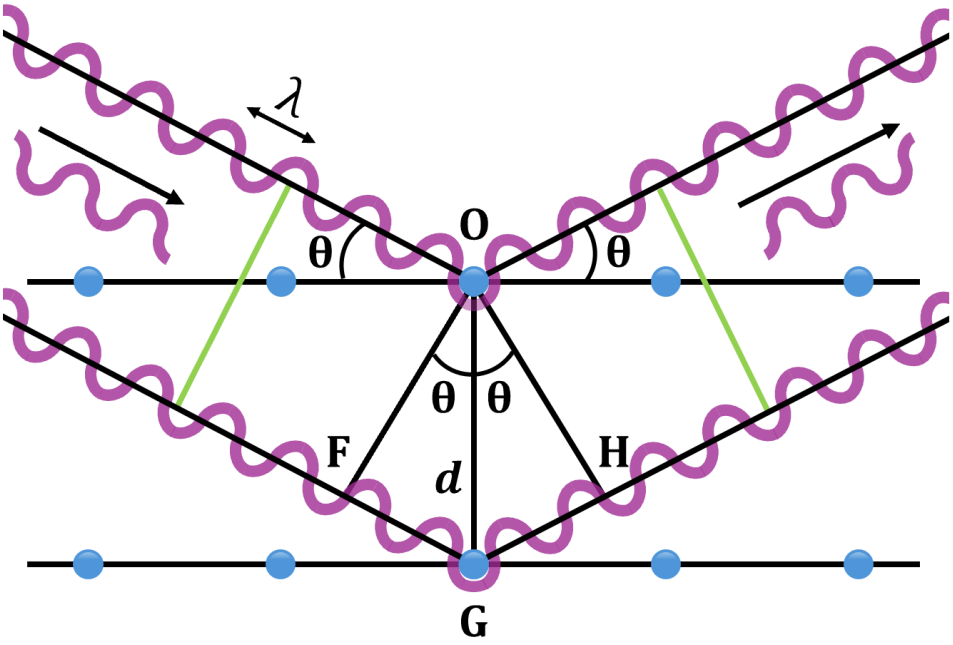


Figure 2.10. Schematic representation of the X-ray diffraction technique, illustrating incident X-rays interacting with a crystal lattice planes, the interplanar spacing (d), diffraction angle (θ), and the condition for constructive interference.

2.6.6.1 Single Crystal X-ray Diffraction (SCXRD)

Single-crystal X-ray Diffraction (SCXRD) measurements were performed on silicotungstic acid to examine its solid-state structure following chemical treatment.[22] The analysis focused on whether the polyoxometalate framework remained intact after reduction. A schematic illustration of the SCXRD experiment is shown in Figure 2.11, where incident X-rays interact with a single crystal to produce diffracted beams that are detected and used for structure determination.

Crystals were obtained under two crystallisation conditions, at 0 °C and –20 °C, in order to examine the influence of temperature on crystal quality. Crystals suitable for analysis were selected under an optical microscope based on size, shape and optical clarity.

Data were collected at 150 K to reduce thermal effects during structure determination. Measurements were obtained using a Rigaku XtaLAB Synergy-R diffractometer fitted with a HyPix-Arc 150 detector. Mo Kα radiation (λ = 0.71073 Å) generated from a micro-focus sealed X-ray source operating at 50 kV and 24 mA was used. Data processing was carried out using the CrysAlisPro software package, and structure solution and refinement were carried out with Olex 2.[23]

Refinement of the structures showed that the characteristic Keggin-type framework was retained. The atomic arrangement obtained from the single-crystal data was consistent with the results from powder X-ray diffraction and provided additional information on the solid-state structure of silicotungstic acid.

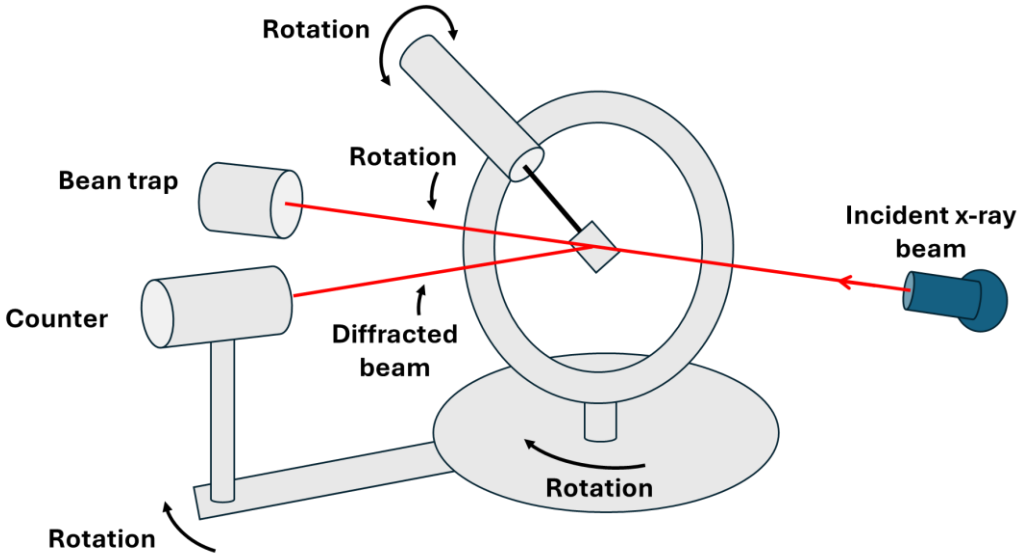


Figure 2.11. Schematic illustration of single-crystal X-ray diffraction experiment, showing interaction of incident X-rays with a single crystal and detection of diffracted beams.

2.6.7 Nuclear Magnetic Resonance (NMR) Spectroscopy

Nuclear magnetic resonance (NMR) spectroscopy formed the main basis for product identification in this study and was used to determine product ratios after extraction, based on ^{1}H NMR peak integration.[24,25] Spectra of the extracted organic phases dissolved in $CDCl_3$ were recorded under identical conditions to allow direct comparison. The product identities suggested by NMR were

compared with results from GC-MS and FT-IR analyses. GC-MS data supported compound identification, while FT-IR spectra showed changes in functional groups following reduction.

A nucleus must possess a non-zero spin quantum number (*I*) to be NMR active. This spin generates a magnetic moment (μ).[26] For a nucleus such as ^{1}H (where $I = ½$), when placed in a static magnetic field (B_0) its magnetic moment can adopt one of two discrete orientations relative to the field: a lower-energy state aligned with the field (α state, m = +1/2) and a higher-energy state aligned against the field (β state, m= –1/2). The energy difference (ΔE) between these states is directly proportional to the strength of B_0[26,27] (Figure 2.12).

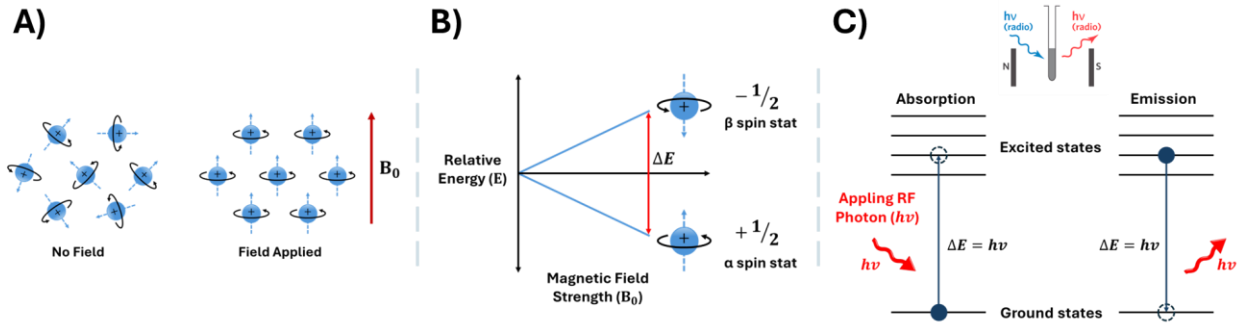


Figure 2.12. A) The NMR resonance condition for a spin -½ nucleus. B) In a static magnetic field (B_0), nuclei populate two energy states (α and β). C) Resonance occurs when the applied RF photon energy (hv) equals the energy difference (ΔE) between states.

When the sample is irradiated with a radiofrequency (RF) pulse that matches this energy gap (the Larmor frequency), nuclei in the lower state can absorb energy and flip to the higher state, this is resonance. After the pulse, the excited nuclei relax back to their original state, emitting RF energy as they do so.

This emitted signal from all the nuclei is called the Free Induction Decay (FID). The FID is a complex signal that decays over time.[24] A mathematical process called a Fourier Transform converts this time-domain FID into the frequency-domain spectrum, giving a plot of signal intensity versus frequency.[24,28]

Interpreting the Spectrum: Chemical Shift and Coupling

The position of a signal in the spectrum is called its chemical shift (δ). It provides information about the chemical environment of the proton. Electrons around a nucleus create a small magnetic field that opposes B_0, shielding the nucleus. The amount of shielding depends on the electron density.[24]

- **Deshielded protons** (e.g., next to an oxygen atom) have less electron density, feel more of B_0, resonate at a higher frequency, and appear on the left (down field) side of the spectrum.
- **Shielded protons** (e.g., in a methyl group) have more electron density, are better shielded, resonate at a lower frequency, and appear on the right (up field) side of the spectrum (Figure 2.13).

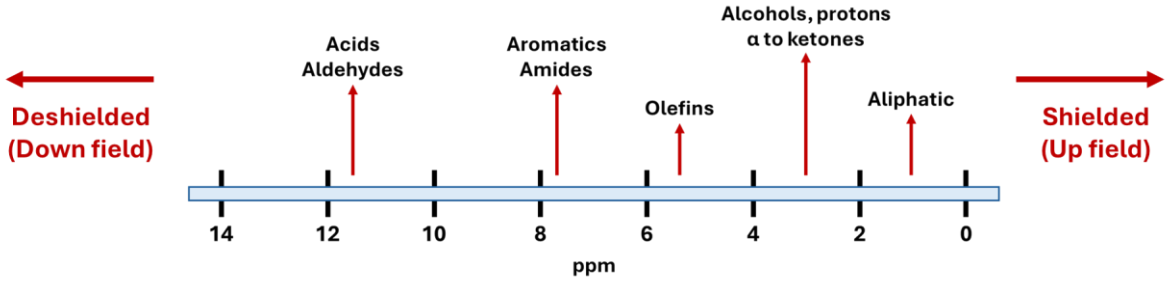


Figure 2.13. Characteristic ^{1}H NMR chemical-shift ranges for common proton environments (e.g., alcohol, aldehyde) in ppm.

To allow direct comparison of spectra acquired on different spectrometers, chemical shift values (δ) are reported on a universal, dimensionless scale in parts per million (ppm), which is defined relative to a standard reference.[26] In the experiments described herein, the proton signal from residual $CHCl_3$ in the $CDCl_3$ solvent (δ = 7.26 ppm) was designated as the internal reference for all ^{1}H NMR measurements.

Protons can also interact with their neighbours through bonds, a phenomenon called spin-spin coupling or *J*-coupling. In simple cases, the resulting splitting pattern often follows the familiar $n+1$ peaks. This is illustrated in Figure 2.14 using a J-coupling splitting tree, showing how doublets and triplets arise from neighbouring proton interactions. The pattern and spacing (J in Hz) provide crucial information about how atoms are connected in the molecule.[28]

Quantitative Analysis by ^{1}H NMR

In this work, quantification of product ratios was based on the integration of characteristic proton signals in the ^{1}H NMR spectra.[24] For each compound (starting material and products), a single, well-resolved peak corresponding to a known number of protons (H) was selected.

The mole ratio between ant two components, A and B, was calculated using the relationship:

$$\frac{n_A}{n_B} = \frac{I_A/H_A}{I_B/H_B} \qquad \text{(Equation 2.4)}$$

Where, n_A and n_B are the molar amounts, I_A and I_B are the integrated area of the selected peaks, and H_A and H_B are the number of protons giving rise to those respective signals.

The mole fraction (X) of any component (i) in the mixture was then determined as:

$$X_i = \frac{I_i/H_i}{\sum(I_j/H_j)} \qquad \text{(Equation 2.5)}$$

Where the summation runs over all quantified components (j). This approach accounts for differences in the number of equivalent protons per molecule, allowing for the direct calculation of molar conversions and product distributions.[24]

^{1}H NMR measurements were carried out at 400 MHz. Clear spectral changes were observed between starting materials and products. Integration of distinct proton signals allowed the relative amounts of each product to be determined quantitatively. The product identities derived from ^{1}H NMR integration were consistent with the products observed by GC-MS and FT-IR, together confirming the product distribution resulting from the reduction process.

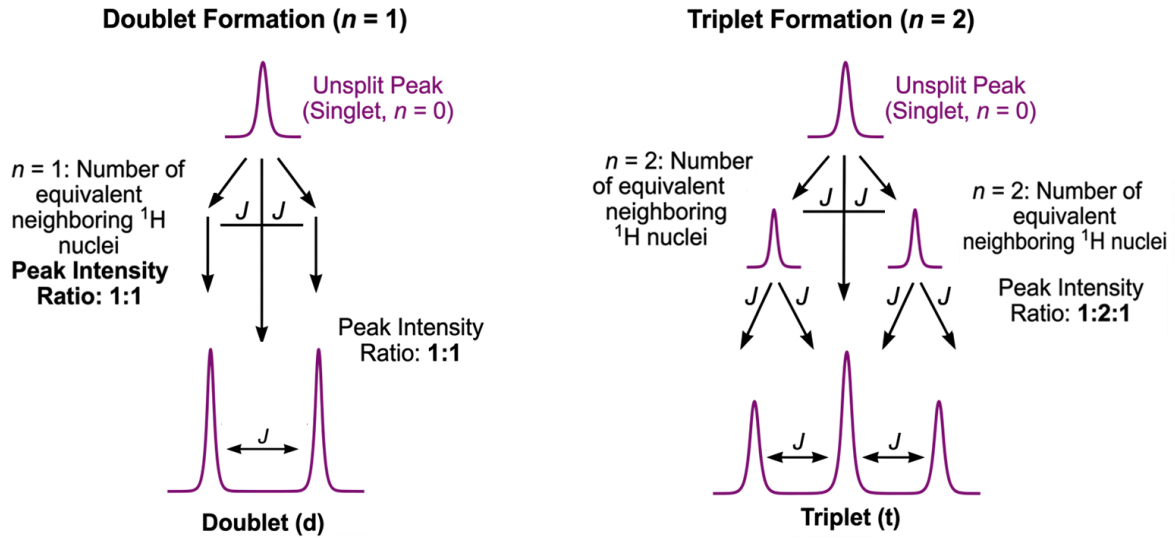


Figure 2.14. J-coupling splitting tree illustrating the n+1 rule in ^{1}H NMR spectroscopy, A proton with one neighbouring proton (n = 1) gives a doublet (1:1), while a proton with two neighbouring protons (n = 2) gives a triplet (1:2:1). Peak separations correspond to the coupling constant, J (Hz).

2.7 References

1 A. J. Bard and L. R. Faulkner, *Electrochemical methods: fundamentals and applications*, John Wiley & Sons, Inc., 2001.

2 N. Elgrishi, K. J. Rountree, B. D. McCarthy, E. S. Rountree, T. T. Eisenhart and J. L. Dempsey, *J. Chem. Educ.*, 2018, **95**, 197–206.

3 C. Schotten, T. P. Nicholls, R. A. Bourne, N. Kapur, B. N. Nguyen and C. E. Willans, *Green Chem.*, 2020, **22**, 3358–3375.

4 G. Inzelt, A. Lewenstam and F. Scholz, eds., *Handbook of reference electrodes*, Springer, 2013.

5 D. Pletcher, *A First Course in Electrode Processes*, The Royal Society of Chemistry, 2009.

6 K. A. Mauritz and R. B. Moore, *Chem. Rev.*, 2004, **104**, 4535–4586.

7 F. Barbir, *Solar Energy*, 2005, **78**, 661–669.

8 Z. Wang, *Electrochemical membrane technology for water and wastewater treatment*, Elsevier, 2022.

9 M. C. Leech, A. D. Garcia, A. Petti, A. P. Dobbs and K. Lam, *React. Chem. Eng.*, 2020, **5**, 977–990.

10 P. T. Kissinger and W. R. Heineman, *J. Chem. Educ.*, 1983, **60**, 702.

11 P. Zanello, *Inorganic electrochemistry: theory, practice and applications*, Royal Society of Chemistry, 2003.

12 C. E. Banks, R. R. Moore, T. J. Davies and R. G. Compton, *Chem. Commun.*, 2004, 1804.

13 C. Gütz, B. Klöckner and S. R. Waldvogel, *Org. Process Res. Dev.*, 2016, **20**, 26–32.

14 M. Faraday, *Philos. Trans. R. Soc. Lond.*, 1834, 77–122.

15 D. Voiry, M. Chhowalla, Y. Gogotsi, N. A. Kotov, Y. Li, R. M. Penner, R. E. Schaak and P. S. Weiss, *ACS Nano*, 2018, **12**, 9635–9638.

16 O. D. Sparkman, Z. E. Penton and F. G. Kitson, *Gas chromatography and mass spectrometry: a practical guide*, Academic Press, 2011.

17 D. A. Skoog, F. J. Holler and S. R. Crouch, *Principles of instrumental analysis*, Thomson Brooks/Cole, 2007.

18 E. de Hoffmann and V. Stroobant, *Mass spectrometry: principles and applications*, J. Wiley, 2007.

19 A. B. D. Nandiyanto, R. Ragadhita and M. Fiandini, *Indones. J. Sci. Technol.*, 2023, **8**, 113–126.

20 A. B. D. Nandiyanto, R. Oktiani and R. Ragadhita, *Indones. J. Sci. Technol.*, 2019, **4**, 97–118.

21 J. D. Menczel and R. B. Prime, *Thermal analysis of polymers*, John Wiley, 2009.

22 R. Jenkins and R. L. Snyder, *Introduction to X-ray powder diffractometry*, Wiley, 1996.

23 O. V. Dolomanov, L. J. Bourhis, R. J. Gildea, J. A. K. Howard and H. Puschmann, *J. Appl. Crystallogr.*, 2009, **42**, 339–341.

24 J. Keeler, *Understanding NMR spectroscopy*, Wiley, 2005.

25 B. Blümich, *Essential NMR: for scientists and engineers*, Springer, 2019.

26 J. W. Akitt and B. E. Mann, *NMR and Chemistry: an introduction to modern NMR spectroscopy*, CRC Press, 2017.

27 M. Balci, *Basic ^{1}H- and ^{13}C-NMR spectroscopy*, Elsevier, 2005.

28 J. D. Rawn and R. J. Ouellette, *Organic chemistry: structure, mechanism, synthesis*, Academic Press, 2018.

Chapter 3: Controlled Multi-Electron Reduction and Redox Stability of Silicotungstic Acid

This chapter contains expanded and updated sections from the version submitted for publication in RSC Advances, titled: Preparation, characterization and hydrogenation activities of multiply reduced silicotungstic acid.

Synopsis

This chapter examines the electrochemical reduction of silicotungstic acid and its ability to undergo controlled multi-electron redox processes in aqueous solution. The preparation of reduced forms of the mediator beyond two-electron form is described, together with comprehensive electrochemical, structural, and spectroscopic characterisation. The stability, reversibility, and re-oxidation behaviour of the reduced species are evaluated using cyclic voltammetry, controlled potential and galvanostatic bulk electrolysis, chronopotentiometry, hydrogen quantification, UV-visible spectroscopy, powder and single-crystal X-ray diffraction, and thermogravimetric analysis. The combined electrochemical and structural data demonstrate that although deeper reduction (up to 12e^- per Keggin unit) can be achieved under strongly reducing conditions, such regimes are accompanied by hydrogen evolution, membrane crossover, precipitation, and incomplete charge recovery. Fully reversible and structurally stable electron storage is therefore effectively confined to the 2e^- and 4e^- reduced forms under mild electrochemical conditions. These findings define the practical redox stability window of silicotungstic acid and establish the basis for its application as a multi-electron redox mediator in the indirect electrochemical reduction studies presented in the following chapter.

Acknowledgements and Declarations

I would like to sincerely thank Dr Sarah K. Dugmore and Dr Claire Wilson for their assistance with the single-crystal X-ray diffraction measurements and structural refinement. The content of this chapter was initially developed in collaboration with Zeliha Ertekin and my supervisor. Prof. Mark Symes. I am grateful for their valuable input during the early stages of the work. Any sections not authored by me in the original collaborative manuscript have been either omitted or substantially rewritten, and the work presented in this chapter represents my own independent research and analysis.

Abstract

Silicotungstic acid ($H_4SiW_{12}O_{40}$) is a commercially available, well-established Keggin-type polyoxometalate that has been employed as a redox mediator in indirect electrochemical hydrogenation reactions in its two-electron reduced form.[1] Although silicotungstic acid is known to undergo multiple sequential electron-transfer processes,[2] controlled electrochemical access to more deeply reduced states, together with their stability, reversibility, and characterisation under aqueous acidic conditions, has received limited systematic investigation.[3,4]

In this chapter, the electrochemical reduction of silicotungstic acid beyond the conventional two-electron form is examined under acidic aqueous conditions. Experimental approaches for generating multi-electron reduced forms of silicotungstic acid are described, and their redox behaviour is characterised using cyclic voltammetry and bulk electrolysis. UV–visible spectroscopy is employed to probe the electronic structure of reduced silicotungstic acid species in both solution and solid form, while re-oxidation processes are examined electrochemically. Structural and compositional integrity are evaluated using powder and single-crystal X-ray diffraction and thermogravimetric analysis, and competing hydrogen evolution during bulk electrolysis is monitored by gas chromatography analysis of the H-cell headspace. Particular attention is given to identifying conditions under which deeper reduction can be achieved without precipitation, electrode degradation, or significant hydrogen evolution.[3,4]

Under the electrochemical conditions employed in this work, silicotungstic acid can be reduced reproducibly to the $2e^-$ and $4e^-$ forms with essentially complete charge recovery, demonstrating reversible redox behaviour and structural stability within this regime. Although further electron uptake up to $12e^-$ per Keggin unit is accessible under more strongly reducing or higher current conditions, these deeper reduced forms exhibit diminished reversibility, increased hydrogen evolution, membrane crossover effects, precipitation, and incomplete charge recovery upon re-oxidation. Comparative potentiostatic experiments at −0.55 V vs NHE further demonstrate that excessively negative potentials promote structural instability even when the electron count corresponds to $4e^-$. These findings define

the practical limits of reversible multi-electron storage in silicotungstic acid and clarify the redox and structural characteristics of its reduced forms,[2,5] thereby establishing a foundation for the indirect electrochemical hydrogenation reactions examined in the subsequent chapter.

3.1 Introduction

In this chapter, the electrochemical reduction of silicotungstic acid beyond the conventional two-electron form is examined under acidic aqueous conditions. The experimental parameters required to access multi-electron reduced forms are established, and the resulting species are characterised using cyclic voltammetry, UV–visible spectroscopy, and electrochemical re-oxidation studies. Structural information is obtained from powder and single-crystal X-ray diffraction, while thermogravimetric analysis probes mass and thermal behaviour associated with reduction. Gas chromatography is additionally employed to analyse the H-cell headspace during bulk electrolysis in order to quantify competing hydrogen evolution.

Electrochemically generated redox mediators provide an alternative approach to hydrogenation reactions in which reducing equivalents are transferred indirectly, rather than via direct electron transfer at the electrode surface.[6,7] In such mediated systems, a soluble redox-active species is first reduced electrochemically and subsequently reacts with a substrate in solution.[7] By decoupling the electrochemical and chemical steps, this approach can suppress unselective electrode reactions, minimise electrode passivation, and enable transformations to proceed under comparatively mild conditions.[6] Polyoxometalates (POMs) are well suited to mediated electrochemical systems owing to their ability to undergo reversible multi-electron redox processes while largely preserving their structural integrity.[7,8]

Silicotungstic acid ($H_4SiW_{12}O_{40}$) is a well-known Keggin-type polyoxometalate that has been widely employed as a redox mediator in aqueous electrochemical systems.[1,9] Its strong Brønsted acidity, high solubility in water, and well-defined electrochemical behaviour make it particularly suitable for operation under acidic conditions.[8,9] Most previous studies have focused on the two-electron reduced form of silicotungstic acid, which can be generated reversibly and has been shown to mediate hydrogen

transfer to a range of organic functional groups.[1,10] In particular, two-electron reduced silicotungstic acid can selectively reduce nitroarenes to the corresponding anilines under mild conditions without the use of molecular hydrogen, elevated temperatures, or additional co-catalysts,[1,10] demonstrating its effectiveness as an indirect electrochemical hydrogenation mediator.[6,11]

Beyond the two-electron reduced form, silicotungstic acid is capable of undergoing further sequential electron-transfer processes.[2] Electrochemical studies of Keggin-type tungstates indicate that additional reduction can occur under sufficiently cathodic conditions, producing species containing mixtures of W^{6+}, W^{5+}, and W^{4+} centres.[2,12] While the initial reduction steps are only weakly dependent on proton activity, subsequent reductions are strongly proton coupled and sensitive to solution pH.[2,5] Under more extreme reducing conditions, highly reduced species, commonly termed tungsten blues, browns, and reds may form. However, achieving controlled access to these deeper reduced forms without mediator degradation, hydrogen evolution, or structural transformation remains a significant experimental challenge, an issue systematically examined in this chapter.[3,4]

Despite extensive interest in silicotungstic acid as a redox mediator, the controlled preparation, stability, and reversibility of multi-electron reduced forms under mild aqueous electrochemical conditions remain insufficiently understood.[3,4] Addressing these questions is important because variations in electron and proton storage are expected to influence the reducing behaviour, efficiency, and practical applicability of the mediator.[5]

The hypothesis investigated in this chapter was that silicotungstic acid could access well-defined multi-electron reduced states beyond the conventional two-electron form while retaining electrochemical reversibility and structural integrity. The rationale was therefore to systematically investigate the extent of electron storage in silicotungstic acid and establish the practical reduction window within which stable and reversible reduced forms could be generated.

A conceptual overview of the electrochemical reduction and subsequent characterisation of silicotungstic acid is shown in Figure 3.1.

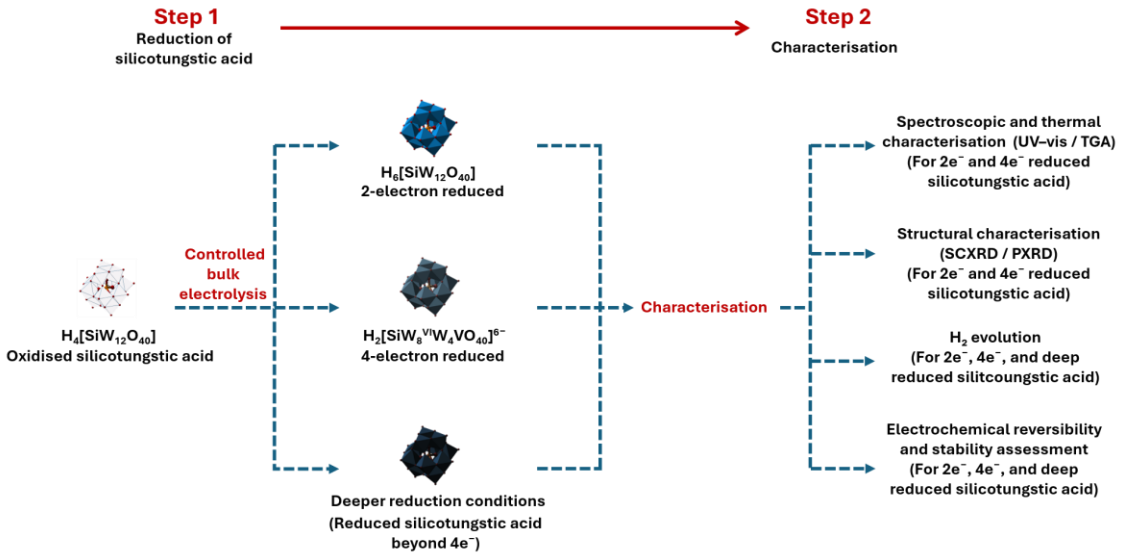


Figure 3.1. Conceptual overview of the electrochemical reduction of silicotungstic acid and the subsequent characterisation and assessment of the reduced forms.

The overall objective of this chapter is therefore to define the stability, reversibility, and structural integrity of multi-electron reduced silicotungstic acid species and to determine the practical limits of reversible electron storage within the Keggin framework.[3,4] These results establish the fundamental redox characteristics of reduced silicotungstic acid and provide the foundation for evaluating its hydrogen transfer reactivity in the following chapter.

3.2 Experimental Methods

3.2.1 Materials and Reagents

Silicotungstic acid (tungstosilicic acid hydrate, $H_4SiW_{12}O_{40}\cdot xH_2O$, reagent grade) was used as received without further purification. Unless stated otherwise, electrolyte solutions were prepared using 1.0 M aqueous phosphoric acid (Fisher Scientific, 85%). Nafion® 117 membranes were employed as separators between the catholyte and anolyte compartments in bulk electrolysis experiments; prior to use the membranes were preconditioned by immersion in 1.0 M sulfuric acid for 24 h. Deionised water was used for all solution preparation, and dissolved gases were removed by purging with nitrogen before electrochemical measurements.

3.2.2 Electrochemical Setup and Procedures

Electrochemical measurements were conducted using the equipment and experimental arrangements described in Chapter 2. Cyclic voltammetry, chronoamperometry, and bulk electrolysis experiments were performed under potentiostatic control using a Gamry Reference 1010E potentiostat. Chronopotentiometric measurements were conducted to monitor the electrode potential under constant-current conditions during extended reduction. While the Gamry Reference 1010E was used for most experiments, its software did not permit real-time logging of cumulative charge during galvanostatic operation. Therefore, a BioLogic SP-150 potentiostat was employed for chronopotentiometry, as its software allowed for continuous recording of both potential and passed charge, enabling accurate coulometric tracking and stability assessment over prolonged electrolysis periods.

Cyclic voltammetric measurements were conducted in single-compartment electrochemical cells operated at room temperature (≈20 °C) using a three-electrode configuration. Data were recorded with a Gamry Reference 1010E potentiostat at a scan rate of 100 mV s^{-1}, without stirring and without iR compensation. Electrolyte solutions (10 mL) were degassed with nitrogen for 15 minutes prior to measurement and maintained under an inert atmosphere throughout the experiments. Electrochemical reactions occurred at a glassy carbon disc working electrode (geometric area = 0.071 cm^2), with a platinum wire serving as the counter electrode. All electrode potentials were recorded relative to an Ag/AgCl reference electrode (3 M NaCl) and are reported vs the normal hydrogen electrode (NHE). The working electrode surface was refreshed prior to each measurement following the cleaning protocol outlined in Chapter 2.

Bulk electrolysis experiments were performed in a two-compartment H-cell incorporating a Nafion® 117 proton-exchange membrane to separate the anodic and cathodic chambers. The cathodic compartment contained a 0.5 M aqueous solution of silicotungstic acid and was equipped with a carbon felt working electrode (2.5 × 4.0 cm^2) together with an Ag/AgCl reference electrode. The anodic compartment contained 1.0 M aqueous phosphoric acid (pH ≈ 0.5) and a platinised titanium electrode, which served as the counter electrode. All bulk reduction experiments were performed under continuous

inert-gas purging to minimise oxidative degradation of reduced species and to limit competing hydrogen evolution reactions. Following electrolysis, reduced silicotungstic acid solutions were transferred under nitrogen to airtight vials for subsequent spectroscopic and analytical characterisation.

3.2.3 Spectroscopic and Structural Characterisation

UV-visible spectra of solution-phase silicotungstic acid samples were recorded over the range 200-800 nm using an Agilent Cary 60 UV-visible spectrophotometer. Solid-state UV-visible measurements were performed over the range 200-1300 nm using a Shimadzu UV-2600 spectrophotometer in diffuse reflectance mode. Solid samples were prepared by drop-casting reduced silicotungstic acid solutions onto quartz substrates and drying under a nitrogen atmosphere prior to analysis.

Fourier-transform infrared (FT-IR) spectra were recorded in the solid form using attenuated total reflectance (ATR) mode. Oxidised and electrochemically reduced samples were isolated by removal of water from aqueous solutions under reduced pressure at room temperature using a rotary evaporator. The resulting solids were further dried under a nitrogen atmosphere prior to analysis to minimise air oxidation. Spectra were collected at room temperature over the range 4000–600 cm^{-1}.

Crystalline samples of silicotungstic acid, before and after electrochemical reduction, were analysed by powder X-ray diffraction. Measurements were performed with a Rigaku MiniFlex instrument employing Cu-Kα radiation, operated at 40 kV and 15 mA. Samples were prepared under conditions designed to minimise exposure to air prior to analysis.

Single-crystal X-ray diffraction was performed on selected samples to obtain detailed information on the solid-state structure of the reduced material. Single-crystal diffraction data were acquired at 150 K using a Rigaku XtaLAB Synergy-R diffractometer equipped with a Mo-Kα radiation source. Data processing and structural refinement were carried out following standard crystallographic procedures.

Thermal mass-loss behaviour of electrochemically reduced silicotungstic acid was investigated using a TA Instruments Discovery TGA-550 thermogravimetric analyser. Measurements were conducted under

a continuous nitrogen flow, with the temperature increased from ambient to 600 °C at a controlled heating rate of 10 °C min^{-1} while monitoring changes in sample mass.

Gas-phase species accumulating in the H-cell during bulk electrolysis were periodically removed for analysis to determine whether hydrogen was formed. Chromatographic separation and detection were achieved on an Agilent 8890 instrument equipped with a thermal conductivity detector and an appropriate column. Fixed volumes of headspace gas (500 μL) were withdrawn using a gas tight syringe and injected into the gas chromatograph. Hydrogen was identified by comparison of retention times with certified reference standards and quantified using external calibration. The resulting data were used to assess the extent of hydrogen evolution as a competing process during electrochemical reduction of the mediator.

3.2.4 Reoxidation Experiments

Reoxidation of reduced silicotungstic acid species was investigated using electrochemical techniques. Following bulk electrolysis or controlled electrochemical reduction, reoxidation was achieved either by reversing the applied potential or by subsequent cyclic voltammetric scans. Changes in current-potential response were monitored in order to assess the reversibility and stability of the reduced species. No spectroscopic methods were employed to monitor reoxidation processes.

3.3 Results and Discussion

3.3.1 Electrochemical reduction of silicotungstic acid

The electrochemical reduction behaviour of silicotungstic acid (STA) was investigated in 1 M H_3PO_4 (pH ≈ 0.5) to define the range of accessible reduced states and to assess their reversibility and stability. Initial studies were carried out using cyclic voltammetry to establish the fundamental redox processes of the Keggin anion. A representative cyclic voltammogram (Figure 3.2) exhibits three well-defined reduction processes, labelled a, b, and c, with formal potentials at −0.043 V, −0.273 V, and −0.450 V vs. NHE, respectively. Processes a and b correspond to successive one-electron reductions of the

polyoxometalate framework, whereas process c involves a proton-coupled two-electron transfer. This sequence of two successive one-electron reductions followed by a proton-coupled two-electron process is consistent with previous electrochemical studies of silicotungstate in acidic aqueous media.[13,14] The potentials and proton-coupling behaviour of these processes are dependent on the acidity and composition of the electrolyte.[13,15] The involvement of protons in this process is consistent with the protonated 4-electron reduced species identified by subsequent structural characterisation, as discussed later in this chapter. While these initial redox processes are established in the literature, the present work focuses on the controlled preparative generation of multiply reduced silicotungstic acid and the systematic evaluation of the reversibility, stability, and structural integrity of the resulting reduced forms.

The literature basis for those additional is strong: Guo et al. describe two successive $1e^-$ reductions followed under acidic conditions by an overall $2e^-/2H^+$ process. They also show explicitly that the behaviour of the third process depends on pH.

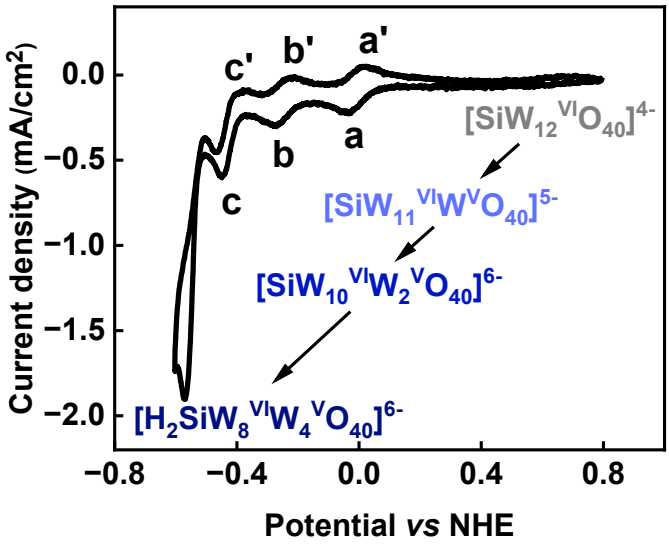


Figure 3.2. The cyclic voltammogram of 50 mM silicotungstic acid in water was obtained using a glassy carbon electrode (0.071 cm^2) as the working electrode, with platinum wire and Ag/AgCl serving as the counter and reference electrodes, respectively. Measurements were carried out at 100 mV s^{-1} over the potential interval 0.8 to −0.6 V relative to NHE. The labels correspond to the oxidised form and successive 1-, 2-, and 4-electron reduced Keggin species.

The corresponding anodic peaks observed on the reverse scan indicate near-reversible electrochemical behaviour, with peak separations ($\Delta E_p \approx 60$ mV) consistent with near-reversible one-electron processes for the first two reductions. The third reduction step, which involves a proton-coupled multi-electron transfer, deviates from ideal Nernstian behaviour. These redox transformations can be described by the sequential reactions given in Equations (3.1–3.3).

$$[SiW_{12}{}^{VI}O_{40}]^{4-} + e^- \rightleftharpoons [SiW_{11}{}^{VI}W^{V}O_{40}]^{5-} \quad \text{Equations 3.1}$$

$$[SiW_{11}{}^{VI}W^{V}O_{40}]^{5-} + e^- \rightleftharpoons [SiW_{10}{}^{VI}W_2{}^{V}O_{40}]^{6-} \quad \text{Equations 3.2}$$

$$[SiW_{10}{}^{VI}W_2{}^{V}O_{40}]^{6-} + 2e^- + 2H^+ \rightleftharpoons H_2[SiW_8{}^{VI}W_4{}^{V}O_{40}]^{6-} \quad \text{Equations 3.3}$$

The initial one-electron reduction of $[SiW_{12}{}^{VI}O_{40}]^{4-}$ produces the mixed-valence species $[SiW_{11}{}^{VI}W^{V}O_{40}]^{5-}$ and is accompanied by the development of a faint blue colouration in solution. Further reduction to the 2-electron reduced species $[SiW_{10}{}^{VI}W_2{}^{V}O_{40}]^{6-}$ leads to a pronounced intensification of the blue colour. The third reduction step involves transfer of two electrons and two protons to yield the 4-electron reduced species $H_2[SiW_8{}^{VI}W_4{}^{V}O_{40}]^{6-}$, generating a deep blue solution characteristic of intervalence charge-transfer transitions within the reduced tungsten oxide framework.

Controlled bulk electrolysis was employed to access these reduced forms in a preparative and quantitative manner using a divided H-cell. Current-time responses recorded during potentiostatic electrolysis at −0.36 V vs NHE (Figure 3.3) show sustained cathodic currents for both the 2-electron and 4-electron reduction processes, whereas a control experiment conducted in the absence of silicotungstic acid exhibits only negligible background current. The initially high cathodic current decreases rapidly as electrolysis proceeds, consistent with depletion of silicotungstic acid at the electrode surface. The subsequent sustained current reflects continued reduction as stirring promotes transport of silicotungstic acid from the bulk solution to the electrode surface.

The corresponding charge-time plots (Figure 3.4) demonstrate that the total charge passed during electrolysis closely matches the theoretical values required for complete $2e^-$ and $4e^-$ reduction

(approximately 2895 C and 5789 C, respectively). The theoretical charge required for each reduction state was calculated using Faraday's law:

$$Q = znF \qquad \text{Equations 3.3}$$

where z is the number of electrons transferred per silicotungstic acid cluster, n is the amount of silicotungstic acid, and F is the Faraday constant (96,485 C mol^{-1}). For 30 mL of 0.5 M silicotungstic acid, the amount of silicotungstic acid was:

$$n = CV = (0.5\ ml\ L^{-1})(0.030\ L) = 0.015\ mol$$

Therefore, the theoretical charges required for the 2e$^-$ and 4e$^-$ reductions were:

$$Q_{2e^-} = 2(0.015)(96{,}485) = 2895\ \text{C}$$

$$Q_{4e^-} = 4(0.015)(96{,}485) = 6789\ \text{C}$$

In both cases, the charge recovered during the subsequent oxidation step closely matches that passed during reduction (see Figure 3.26), confirming quantitative reversibility of electron transfer up to the 4-electron reduced form.

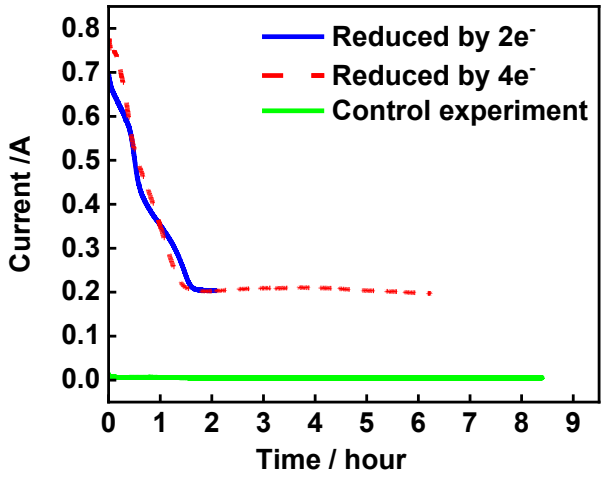


Figure 3.3. Current-time responses recorded during controlled-potential electrolysis at −0.36 V vs NHE in a divided H-cell. Traces correspond to the 2-electron reduction of 30 mL of 0.5 M silicotungstic acid (blue), the 4-electron reduction under identical conditions (red), and a control experiment containing only 1 M phosphoric acid electrolyte (green). Sustained cathodic currents in the presence of silicotungstic acid confirm bulk electrochemical reduction of the mediator, whereas the negligible current in the control indicates minimal background activity.

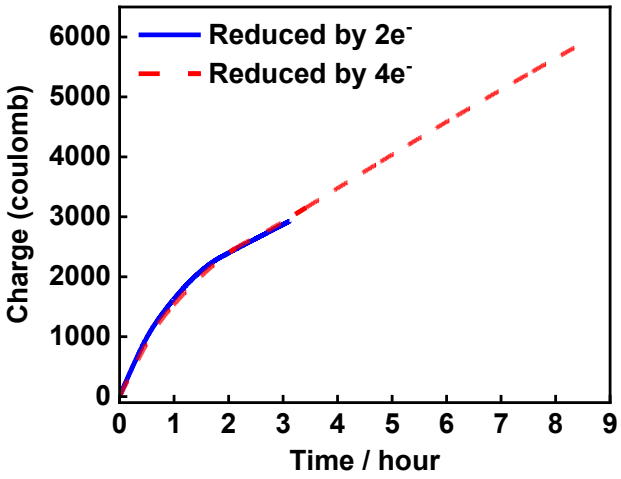


Figure 3.4. Charge passed as a function of electrolysis time corresponding to the current–time data shown in Figure 3.3. The blue solid line represents the 2-electron reduction, while the red dashed line represents the 4-electron reduction. The experimentally measured charges show good agreement with the theoretical charges required for complete 2-electron (2895 C) and 4-electron (5789 C) reduction.

The reversibility of the 4-electron reduced form was further verified by potentiostatic reduction at −0.36 V vs NHE followed by subsequent anodic re-oxidation at +0.76 V vs NHE. Quantitative recovery of the delivered charge confirms that the 4-electron reduced form remains fully electrochemically reversible under these conditions and provides direct experimental validation of structural integrity within this reduction regime.

Consistent with this electrochemical reversibility, the solution returned to colourless following re-oxidation of the 4-electron reduced species, consistent with restoration of the original silicotungstic acid. Under galvanostatic reduction to approximately 6-electron reduced at −100 mA, the solution similarly exhibited a blue colour during reduction and returned to an almost colourless form upon re-oxidation, indicating substantial reversibility under controlled current conditions Figure 3.5.

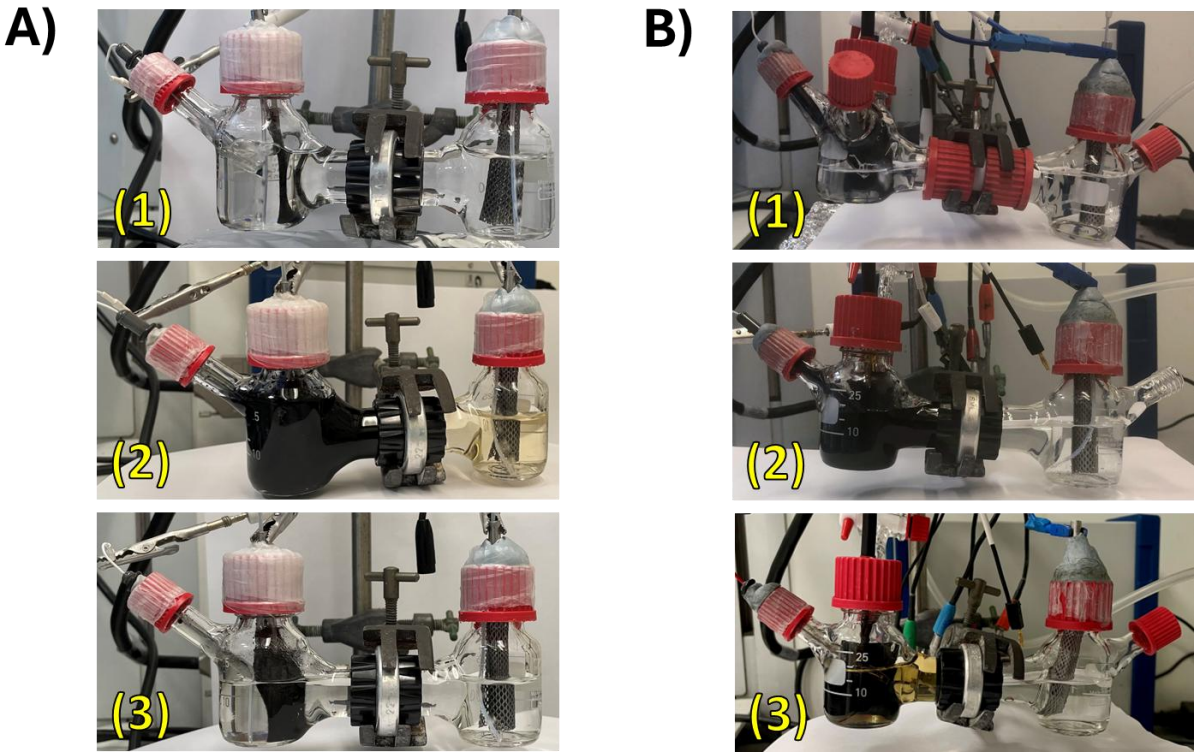


Figure 3.5. Visual evidence of reduction and reoxidation of silicotungstic acid in H-cell. (A) Potentiostatic 4-electron reduction at −0.36 V vs NHE produces a deep blue solution that returns to colourless upon reoxidation at +0.76 V vs NHE, confirming reversible redox cycling. (B) Galvanostatic reduction to approximately 6-electron reduced at −100 mA similarly yields a blue solution that largely returns to colourless after re-oxidation, indicating substantial electrochemical reversibility under controlled conditions.

To examine the influence of applied potential on structural stability, a separate experiment was performed in which silicotungstic acid was reduced potentiostatically at −0.55 V vs NHE to a 4-electron level, followed by re-oxidation at +0.95 V vs NHE. The reduction process was monitored by charge−time and current−time measurements (Figure 3.5. A,B). Although the total charge passed corresponded approximately to four electron equivalents per Keggin unit, visible precipitate formation was observed during reduction.

Upon subsequent re-oxidation (Figure 3.7. A,B), the solution did not return to its original colourless state but remained slightly turbid with a light brown appearance, indicating incomplete restoration of the oxidised form despite the strongly anodic potential applied. The current−time response during re-oxidation also differed from that observed for the −0.36 V experiment, suggesting partial irreversibility.

This is further supported by the charge balance, as the total charge recovered during re-oxidation (3554 C) is lower than passed during reduction (3860 C), corresponding to approximately 92% charge recovery and indicating incomplete electrochemical reversibility under these conditions.

The persistence of a brown colour after re-oxidation suggests the formation of reduced or structurally modified species that are not fully converted back to the parent Keggin anion. In polyoxometalate systems, deep reduction is known to be coupled to proton uptake, leading to structural reorganisation of the framework, including changes in coordination environment and, in some cases, formation of metal-metal bonded reduced species.[11]

These processes can result in chemically altered species that are not fully re-oxidised to the original colourless W(VI) state, thereby explaining both the residual colour and the observed partial irreversibility. These results indicate that although a 4e⁻ reduction can be achieved at −0.55 V, the more negative potential promotes competing processes and structural instability. Applying a milder potential for a longer duration therefore better preserves the system compared to applying a more negative potential for a shorter time.

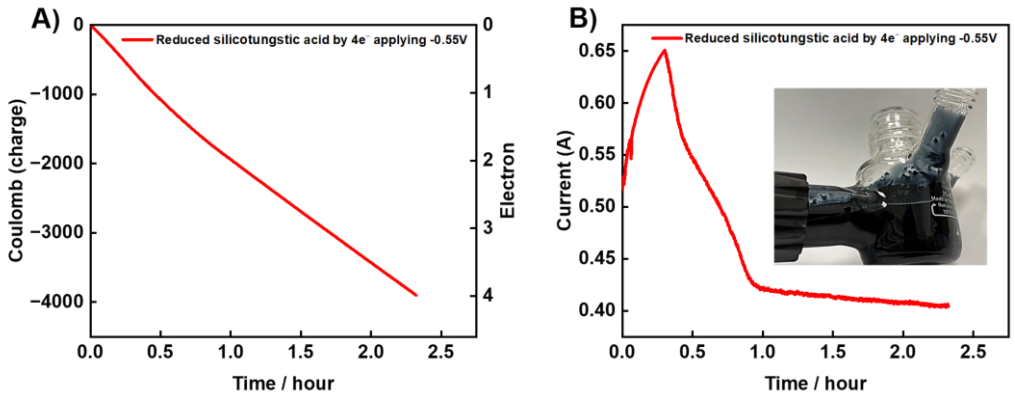


Figure 3.6. (A) Charge−time and (B) current−time profiles recorded during potentiostatic reduction of 0.5 M silicotungstic acid at −0.55 V vs NHE to a 4-electron level.

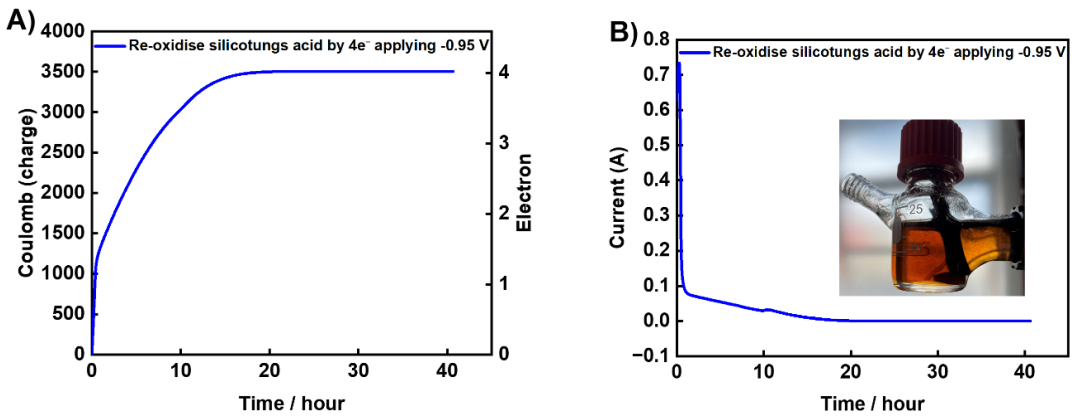


Figure 3.7. (A) Charge−time and (B) current-time profiles recorded during subsequent re-oxidation at +0.95 V vs NHE. Incomplete charge recovery and altered current response indicate partial irreversibility under these conditions.

Long-term electrolysis experiments were conducted to probe the stability of silicotungstic acid under sustained reducing conditions. Continuous electrolysis over eight days (Figure 3.8) resulted in the passage of approximately 17-electron equivalents per initial silicotungstic acid cluster. A brown precipitate was observed following the prolonged eight-day electrolysis, providing additional evidence of irreversible chemical transformation under these strongly conditions. This value represents the total charge passed and does not necessarily correspond to formation of a discrete 17-electron reduced silicotungstic acid species, as competing cathodic processes, including hydrogen evolution, may contribute to the charge passed during prolonged electrolysis. However, subsequent re-oxidation recovered only around 3-electron equivalents. The large difference between the charge passed during reduction and that recovered during re-oxidation demonstrates that the prolonged reduction process is not fully reversible, with a substantial proportion of the charge being consumed by competing and irreversible processes rather than stored reversibly within the silicotungstate framework. This pronounced loss of reversibility indicates irreversible chemical transformation during deep reduction, most plausibly arising from degradation of the Keggin framework together with competing side processes such as proton-induced structural distortion, formation of reduced tungsten-oxide species, and hydrogen evolution.

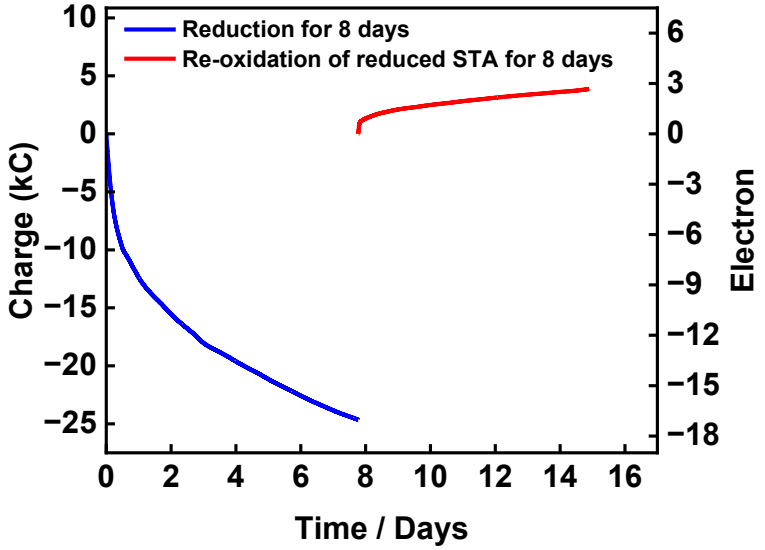


Figure 3.8. Charge–time profile for a 0.5 M aqueous silicotungstic acid electrolyte subjected to electrolysis at −0.36 V versus the normal hydrogen electrode for eight days, followed by re-oxidation at +0.76 V versus the normal hydrogen electrode. The reduction and re-oxidation charges were integrated separately, with the charge referenced to zero at the beginning of each electrolysis step. Therefore, the apparent discontinuity between the two traces does not represent a temporal gap between the experiments. The electrochemical measurements employed a compartment-separated H-type cell operated under inert gas at ambient temperature, incorporating carbon felt, platinized titanium, and Ag/AgCl electrodes as the working, counter, and reference electrodes, respectively. The results demonstrate only partial recovery of charge after extensive reduction.

Cyclic voltammograms recorded after bulk electrolysis provide additional confirmation of the formation of a distinct reduced form (Figure 3.9). Although peak positions and current magnitudes differ from those of the fully oxidised species, the voltammetric responses of the 2-electron and 4-electron reduced forms remain largely reversible, supporting retention of the Keggin structure following reduction within this regime.

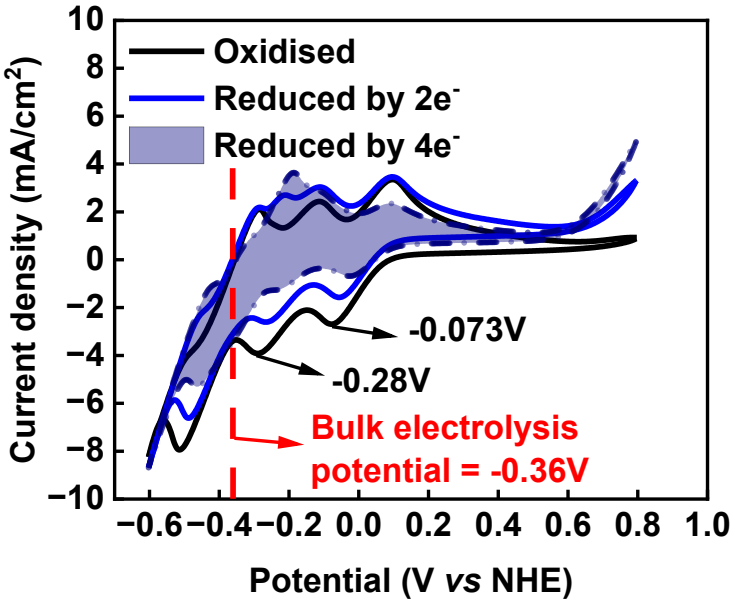


Figure 3.9. Cyclic voltammograms of silicotungstic acid recorded in the fully oxidised form and after electrochemical reduction to the 2-electron and 4-electron forms. Measurements are conducted using the same electrode configuration as in Figure 3.1 at a scan rate of 100 mV s^{-1}, illustrating the changes in redox response associated with progressive reduction while retaining electrochemical reversibility up to the 4-electron form.

Reduction beyond 4-electron regime was investigated using galvanostatic control to mitigate the slow electrolysis and membrane crossover observed under mild potentiostatic conditions. Under these conditions, the applied current drives the working electrode to more negative potentials than those required for 4-electron reduction, enabling access to more deeply reduced states. Application of cathodic currents allowed delivery of higher charge within shorter electrolysis times, delaying the onset of hydrogen evolution.

To further probe reduction beyond the 4-electron regime, a dedicated galvanostatic reduction/re-oxidation experiment was performed. Silicotungstic acid was first reduced under a constant cathodic current of −100 mA until the charge corresponding to approximately 6 electrons per Keggin unit had been delivered. The current direction was subsequently reversed, and anodic oxidation was carried out at +100 mA for a corresponding charge.

Under galvanostatic conditions, charge was passed during both the reduction and subsequent oxidation steps (Figure 3.10. A, B). However, this charge balance alone does not demonstrate electrochemical reversibility, since the potentiostat adjusts the potential to maintain the applied current and the recovered charge may arise from oxidation of chemically altered species rather than regeneration of the original reduced silicotungstic acid. Additional product or structural analysis would therefore be required to establish whether the original Keggin species is restored after deep reduction.

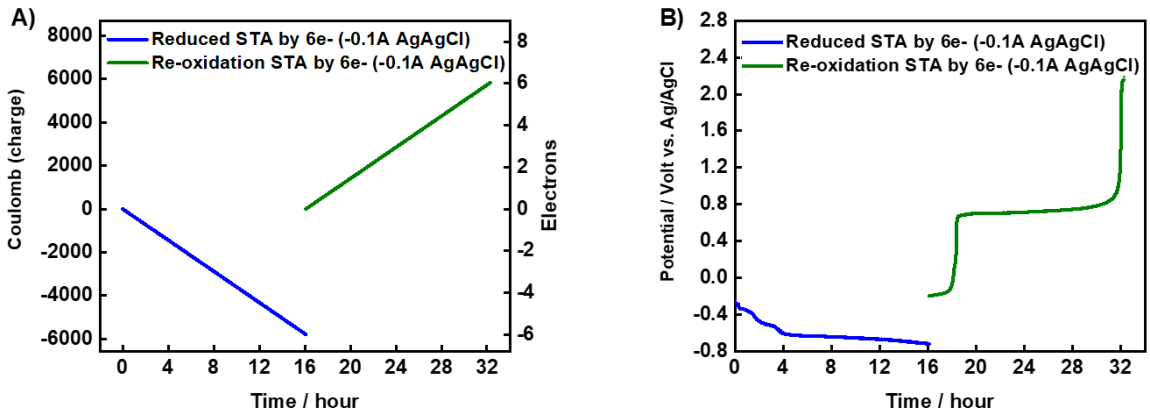


Figure 3.10. (A) Charge–time and (B) potential–time profiles recorded during galvanostatic reduction of 20 mL of 0.5 M silicotungstic acid at −100 mA, followed by anodic re-oxidation at +100 mA. Approximately 6 electrons equivalents per Keggin unit were delivered during the cathodic step. A substantial amount of charge was also passed during the anodic step. However, under galvanostatic conditions, this does not by itself demonstrate electrochemical reversibility, as the recovered charge may arise from oxidation of chemically altered species rather than regeneration of the original reduced silicotungstic acid.

However, this behaviour contrasts with experiments performed at higher driving currents or deeper reduction levels, where incomplete charge recovery, increasing hydrogen evolution, and formation of insoluble blue-brown tungsten-oxide species were observed (Figure 3.11–3.12), indicating the onset of irreversible chemical transformation. As shown in Figure 3.11, the contribution of hydrogen evolution increases markedly beyond approximately 4 electrons per Keggin unit. Direct evidence for hydrogen formation was obtained by gas chromatography (Figure 3.12), which shows a clear H_2 peak at a

retention time of 1.77 min. In addition, red–brown precipitates were observed on the cathode surface following electrolysis under these more aggressive conditions (Figure 3.13), consistent with the formation of reduced tungsten-oxide species.

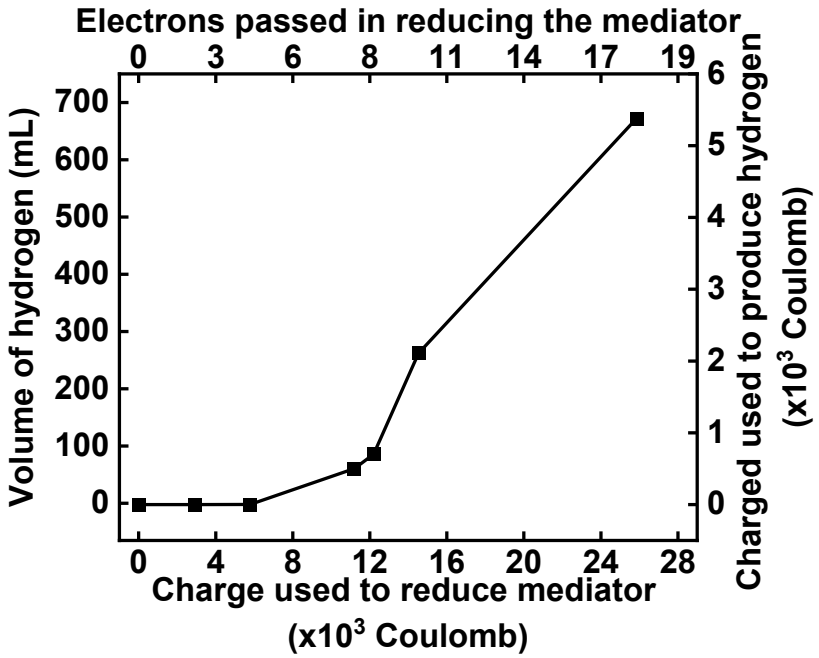


Figure 3.11. Correlation between the total charge passed during electrochemical reduction of 0.5 M silicotungstic acid and the quantity of hydrogen generated. The lower x-axis represents cumulative charge, while the upper axis indicates the estimated number of electrons transferred per molecule. The left y-axis shows the measured hydrogen volume and the right y-axis the corresponding charge associated with hydrogen evolution, highlighting the increasing contribution of hydrogen formation beyond approximately 4 electron per cluster.

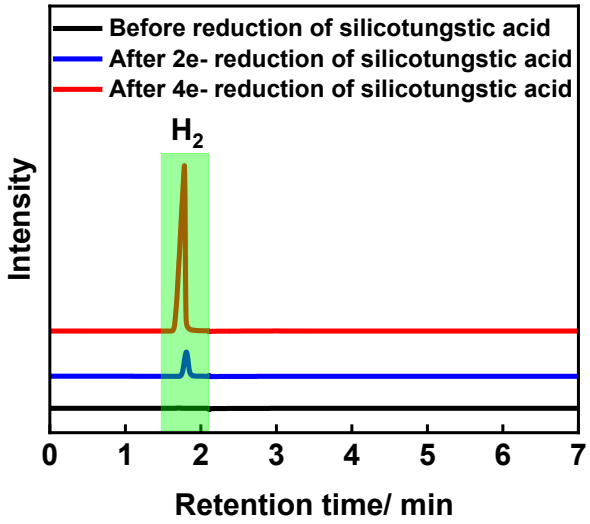


Figure 3.12. Gas chromatogram showing detection of hydrogen during electrochemical reduction of silicotungstic acid (H_2 retention time = 1.77 min), confirming hydrogen evolution under strongly reducing conditions.



Figure 3.13. Red-brown precipitate formed on the cathode side of the H-cell following electrochemical reduction under more aggressive current conditions, consistent with the formation of reduced tungsten-oxide species.

To probe the effect of more aggressive reduction conditions, electrolysis was conducted under galvanostatic control at −300 mA. Under these conditions, rapid charge accumulation was accompanied by significant hydrogen evolution and the formation of brown-red precipitates on the cathode surface, indicating the onset of irreversible chemical transformation (Figure 3.14)

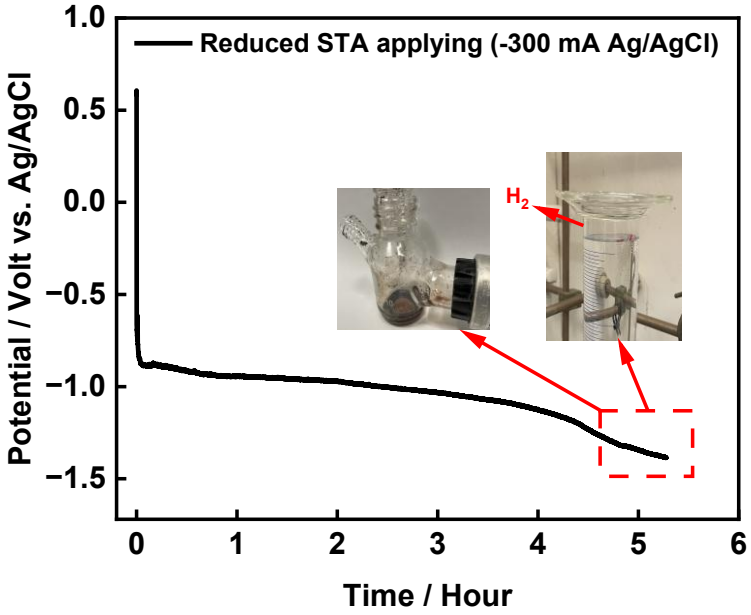


Figure 3.14. Charge-time curves recorded at −300 mA for 20 mL of 0.5 M silicotungstic acid. Inset: Formation of brown-red precipitates on the H-cell cathode after electrolysis, together with the corresponding volume of H_2 evolved. The data illustrate the onset of irreversible chemical transformation and competing hydrogen evolution under high current conditions.

As reduction progressed, increasingly negative electrode potentials were required to sustain electron uptake, reflecting the growing energetic cost associated with further reduction of the polyoxometalate framework. Concurrently, solution colour evolved from deep blue to darker blue-brown hues, consistent with the onset of irreversible chemical change. In contrast to the reversible $2e^-$ and $4e^-$ reduced species, the most highly reduced solution could not be fully re-oxidised, demonstrating progressive loss of electrochemical reversibility.

To evaluate the reversibility of deep reduction, silicotungstic acid was reduced galvanostatically at −100 mA to a 12-electron reduction level based on the total charge passed (Figure 3.15. A, B). During the reduction process, visible hydrogen evolution became pronounced after approximately 9 electron equivalents per Keggin unit, as confirmed by gas accumulation in the measuring cylinder. This behaviour is consistent with the trend observed in Figure 3.11, where hydrogen evolution becomes increasingly significant at higher charge and more negative potentials. Hydrogen evolution under strongly cathodic conditions in the presence of heteropolyoxometalates has also been reported previously.[16] Concomitantly, the potential−time profile exhibited a marked change in slope and a progressive shift to more negative potentials, reflecting the increasing energetic demand for further electron uptake and the onset of competing hydrogen evolution.

Subsequent re-oxidation was performed under galvanostatic control at +100 mA (Figure 3.16. A,B). Based on the total anodic charge recorded, approximately 9 electron equivalents were recovered, within the experimental time window. As the re-oxidation period 24h was shorter that the preceding reduction period 32 h, this does not necessarily reflect complete charge recovery. Nevertheless, the combination of incomplete charge recovery within this timeframe, together with the observed instability in the potential–time response, suggests that a significant fraction of the cathodic charge passed beyond ~9e^- does not correspond to reversibly stored electrons within the Keggin framework. During re-oxidation, membrane crossover effects were observed, leading to instability in the potential−time trace due to electrolyte leakage. This leakage likely disrupted the electrode–electrolyte interface and, together with gas evolution and mechanical disturbance within the cell, resulted in intermittent electrical contact at the electrode connections. These factors further illustrate the practical limitations associated with deep reduction.

Overall, these results indicate that reduction beyond the 4e^- regime becomes progressively inefficient and partially irreversible, with increasing contributions from hydrogen evolution and the formation of reduced tungsten-oxide species.

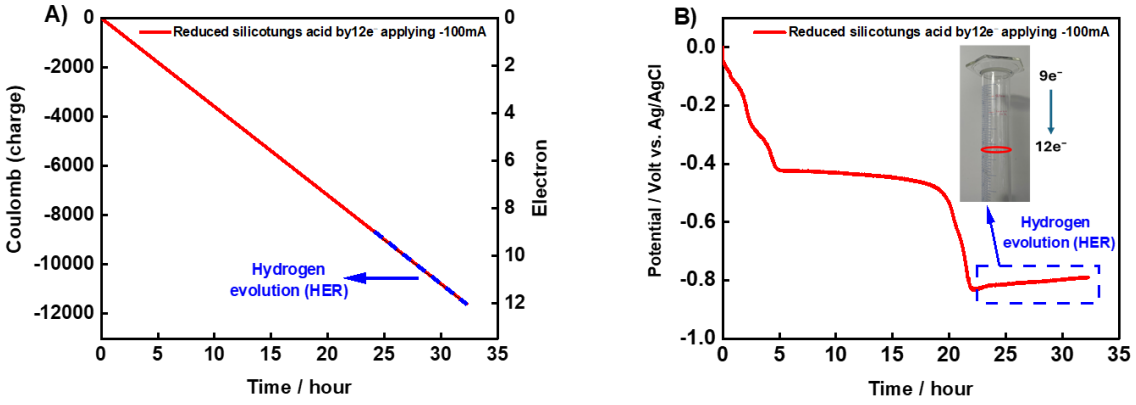


Figure 3.15. (A) Charge−time curve showing cumulative charge passed during galvanostatic reduction of 0.5 M silicotungstic acid at −100 mA to a 12-electron level per Keggin unit. (B) Potential−time profile recorded under the same conditions. The increasingly negative potential and change in slope beyond ~9e⁻ reflect the growing energetic demand for further reduction and correspond with the onset of competing hydrogen evolution.

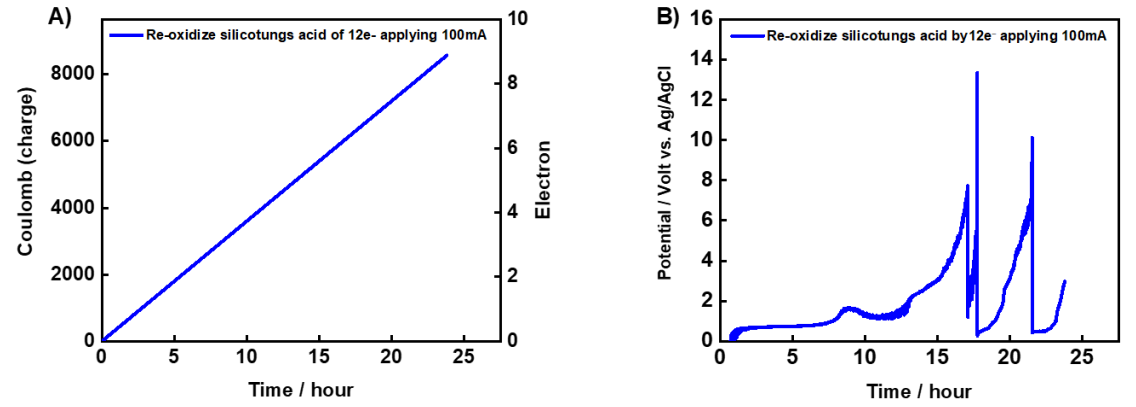


Figure 3.16. (A) Charge−time curve recorded during re-oxidation at +100 mA following 12-electron reduction. Only approximately 9 electron equivalents were recovered within the experimental time window, which was shorter than the preceding reduction period and therefore does not necessarily reflect complete charge recovery. (B) Potential−time profile during re-oxidation. Instabilities in the potential trace arise from membrane crossover and electrolyte leakage observed under deep reduction conditions.

Overall, these results show that although silicotungstic acid can accommodate extensive electron uptake under strongly reducing conditions, practical and reversible electron storage in aqueous acidic media is effectively limited to the $2e^-$ and $4e^-$ reduced forms.

Independent confirmation of these electronically distinct and structurally preserved reduced forms is provided by spectroscopic analysis in the following section.

3.3.2 Spectroscopic evidence of multi-electron reduction

Spectroscopic characterisation was undertaken to provide independent confirmation of the reduced forms of silicotungstic acid (STA) identified electrochemically and to evaluate how progressive electron uptake influences the electronic structure of the Keggin anion. In reduced polyoxometalates, visible colour changes and intervalence charge-transfer (IVCT) absorption bands are well-established indicators mixed-valence metal centres. Accordingly, particular attention was given to solution colour, solid-state appearance, and UV-vis absorption behaviour.

Stepwise electrochemical reduction of silicotungstic acid is accompanied by systematic colour evolution. The fully oxidised species is colourless, whereas formation of the reduced forms produces increasingly intense blue solutions. Reduction to the 4-electron form yields a deep blue colour characteristic of mixed-valence tungsten centres. These colour changes are reversible within the $2e^-$ and $4e^-$ regimes, consistent with the quantitative charge recovery observed electrochemically (Section 3.3.1) and indicating preservation of the Keggin framework under moderate reduction conditions. Photographs of the corresponding lyophilised solids further illustrate the progressive darkening from oxidised to $2e^-$ and $4e^-$ reduced forms (Figure 3.17), consistent with the increasing degree of tungsten reduction.



Figure 3.17. Photograph of silicotungstic acid samples in an X-ray diffraction sample holder showing the white oxidised form together with the blue two-electron and deep-blue four-electron reduced forms. The progressive colour reflects increasing intervalence charge-transfer interactions associated with multi-electron reduction of the Keggin anion.

Electronic absorption spectra of the reduced species provide more direct insight into their electronic structure. Solution-phase UV-vis spectra of the $2e^-$ and $4e^-$ reduced forms were recorded from diluted aliquots of the corresponding electrolysis solutions at a final silicotungstic acid concentration of approximately 11 μM. The spectra exhibit absorption features in the UV region, with maxima at approximately 262 nm and 259 nm for the $2e^-$ and $4e^-$ reduced forms, respectively (Figure 3.18A). These features occur in the UV region and are distinct from the visible-region absorption associated with the characteristic blue colour of the reduced species.

To investigate the absorption associated with this characteristic blue colour, solution-phase spectra were also recorded over an extended wavelength range (Figure 3.18B). For these measurements, the $2e^-$ and $4e^-$ reduced samples were diluted to approximately 0.25 mM and 0.62 mM, respectively. Both reduced species exhibit broad absorption bands in the visible/NIR region, with maxima at approximately 729 nm for the $2e^-$ reduced form and 724 nm for the $4e^-$ reduced form. These broad bands are consistent with intervalence charge-transfer (IVCT) transitions between W(V) and W(VI) centres in the mixed-valence reduced silicotungstate species and are consistent with the characteristic blue colour of the reduced forms. Because the two samples were measured at different concentrations, comparison is

restricted to the positions and general characteristics of the absorption bands rather than their absolute absorbance intensities.

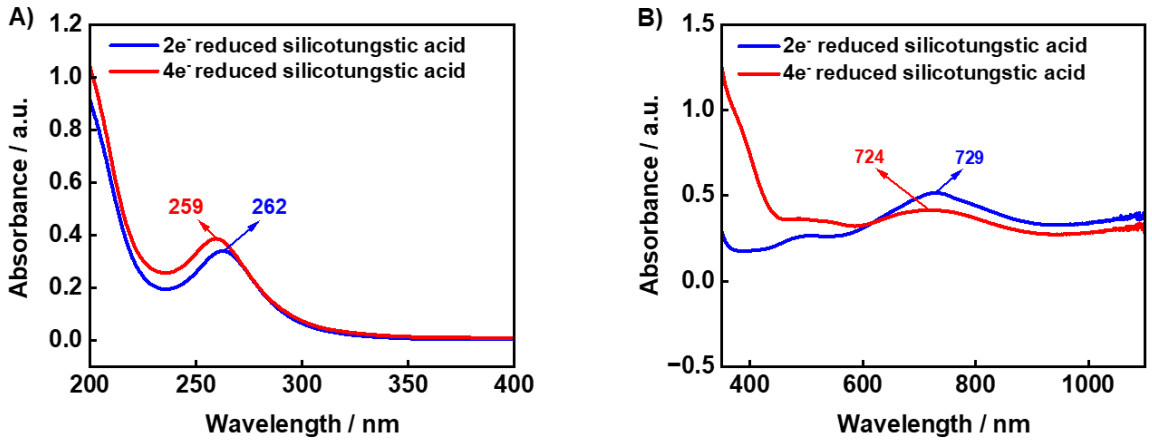


Figure 3.18. Solution-phase UV–vis absorption spectra of reduced silicotungstic acid. A) UV-region spectra of the $2e^-$ and $4e^-$ reduced forms, showing absorption maxima at approximately 262 nm and 259 nm, respectively. B) Extended wavelength spectra of the $2e^-$ and $4e^-$ reduced forms, showing broad visible/NIR absorption bands with maxima at approximately 729 nm and 724 nm, respectively, consistent with intervalence charge-transfer (IVCT) transitions in the mixed-valence reduced species.

More pronounced distinctions are observed in the corresponding solid-state spectra (Figure 3.19). The 2-electron reduced species displays an absorption maximum at approximately 527.5 nm, whereas the 4-electron reduced form exhibits a red-shifted maximum near 549.6 nm. This bathochromic shift indicates a change in the electronic structure of the mixed-valence reduced species as the degree of reduction increases, consistent with the well-established behaviour of reduced Keggin-type polyoxometalates.[17]

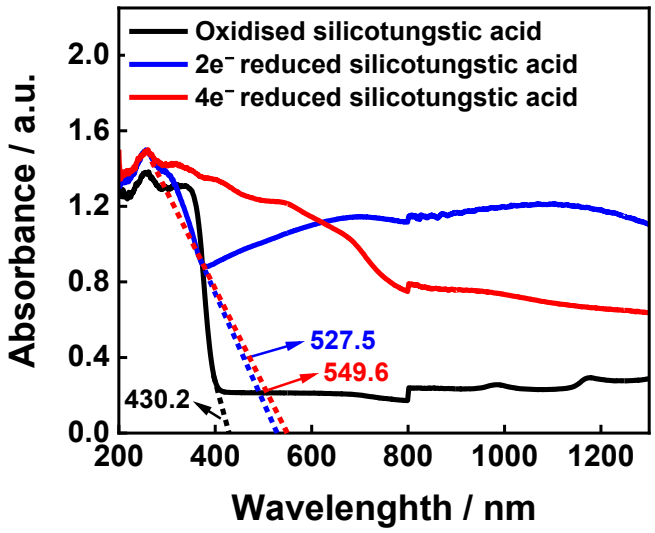


Figure 3.19. Solid-state UV–vis spectra of oxidised silicotungstic acid and the corresponding $2e^-$ and $4e^-$ reduced forms. The reduced species display absorption features at approximately 527.5 nm and 549.6 nm for the $2e^-$ and $4e^-$ reduced forms, respectively.

Complementary vibrational analysis was performed using FT-IR spectroscopy to evaluate structural changes within the Keggin framework upon reduction (Figure 3.20). The oxidised silicotungstic acid displays the characteristic vibrational bands of a Keggin type polyoxometalate, including the Si–O stretching vibrations (~1020−1040 cm^{-1}), the terminal W=O stretching mode (~980 cm^{-1}), and the bridging W–O–W vibrations in the 900–800 cm^{-1} region, consistent with literature reports for Keggin type silicotungstates.[17] Upon reduction to the $2e^-$ form, modest band broadening and slight intensity changes are observed in the W=O and W–O–W regions, consistent with partial reduction of W^{6+} to W^{5+} and minor perturbation of the tungsten–oxygen bonding environment.[18] Further reduction to the $4e^-$ form results in more pronounced broadening of these bands, indicating increased distortion of the metal–oxygen framework. Importantly, the persistence of the diagnostic Si–O, W=O, and W–O–W vibrations suggests retention of the Keggin framework during stepwise multi-electron reduction, in agreement with the well-established redox robustness of Keggin polyoxometalates.[17,18]

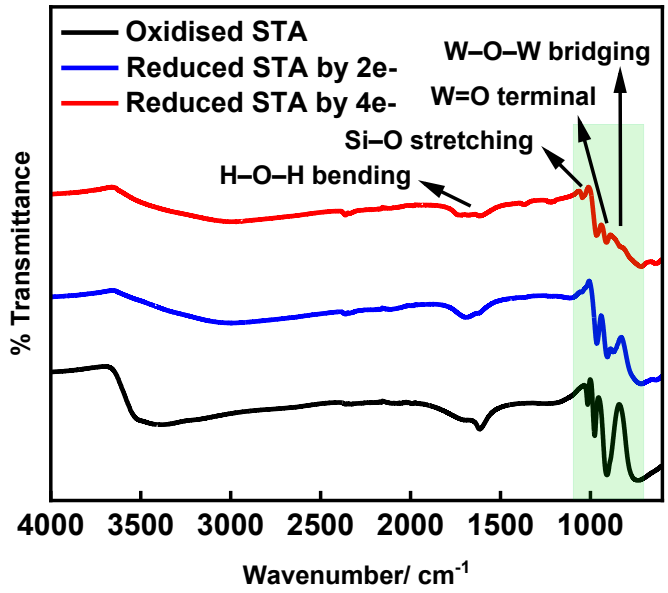


Figure 3.20. FT-IR spectra of oxidised, 2e⁻, and 4e⁻ reduced silicotungstic acid showing progressive broadening of tungsten–oxygen vibrational bands upon reduction while preserving the characteristic Keggin framework features.

Spectroscopic measurements were also performed on the 6-electron reduced form generated under galvanostatic conditions. Comparison of spectra obtained at applied currents of −100 mA and −200 mA revealed only minor differences, with absorption maxima observed at approximately 259 nm and 261 nm, respectively (Figure 3.21). The small magnitude of this shift indicates that the UV absorption features are only weakly affected by the applied reduction current. As these measurements are presented only in the UV region, no conclusions regarding visible/NIR IVCT absorption can be drawn from these spectra. Electrochemical measurements discussed in Section 3.3.1 nevertheless show reduced stability and incomplete reversibility at higher reduction levels, consistent with reported behaviour of highly reduced Keggin-type polyoxometalates under strongly reducing conditions.

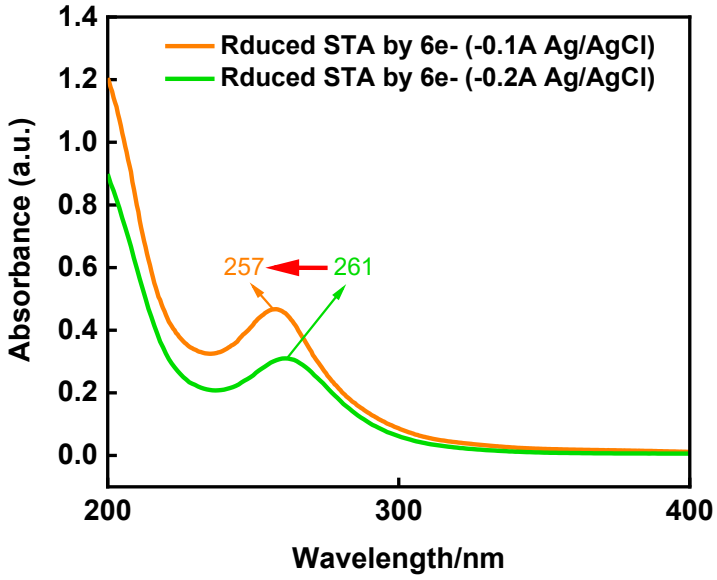


Figure 3.21. UV-vis absorption spectra of the 6-electron reduced silicotungstic acid generated under galvanostatic conditions at applied currents of −100 mA and −200 mA. The small shift in absorption maximum from approximately 259 nm to 261 nm indicates only minor variation in electronic structure with applied current and the absence of well-defined visible intervalence charge-transfer beyond the 4-electron reduction regime.

Overall, the combined colour evolution and UV-vis spectroscopic data provide independent evidence for controlled and reversible multi-electron storage in silicotungstic acid up to the 4-electron reduced form, while indicating progressive loss of electronic definition at higher degrees of reduction. These findings reinforce the conclusion that, under mild aqueous conditions, the $2e^-$ and $4e^-$ reduced forms represent the most electronically coherent, structurally preserved, and chemically stable forms of silicotungstic acid. Direct structural confirmation of framework retention within this reduction regime is provided by single-crystal X-ray diffraction analysis, discussed in the following section.

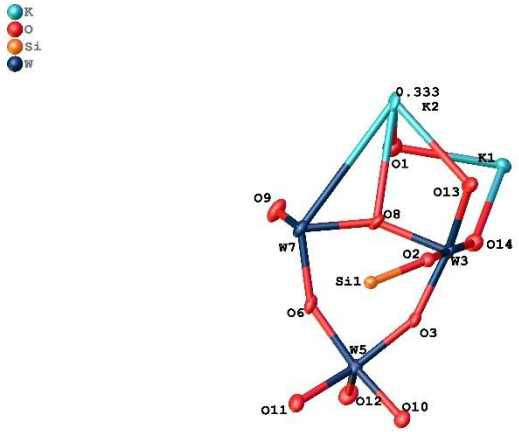
3.3.3 Structural analysis by single-crystal X-ray diffraction

Single-crystal X-ray diffraction (SCXRD) was employed to determine whether multi-electron reduction of silicotungstic acid (STA) induces measurable structural changes within the Keggin framework and to compare the reduced species with the crystallographic parameters reported for the fully oxidised anion. Structural characterisation focused on the 2-electron reduced species, $[SiW_{10}{}^{VI}W_2{}^{V}O_{40}]^{6-}$, and the 4-electron reduced species, $H_2[SiW_8{}^{VI}W_4{}^{V}O_{40}]^{6-}$, which correspond to the electrochemically reversible reduction regime identified in Sections 3.3.1 and 3.3.2. To the best of our knowledge, the crystal structures of these reduced species have not been previously reported. Crystals suitable for SCXRD analysis were obtained by slow crystallisation of the reduced solution under a nitrogen atmosphere at 4°C. The crystals exhibited a progressive colour change upon reduction, from colourless in the oxidised form to deep blue in the 2-electron reduced form and almost black in the 4-electron reduced form.

Both reduced compounds crystallise in the hexagonal space group $P6_222$ and retain the characteristic Keggin-type metal-oxide framework. Bond-valence-sum analysis yields average tungsten oxidation states of approximately +5.83 for the 2-electron reduced species and +5.67 for the 4-electron reduced species, consistent with reduction of two and four W(VI) centres to W(V), respectively. Three crystallographically independent tungsten sites are present in each structure, generated through symmetry operations. Consequently, the added electron density is statistically distributed across the tungsten centres rather than localised at specific metal sites. This is consistent with valence delocalisation, in which the added electrons are distributed among the tungsten centres rather than being localised at individual W(V) sites.

A full comparison of crystallographic parameters for oxidised silicotungstic acid and the 2-electron and 4-electron reduced species is provided in Table A3.1. The single-crystal X-ray representations of the 2-electron and 4-electron reduced silicotungstate structures are shown in Figure 3.22.

A)



B)

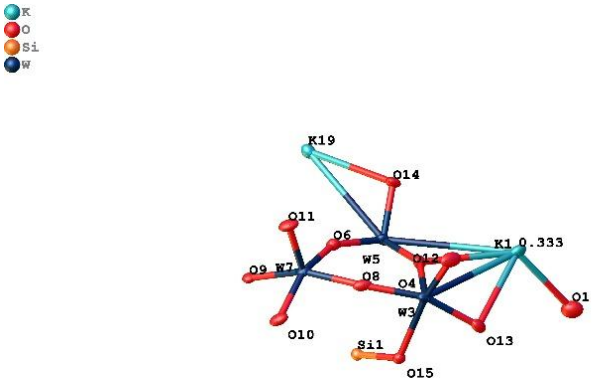


Figure 3.22. Single-crystal X-ray representations of the asymmetric units of the (A) 2-electron and (B) 4-electron reduced silicotungstate structures. Displacement ellipsoids are shown at the 50% probability level, with hydrogen atoms omitted for clarity.

Comparison of the reduced structures with the oxidised analogue reveals no statistically significant changes in W–O bond lengths or overall framework geometry. Only minor unit-cell contractions are observed, attributable primarily to differences in data collection temperature and subtle electrostatic effects rather than fundamental structural rearrangement. These trends are summarised in Table A3.1. Such resilience is typical of polyoxometalates, which can accommodate multiple added electrons with

minimal geometric distortion owing to their well-known electron-sponge character. These observations indicate that incorporation of up to four electrons primarily modifies the electronic distribution within the cluster while preserving the underlying Keggin architecture.

Refinement of both reduced structures required modelling of partial potassium occupancies corresponding to approximately 2.7 K^+ ions per anion, together with treatment of disordered solvent molecules using a solvent-masking (SQUEEZE) procedure. The masked electron density corresponds to approximately four water molecules per asymmetric unit located within channels running parallel to the crystallographic c-axis. Complete crystallographic parameters for the 4-electron reduced structure are summarised in Tables A3.2–A3.4. The corresponding crystallographic information for the two-electron reduced structure is provided in Tables A3.5–A3.7.

Crystallographic data for both reduced structures have been deposited with the Cambridge Crystallographic Data Centre (CCDC) under the deposition numbers listed above. These data can be obtained free of charge from the CCDC via www.ccdc.cam.ac.uk/structures

Additional crystallographic representations, including the solvent-accessible channels and packing arrangements, are presented in Figures A3.1–A3.2.

Although the $2e^-$ and $4e^-$ reduced forms exhibit only subtle crystallographic differences from one another, comparison with oxidised silicotungstic acid shows a small but measurable unit-cell contraction (Table A3.1). Importantly, no evidence of framework distortion, bond cleavage, or symmetry change is detected within the reversible reduction regime.

These structural observations correlate directly with the electrochemical and spectroscopic results presented in Sections 3.3.1 and 3.3.2. Preservation of the Keggin framework in the $2e^-$ and $4e^-$ reduced forms confirms that reversible electron uptake occurs without significant atomic rearrangement, supporting their identification as the chemically stable and electronically coherent reduced forms of silicotungstic acid. In contrast, the loss of reversibility observed during deeper reduction is therefore attributed not to gradual distortion of an intact Keggin structure, but rather to irreversible chemical

transformation or framework degradation that prevents formation of well-defined crystalline products suitable for diffraction analysis.

Overall, single-crystal X-ray diffraction provides definitive structural confirmation that multi-electron reduction of silicotungstic acid up to four electrons preserves the integrity of the Keggin framework, whereas the electrochemical and spectroscopic evidence indicates reduced stability under deeper reduction conditions. Together, these findings establish the $2e^-$ and $4e^-$ reduced forms as stable, well-defined redox forms of silicotungstic acid under mild aqueous conditions.

3.3.4 Structural Characterisation by Powder X-ray Diffraction

Powder X-ray diffraction (PXRD) patterns were recorded for oxidised silicotungstic acid and for samples electrochemically reduced to the $2e^-$ and $4e^-$ forms (Figure 3.23). The samples were prepared by rotary evaporation of aqueous solutions under reduced pressure at room temperature, followed by drying under a nitrogen atmosphere to minimise air oxidation. Where possible, the experimental PXRD patterns were compared with those expected from the corresponding single-crystal structures. However, reference patterns for reduced Keggin species are limited in the literature.

The diffraction pattern of the oxidised material is consistent with reported PXRD data for crystalline $H_4SiW_{12}O_{40}$ and its hydrated phases,[19] confirming the presence of the Keggin type polyoxometalate framework. The relatively broad reflections observed are characteristic of partially hydrated heteropolyacids and indicate a semi-crystalline solid form.

Upon reduction to the $2e^-$ form at −0.36 V vs NHE, modest changes in peak intensity and definition are observed relative to the oxidised material. These variations suggest alterations in solid state ordering of the Keggin units, potentially associated with changes in proton distribution or hydration accompanying electron uptake. Further reduction to the $4e^-$ form results in slightly reduced peak definition compared to the $2e^-$ form, consistent with increased lattice disorder at higher levels of electron accumulation.

Importantly, no additional diffraction peaks corresponding to crystalline tungsten oxide phases (for example WO_3), are detected in either reduced sample. The overall diffraction profiles remain characteristic of the Keggin type structure, demonstrating that electrochemical reduction up to the $4e^-$ form does not induce structural decomposition of the polyoxometalate framework. The PXRD findings are consistent with the FT-IR, UV−visible, and electrochemical data, collectively supporting retention of the Keggin framework up to the $4e^-$ reduced form.

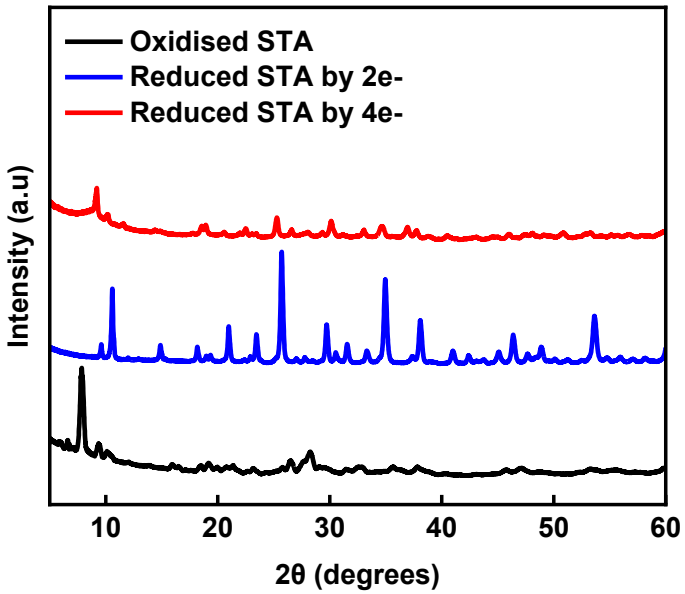


Figure 3.23. Powder X-ray diffraction (PXRD) patterns of oxidised silicotungstic acid and the corresponding $2e^-$ and $4e^-$ electrochemically reduced forms prepared under identical conditions.

3.3.5 Thermal behaviour and hydration state (TGA)

The hydration behaviour and thermal stability of silicotungstic acid were investigated using thermogravimetric analysis (TGA) (Figure 3.24). The as-received sample exhibits a significant mass loss of approximately 9.5% below 100 °C, corresponding to the removal of loosely bound hydration water (~17 mol H_2O per formula unit). A further gradual mass loss up to 250 °C results in a total weight loss of approximately 12.6%, consistent with the presence of ~23 mol of water in the fully hydrated

material.[19] These values are summarised in the Table 3.1 and are consistent with reported hydration levels for commercial $H_4SiW_{12}O_{40}\cdot nH_2O$.

Table 3.1. Summary of mass loss and estimated hydration levels of silicotungstic acid determined from TGA analysis.

Sample	Temperature Range	Weight Loss (%)	Estimated H_2O (mol per silicotungstic acid)
As received	< 100 °C	9.5	~17
As received	< 250 °C	12.6	~23
Dried (85 °C)	< 250 °C	~5	~9-10

In contrast, the sample pre-dried at 85 °C overnight exhibits substantially reduced mass loss below 100 °C, confirming removal of the majority of weakly bound water during pre-treatment. Nevertheless, a gradual decrease in mass at higher temperatures indicates the persistence of more strongly hydrogen bonded or structural water within the solid. No abrupt mass loss associated with framework decomposition is observed below 400 °C, demonstrating the thermal robustness of the Keggin structure under the applied conditions.

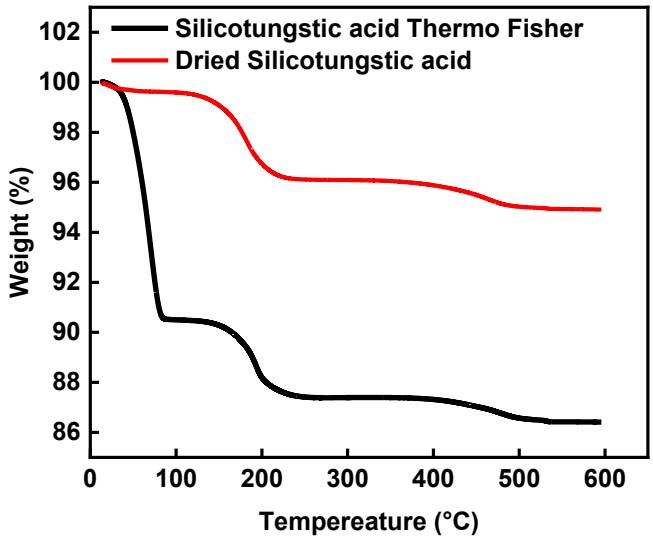


Figure 3.24. Thermogravimetric analysis (TGA) curves of silicotungstic acid ($H_4SiW_{12}O_{40}$). Black curve: as-received material, red curve: sample dried at 85 °C overnight. The staged mass losses correspond to removal of physiosorbed and structurally bound water.

3.4 Redox stability and reactivity

3.4.1 Re-oxidation behaviour and stability

The practical utility of reduced silicotungstic acid as a multi-electron redox mediator depends critically on both the reversibility of electron uptake and the chemical stability of the resulting reduced forms. To evaluate these factors, the re-oxidation behaviour of electrochemically reduced silicotungstic acid was systematically investigated following controlled 2-electron, 4-electron, and deeper reduction conditions.

Potentiostatic re-oxidation experiments performed after bulk 2-electron and 4-electron reduction exhibit essentially quantitative charge recovery (Figure 3.25), demonstrating that electron transfer within this regime is highly reversible. Cyclic voltammograms recorded before reduction and after re-oxidation display nearly identical peak positions and current responses, confirming preservation of the characteristic redox chemistry of the Keggin anion. Consistent with this electrochemical reversibility, UV-visible spectroscopy reveals complete disappearance of the blue intervalence charge-transfer absorption band upon re-oxidation, corresponding to regeneration of the fully oxidised, colourless species. Collectively, these observations establish that the $2e^-$ and $4e^-$ reduced forms of silicotungstic acid are both electrochemically reversible and chemically stable under the experimental conditions employed.

To probe reversibility beyond the 4-electron regime, galvanostatic reduction re-oxidation experiments were conducted under carefully controlled conditions. Reduction toward the 6-electron level at a constant cathodic current of –100 mA, followed by anodic re-oxidation at +100 mA, enabled recovery of a substantial fraction of the charge passed during reduction (Figure 3.10). However, under galvanostatic conditions this charge recovery alone does not demonstrate electrochemical reversibility, as the applied current can be sustained by oxidation of chemically altered species rather than regeneration of the original reduced silicotungstic acid. Nevertheless, these results indicate that

reduction approaching the 6-electron level can be achieved under mild driving conditions, although the extent of reversible electron storage is reduced compared with that observed for the $2e^-$ and $4e^-$ forms.

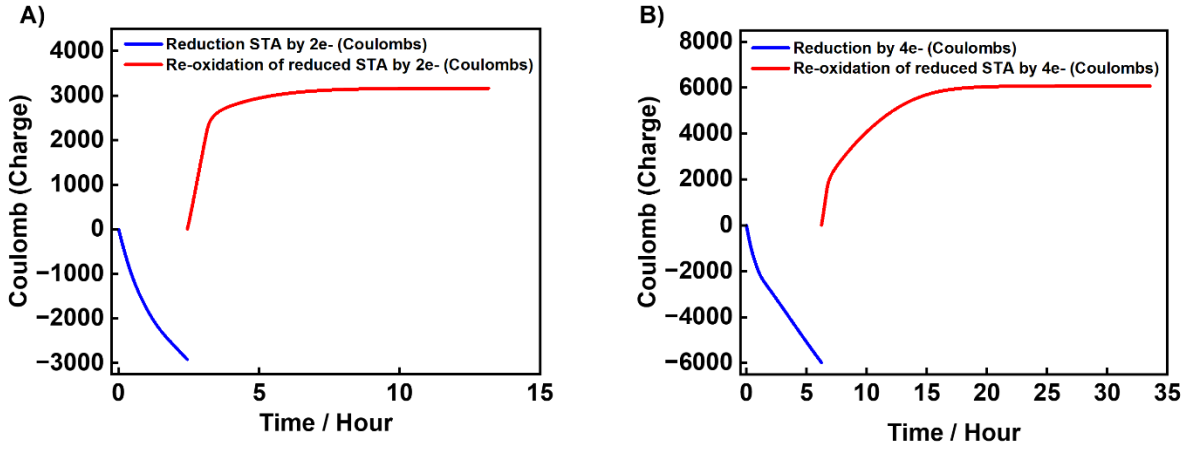


Figure 3.25. Charge-time profile for the two-electron (A) and four-electron (B) reduction and subsequent re-oxidation of 0.5 M silicotungstic acid at room temperature. Reduction was performed potentiostatically at –0.36 V versus the normal hydrogen electrode (NHE), followed by re-oxidation at +0.75 V versus NHE. Experiments were conducted in a divided H-cell using a carbon felt working electrode (2.5 × 4.0 cm^2), a platinum wire counter electrode, and an Ag/AgCl reference electrode.

Markedly different behaviour is observed under more strongly reducing conditions. At higher cathodic currents or during extended electrolysis, re-oxidation recovers only a limited proportion of the inserted charge, indicating pronounced irreversibility. Electrochemical responses following attempted re-oxidation show attenuation of the original redox features together with loss of well-defined reversible behaviour, consistent with degradation of the electroactive Keggin framework. Spectroscopic measurements likewise reveal incomplete restoration of the oxidised UV-visible profile and persistence of broad absorption features associated with reduced tungsten oxide species.

Visual and physical observations further support irreversible chemical transformation at high degrees of reduction. Deeply reduced solutions progressively darken from blue to blue-brown and may form suspended or precipitated materials during prolonged electrolysis. Complementary headspace measurements demonstrate substantially increased hydrogen evolution at higher applied cathodic

currents, confirming that the hydrogen evolution reaction becomes increasingly competitive under strongly reducing conditions. The progressive colour change from blue to blue-brown, together with increased hydrogen evolution, incomplete charge recovery, and precipitate formation under strongly reducing conditions, provides evidence for irreversible chemical transformation and degradation of the Keggin framework during deep reduction. Consistent with this behaviour, galvanostatic reduction at –300 mA drives the working electrode potential to highly negative values approaching –1.3 V vs. NHE, where proton reduction is strongly favoured. Attempts to achieve controlled 6-electron reduction under these conditions were repeatedly terminated by the potentiostat voltage compliance limit before reaching the theoretical charge, indicating an intrinsic electrochemical limitation associated with deep reduction.

During subsequent galvanostatic re-oxidation of deeply reduced solutions, the working electrode potential exhibited a pronounced time dependent increase, rising from approximately –0.2 V to values exceeding +2 V vs Ag/AgCl over the course of the experiment. The requirement for such strongly anodic potentials indicates that oxidation of the reduced mediator alone was insufficient to sustain the imposed current and that additional anodic processes, most plausibly water oxidation, contributed under these conditions. The combination of incomplete charge recovery and extreme anodic polarisation demonstrates that deep reduction introduces parasitic side reactions and irreversible chemical changes that diminish coulombic efficiency and electrochemical reversibility.

Time-dependent stability studies under inert atmosphere further emphasise the contrast between moderately and deeply reduced silicotungstic acid. Solutions containing the $2e^-$ and $4e^-$ reduced forms remain visually homogeneous and electrochemically responsive over extended periods, whereas more highly reduced solutions gradually darken, developing a brown coloration and showing a loss of electrochemical response even in the absence of an applied potential. This behaviour demonstrates that the intrinsic chemical stability of silicotungstic acid decreases sharply once reduction proceeds beyond the structurally preserved Keggin regime.

Overall, these results show that reversible multi-electron storage in silicotungstic acid is most reliably achieved within the $2e^-$ and $4e^-$ reduced forms, which exhibit essentially complete charge recovery upon re-oxidation and retain the Keggin framework in their reduced states, as supported by the structural characterisation described above. Reduction approaching the 6-electron level retains only partial reversibility under carefully controlled conditions, whereas deeper reduction leads to incomplete charge recovery, persistent reduced tungsten species, formation of insoluble decomposition products, and increasingly dominant parasitic reactions including hydrogen and oxygen evolution. Together, these effects define the practical stability window of silicotungstic acid as a redox mediator and provide the basis for evaluating its electron-storage capacity in the following section.

3.4.1.1 Practical limitations during deep electrochemical reduction

Deep electrochemical reduction of silicotungstic acid introduces several practical constraints that limit its usefulness as a reversible multi-electron redox mediator. Under increasingly cathodic conditions, the rate of hydrogen evolution rises sharply, diverting charge towards a competing reaction and reducing coulombic efficiency. In addition, prolonged electrolysis promotes the crossover of species through the membrane, which complicate controlled charge delivery and accurate determination of electron stoichiometry. At high applied currents, instrumental voltage compliance limits may be reached before the theoretical charge required for deeper reduction is achieved, indicating that the potentiostat itself imposes operational boundaries.

Chemical stability also decreases markedly beyond the four-electron regime. Spectroscopic broadening and the formation of blue-brown precipitates indicate the onset of irreversible chemical transformation under deeper reduction conditions. These irreversible transformations prevent complete re-oxidation and lead to progressive loss of electrochemical activity upon re-oxidation. Consequently, although charge corresponding to reduction beyond four electrons per Keggin unit can be passed experimentally, the combined effects of parasitic reactions, instrumental limitations, and structural degradation define a clear practical boundary for stable and reversible electron storage in silicotungstic acid.

3.4.2 Practical Electron Storage Capacity

The ability of silicotungstic acid (STA) to function as a practical multi-electron redox mediator depends not only on the number of electrons that can be formally introduced onto the Keggin framework, but also on the reversibility and stability of the resulting reduced states. Although electrochemical reduction beyond four electrons per cluster can be achieved under strongly cathodic conditions, the results presented in Section 3.3.1-3.4.1 demonstrate that only the $2e^-$ and $4e^-$ reduced forms exhibit consistent electrochemical reversibility and chemical stability under mild aqueous conditions.

Within this accessible regime, bulk electrolysis confirms that silicotungstic acid can reproducibly

Store up to four electrons per Keggin unit, with essentially quantitative charge recovery upon re-oxidation. The associated redox processes occur within a moderate potential window (−0.36 V to +0.76 V vs. NHE), thereby avoiding significant contributions from competing reactions such as hydrogen or oxygen evolution and enabling efficient, repeatable multi-electron cycling.

Although further levels of reduction can be reached, these states do not correspond to practically usable electron storage forms. Instead, they are associated with diminished reversibility, increased hydrogen evolution, and partial degradation of the Keggin framework, which limit their applicability as redox active species.

Importantly, the absence of significant structural changes in the $2e^-$ and $4e^-$ reduced forms, as demonstrated by single crystal X-ray diffraction, indicates that electron uptake occurs without disruption of the Keggin framework. This structural robustness underpins the observed electrochemical stability and distinguishes silicotungstic acid from many molecular redox mediators that undergo irreversible structural changes upon multi-electron reduction.

From a practical perspective, these findings define an effective electron storage capacity of four electrons per Keggin unit under aqueous conditions. This multi-electron capability, combined with favourable redox potentials and structural stability, highlights the potential of silicotungstic acid as a robust redox mediator. Collectively, these results identify the $2e^-$ and $4e^-$ reduced forms as the

functionally relevant redox states of silicotungstic acid, providing a mechanistic foundation for examining their chemical reactivity in the following chapter.

3.5 Conclusions

This chapter systematically examined the electrochemical reduction behaviour, stability, and structural integrity of silicotungstic acid (STA) under acidic aqueous conditions to define the practical limits of reversible multi-electron storage within the Keggin framework.

Electrochemical analysis demonstrates that silicotungstic acid undergoes three sequential reduction processes corresponding to two successive one-electron transfers followed by a proton-coupled 2-electron reduction. Bulk electrolysis confirms that the $2e^-$ and $4e^-$ reduced forms can be generated quantitatively and re-oxidised with essentially complete charge recovery, establishing these species as electrochemically reversible, chemically stable, and well-defined redox forms.

In contrast, deeper reduction under more strongly reducing conditions, including galvanostatic reduction to levels approaching $12e^-$ per Keggin unit, leads to incomplete re-oxidation, increasing hydrogen evolution, membrane crossover effects, precipitation of tungsten containing species, and progressive loss of electrochemical reversibility. Visible hydrogen formation becomes pronounced beyond $9e^-$, indicating that a significant fraction of the charge passed at higher reduction levels does not correspond to reversibly stored electrons within the Keggin framework. These observations demonstrate that reduction beyond 4-electron is increasing dominated by competing side reactions and irreversible chemical transformation rather than stable charge storage.

Spectroscopic and structural measurements provide independent confirmation of these trends. UV−visible and FT-IR analyses reveal progressive broadening and loss of well-defined electronic features at higher reduction levels, while powder and single-crystal X-ray diffraction confirm retention of the Keggin framework only within the $2e^-$ and $4e^-$ regimes. Thermogravimetric analysis further supports the stability of the hydrated framework under controlled conditions.

Taken together, the electrochemical, spectroscopic, and structural results establish that the $2e^-$ and $4e^-$ reduced forms represent the most stable and functionally relevant redox states of silicotungstic acid under mild aqueous conditions. These findings define the operational stability window of silicotungstic acid as a multi-electron redox mediator and provide a mechanistic foundation for understanding the hydrogen-transfer reactivity explored in the following chapter.

3.6 Appendix

Table A3.1. Comparison of crystallographic data and selected structural parameters for oxidised silicotungstic acid and its two-electron and four-electron reduced silicotungstate anions.

Parameter	**Oxidized $K_4[SiW_{12}O_{40}]^{4-}$**	**$2e^-$ reduced $K_3H_3[SiW_{10}^{VI}W_2^{V}O_{40}]^{6-}$**	**$4e^-$ reduced $K_3H_5[SiW_8^{VI}W_4^{V}O_{40}]^{8-}$**
Space group	$P6_22\,2$	$P6_22\,2$	$P6_22\,2$
a/b (**Å**)	19.1618	18.9922	18.9540
c (**Å**)	12.5124	12.5148	12.5283
Volume (**Å^3**)	3978.72	3909.35	3897.84
Temperature (K)	293	150	150
Mean (W–O) (**Å**)	1.92 (est.)	1.93 (est.)	1.94 (est.)
Avg. W Bond Valence	+5.85	+6.09	+6.12
K^+ occupancy per Keggin ion	4	≈ 2.7	≈ 2.7
Solvent mask (e^- per ASU)	-*	42 (≈ 4.2 H_2O)	45 (≈ 4.5 H_2O)

*The oxidised structure published[20] contains ~7 water molecules per Keggin Ion.

Table A3.2. Crystal data for the four-electron reduced silicotungstic acid (CCDC 2500216).

$K_{2.667}O_{44}SiW_{12}\cdot 0.333$	D_x = 3.912 Mg m^{-3}
M_r = 3060.63	Mo $K\alpha$ radiation, λ = 0.71073 Å
Hexagonal, $P6_222$	Cell parameters from 17353 reflections
a = 18.9540 (3) Å	θ = 2.5–35.8°
c = 12.5283 (2) Å	μ = 26.79 mm^{-1}
V = 3897.84 (14) Å^3	T = 150 K
Z = 3	Block, black
F(000) = 3948	0.08 × 0.06 × 0.04 mm

Table A3.3. Data collection parameters for the four-electron reduced silicotungstic acid.

XtaLAB Synergy R, HyPix-Arc 150 diffractometer	3168 reflections with $I > 2\sigma(I)$
Detector resolution: 10.0000 pixels mm^{-1}	$R_{int} = 0.041$
ω scans	$\theta_{max} = 28.3°$, $\theta_{min} = 2.5°$
Absorption correction: multi-scan *CrysAlis PRO* 1.171.43.90 (Rigaku Oxford Diffraction, 2023) Empirical absorption correction using spherical harmonics, implemented in SCALE3 ABSPACK scaling algorithm.	$h = -25 \rightarrow 22$
$T_{min} = 0.606$, $T_{max} = 1.000$	$k = -24 \rightarrow 25$
32721 measured reflections	$l = -16 \rightarrow 16$
3241 independent reflections	

Table A3.4. Structure refinement details for the four-electron reduced silicotungstic acid.

Refinement on F^2	12 restraints
Least-squares matrix: full	$w = 1/[\sigma^2(F_o^2) + (0.0112P)^2 + 7.1204P]$ where $P = (F_o^2 + 2F_c^2)/3$
$R[F^2 > 2\sigma(F^2)] = 0.015$	$(\Delta/\sigma)_{max} = 0.002$
$wR(F^2) = 0.030$	$\Delta\rangle_{max} = 0.56$ e $Å^{-3}$
$S = 1.04$	$\Delta\rangle_{min} = -0.65$ e $Å^{-3}$
3241 reflections	Absolute structure: Flack x determined using 1265 quotients [(I+)-(I-)]/[(I+)+(I-)] (Parsons, Flack and Wagner, Acta Cryst. B69 (2013) 249-259).
140 parameters	Absolute structure parameter: -0.006 (8)

Table A3.5. Crystal data for the two-electron reduced silicotungstic acid (CCDC).

$K_{2.667}O_{44}SiW_{12}·0.333[]$	$D_x = 3.900$ Mg m^{-3}
$M_r = 3060.63$	Mo $K\alpha$ radiation, $\lambda = 0.71073$ Å
Hexagonal, $P6_222$	Cell parameters from 23746 reflections
$a = 18.9922$ (2) Å	$\theta = 2.7–37.4°$
$c = 12.5148$ (1) Å	$\mu = 26.71$ mm^{-1}
$V = 3909.35$ (9) $Å^3$	$T = 150$ K
$Z = 3$	Needle, metallic dark blue
$F(000) = 3948$	0.43 × 0.08 × 0.04 mm

Table A3.6. Data collection parameters for the two-electron silicotungstic acid.

XtaLAB Synergy R, HyPix-Arc 150 diffractometer	3243 independent reflections
Radiation source: micro-focus sealed X-ray tube, Mova (Mo) X-ray Source	3163 reflections with $I > 2\sigma(I)$
Mirror monochromator	$R_{int} = 0.040$
Detector resolution: 10.0000 pixels mm^{-1}	$\theta_{max} = 28.3°$, $\theta_{min} = 2.5°$
ω scans	$h = -24 \rightarrow 25$
Absorption correction: multi-scan *CrysAlis PRO* 1.171.43.90 (Rigaku Oxford Diffraction, 2023) Empirical absorption correction using spherical harmonics, implemented in SCALE3 ABSPACK scaling algorithm.	$k = -25 \rightarrow 25$
$T_{min} = 0.349$, $T_{max} = 1.000$	$l = -15 \rightarrow 16$
36374 measured reflections	

Table A3.7. Structure refinement details for the two-electron reduced silicotungstic acid.

Refinement on F^2	Primary atom site location: dual
Least-squares matrix: full	$w = 1/[\sigma^2(F_o^2) + (0.0153P)^2 + 4.0569P]$ where $P = (F_o^2 + 2F_c^2)/3$
$R[F^2 > 2\sigma(F^2)] = 0.014$	$(\Delta/\sigma)_{max} = 0.001$
$wR(F^2) = 0.031$	$\Delta\rangle_{max} = 0.95$ e Å^{-3}
$S = 1.03$	$\Delta\rangle_{min} = -0.80$ e Å^{-3}
3243 reflections	Absolute structure: Flack x determined using 1263 quotients [(I+)-(I-)]/[(I+)+(I-)] (Parsons, Flack and Wagner, Acta Cryst. B69 (2013) 249-259).
140 parameters	Absolute structure parameter: -0.001 (6)
48 restraints	

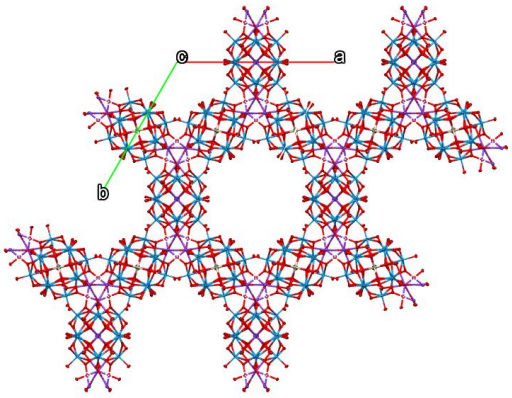


Figure A3.1: Packing diagram of the 2-electron reduced silicotungstic acid structure viewed along the crystallographic *c*-axis, highlighting solvent-accessible channels containing disordered water molecules treated using a solvent-masking (SQUEEZE) procedure.

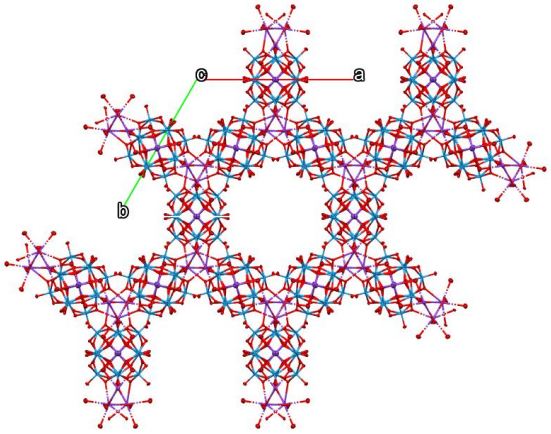


Figure A3.2: Packing diagram of 4-electron reduced silicotungstic acid structure viewed along crystallographic *c*-axis, showing solvent channels parallel to the *c*-axis and overall preservation of the Keggin framework upon multi-electron reduction.

3.7 References

1 L. MacDonald, B. Rausch, M. D. Symes and L. Cronin, *Chem. Commun.*, 2018, **54**, 1093–1096.

2 S. P. E. Smith and J. B. Christian, *Electrochim. Acta*, 2008, **53**, 2994–3001.

3 J. Friedl, M. V. Holland-Cunz, F. Cording, F. L. Pfanschilling, C. Wills, W. McFarlane, B. Schricker, R. Fleck, H. Wolfschmidt and U. Stimming, *Energy Environ. Sci.*, 2018, **11**, 3010–3018.

4 J. Friedl, F. L. Pfanschilling, M. V. Holland-Cunz, R. Fleck, B. Schricker, H. Wolfschmidt and U. Stimming, *Clean Energy*, 2019, **3**, 278–287.

5 C. Boskovic, M. Sadek, R. T. C. Brownlee, A. M. Bond and A. G. Wedd, *J. Chem. Soc., Dalton Trans.*, 2001, 187–196.

6 A. D. Stergiou and M. D. Symes, *Catal. Today*, 2022, **384–386**, 146–155.

7 M. Sadakane and E. Steckhan, *Chem. Rev.*, 1998, **98**, 219–238.

8 M. Misono, *Heterogeneous Catalysis of Mixed Oxides: Chapter 4. Catalysis of Heteropoly Compounds (Polyoxometalates)*, Elsevier Inc. Chapters, 2013, vol. 176.

9 S. Dong, X. Xi and M. Tian, *J. Electroanal. Chem.*, 1995, **385**, 227–233.

10 A. D. Stergiou, D. H. Broadhurst and M. D. Symes, *ACS Org. Inorg. Au*, 2023, **3**, 51–58.

11 C. Falaise, *Eur. J. Inorg. Chem.*, 2025, **28**, e202400827.

12 J. P. Launay, *J. Inorg. Nucl. Chem.*, 1976, **38**, 807–816.

13 S.-X. Guo, A. W. A. Mariotti, C. Schlipf, A. M. Bond and A. G. Wedd, *J. Electroanal. Chem.*, 2006, **591**, 7–18.

14 B. Keita and L. Nadjo, *J. Electroanal. Chem. Interfacial Electrochem.*, 1987, **217**, 287–304.

15 B. Keita and L. Nadjo, *J. Electroanal. Chem. Interfacial Electrochem.*, 1987, **227**, 77–98.

16 B. Keita and L. Nadjo, *J. Electroanal. Chem. Interfacial Electrochem.*, 1988, **243**, 87–103.

17 M. T. Pope, Y. Jeannin and M. Fournier, *Heteropoly and isopoly oxometalates*, Springer, 1983, vol. 33.

18 M. T. Pope and A. Müller, *Angew. Chem. Int. Ed. Engl.*, 1991, **30**, 34–48.

19 F. J. Berry, G. R. Derrick and M. Mortimer, *Polyhedron*, 2014, **68**, 17–22.

20 P. Klonowski, J. C. Goloboy, F. J. Uribe-Romo, F. Sun, L. Zhu, F. Gandara, C. Wills, R. J. Errington, O. M. Yaghi and W. G. Klemperer, *Inorg. Chem.*, 2014, **53**, 13239–13246.

Chapter 4: Application of Electrochemically Reduced Silicotungstic Acid in Indirect Organic Reduction

This chapter contains expanded and updated sections from the version submitted for publication in RSC Advances, titled: Preparation, characterization and hydrogenation activities of multiply reduced silicotungstic acid.

Synopsis

This chapter explores the use of electrochemically reduced silicotungstic acid as a multi-electron redox mediator for the indirect reduction of electron deficient aromatic substrates. Based on the redox stability window established in Chapter 3, the 2-electron, 4-electron, and 6-electron reduced forms were prepared electrochemically and tested under controlled silicotungstic acid : substrate ratios. Reactivity was evaluated using 4-cyanobenzaldehyde as a model substrate, with product formation analysed by ^{1}H NMR spectroscopy and corroborated by GC-MS and FT-IR measurements. The 4-electron reduced form provided the optimal balance between reducing power and selectivity, enabling efficient conversion of the aldehyde to the corresponding benzyl alcohol while preserving the nitrile group. The 2-electron reduced form exhibited moderate activity, whereas the 6-electron reduced form showed lower practical efficiency due to competing processes under strongly reducing conditions. Additional substrates confirmed clear functional group selectivity, with aldehydes reduced preferentially over aromatic nitriles and ketones. Overall, these findings define the scope and limitations of reduced silicotungstic acid as a mediator for indirect electrochemical reductions.

Acknowledgements and Declarations

The content of this chapter was initially developed in collaboration with Zeliha Ertekin and my supervisor, Prof. Mark Symes. I am grateful for their valuable input during the early stages of the work. Any sections not authored by me in the original collaborative manuscript have been either omitted or substantially rewritten, and the work presented in this chapter represents my own independent research and analysis.

Abstract

This chapter investigates the use of electrochemically reduced silicotungstic acid as a multi-electron redox mediator for the indirect reduction of electron deficient aromatic substrates. Based on the redox stability window established in Chapter 3, the $2e^-$, $4e^-$, and $6e^-$ reduced forms of silicotungstic acid were examined under controlled silicotungstic acid to substrate ratios (typically 10:1 electron equivalents relative to substrate) to evaluate their reactivity and selectivity. Reaction mixtures were primarily analysed using ^{1}H NMR spectroscopy to determine substrate conversion and product formation. Product identity was further confirmed by GC-MS analysis, and FT-IR spectroscopy was used as complementary structural evidence where appropriate. Substrate conversion was determined by ^{1}H NMR integration, and total yields were calculated from the mass of the organic residue following extraction and solvent removal.

The reaction of 4-cyanobenzaldehyde showed a clear dependence on the degree of silicotungstic acid reduction. The 4-electron reduced form, generated potentiostatically at −0.36 V vs NHE, gave the highest efficacy, achieving 88% substrate conversion and 81% total yield, with selective reduction of the aldehyde group to the corresponding benzyl alcohol while leaving the nitrile group unaffected. The 2-electron reduced form showed moderate reactivity, which improved with increasing silicotungstic acid loading. In contrast, the 6-electron reduced form (generated galvanostatically at −100 mA and −200 mA) achieved high substrate conversion (>87%) but gave significantly lower yields (~38–40%), indicating that competing side reactions occur alongside the desired transformation under more strongly reducing conditions.

Other substrates, including dicyanobenzenes, trifluoromethyl-substituted ketones, and sterically demanding aldehydes, showed little or no conversion under the same conditions, with high recovery of starting material confirming limited reactivity. Overall, these results indicate that although deeper reduction increases reducing power, it compromises selectivity and synthetic efficiency. The 4-electron reduced form of silicotungstic acid therefore provides the most suitable balance between reducing power, selectivity, and synthetic efficiency for selective aldehyde to alcohol reduction.

4.1 Introduction

Chapter 3 established that silicotungstic acid can undergo controlled multi-electron reduction in aqueous media, with the 2-electron and 4-electron reduced forms exhibiting reversible electrochemical behaviour and structural stability.[1,2] In contrast, deeper reduction beyond the four-electron level leads to diminished reversibility and increased participation of competing processes.[2,3] Having defined the practical redox stability window of silicotungstic acid, it is therefore necessary to evaluate whether these electrochemically generated reduced forms can be applied effectively as soluble multi-electron redox mediators for organic transformations.

Indirect electrochemical reduction using soluble mediators offers several advantages over direct electrode reduction. In mediated systems, electron transfer occurs through a chemically defined reduced species rather than at the electrode surface, which can improve control over reaction conditions, minimise overpotential effects, and enhance chemoselectivity. Polyoxometalates such as silicotungstic acid are particularly attractive in this context due to their ability to store multiple electrons within a single molecular framework and undergo reversible multi-electron redox processes.[2–6] However, whether increasing the number of stored electrons enhances synthetic performance remains unclear, particularly given that deeper reduction compromises electrochemical stability (Chapter 3). Understanding how the degree of electrochemical reduction influences mediator reactivity is therefore essential for the development of selective electrochemical reduction strategies. Despite the well-established redox chemistry of polyoxometalates, systematic studies comparing the reactivity of different multi-electron reduced forms of silicotungstic acid in mediated organic reductions are still limited.[7–9]

The hypothesis investigated in this chapter was that increasing the number of electrons stored within electrochemically reduced silicotungstic acid would influence its ability to transfer reducing equivalents to organic substrates. The rationale for comparing different reduction states was therefore to determine whether increased electron storage could enhance substrate reduction while maintaining selectivity and mediator stability.

In this chapter, the $2e^-$, $4e^-$, and $6e^-$ reduced forms of silicotungstic acid are evaluated as soluble redox mediators for the reduction of electron-deficient aromatic substrates. The study focuses primarily on 4-cyanobenzaldehyde as a model compound, enabling direct comparison between different degrees of reduction and mediator to substrate ratios. The selective transformation of the aldehyde group to the corresponding benzyl alcohol, while retaining the nitrile functionality, provides a convenient probe of chemoselectivity. Additional substrates, including dicyanobenzenes, trifluoromethyl substituted carbonyl compounds, and sterically demanding aromatic aldehydes, are examined to assess the scope and limitations of the system.

By systematically comparing the reactivity of the $2e^-$, $4e^-$, and $6e^-$ reduced forms of silicotungstic acid at defined mediator to substrate ratios, this chapter aims to determine how the degree of electrochemical reduction influences conversion, selectivity, and synthetic efficiency. Particular attention is given to the balance between increased reducing power and the onset of competing pathways under strongly reducing conditions. Through this approach, the suitability of electrochemically generated silicotungstic acid as a tuneable mediator for selective organic reduction is critically assessed (Figure 4.1).

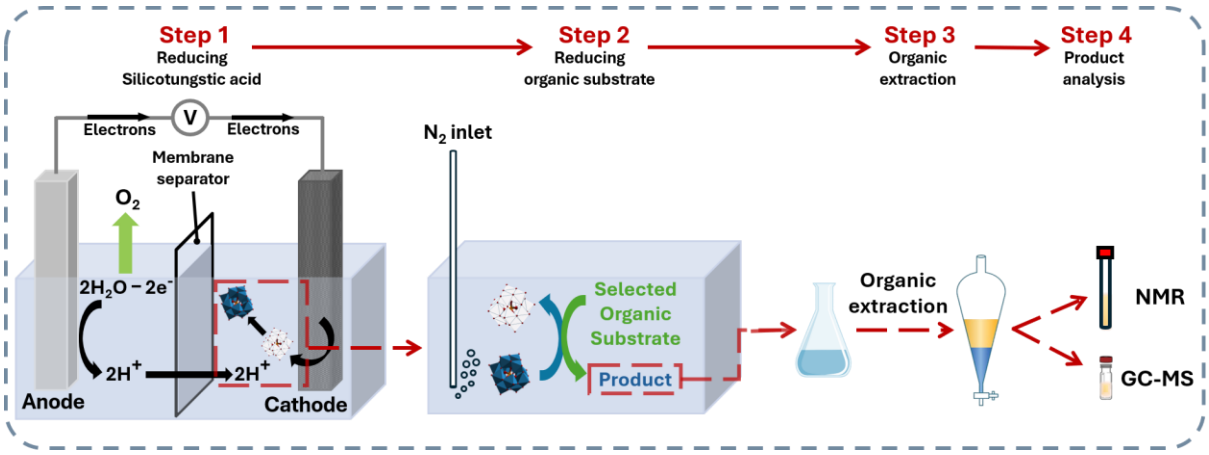


Figure 4.1. Schematic overview of the mediated hydrogenation process. Step 1: electrochemical reduction of silicotungstic acid (oxidised form shown in white, reduced form shown in blue). Step 2: reaction of the reduced mediator with the selected organic substrate (aromatic aldehyde, ketone, or nitrile). Step 3: extraction of the organic products. Step 4: product analysis by ^{1}H NMR and GC-MS.

4.2 Experimental

4.2.1 Materials

Silicotungstic acid hydrate ($H_4[Si(W_3O_{10})_4]\cdot xH_2O$), phosphoric acid (85% aqueous solution), sodium hydroxide, magnesium sulfate, chloroform, dichloromethane, Nafion N-117 membrane, and supporting electrolytes were obtained and handled as described in Section 3.2.1.

The following organic substrates were used without further purification: 4-cyanobenzaldehyde, 4-(trifluoromethyl)benzaldehyde, phthalonitrile, terephthalonitrile, 4-(trifluoromethyl) acetophenone, biphenyl-4-carboxaldehyde, and 2-naphthaldehyde. Commercially available reagents were used directly without further treatment unless explicitly noted.

Deuterated chloroform ($CDCl_3$) was used for NMR analysis. Nitrogen (>99% purity) was employed to maintain an inert atmosphere during electrolysis subsequent reactions.

4.2.2 Electrochemical Generation of Reduced Silicotungstic Acid

Electrochemical reductions were carried out using the three-electrode configuration and divided H-cell described in Section 3.2.2. The H-cell, equipped with a proton-exchange membrane, was used to separate the cathodic and anodic compartments while maintaining ionic conductivity between them. Silicotungstic acid was placed in the cathodic compartment, where electrochemical reduction occurs, while phosphoric acid was used as the supporting electrolyte in the anodic compartment. The proton-exchange membrane allowed proton transport between the compartments while minimising mixing of the catholyte and anolyte.

The 2-electron and 4-electron reduced forms of silicotungstic acid were generated potentiostatically at −0.36 V vs NHE.

The 6-electron reduced form was generated galvanostatically by applying constant cathodic currents of −100 mA or −200 mA. Electrolysis was continued until the charge corresponding to six electrons per

silicotungstic acid cluster had been passed. This assignment assumes that the delivered charge is fully utilised for silicotungstic acid reduction and not consumed by competing side reactions. Following electrolysis, the reduced silicotungstic acid solution was transferred under nitrogen to a separate reaction vessel for subsequent reaction with organic substrates.

4.2.3 General Procedure for the Reduction of Organic Substrates

Organic substrates were added to the electrochemically reduced silicotungstic acid solution at defined molar ratios (typically 10:1 silicotungstic acid: substrate unless otherwise stated). The reaction mixture was stirred magnetically under a nitrogen atmosphere at room temperature (~20 °C) for approximately 18 hours.

Upon completion of the reaction, the acidic aqueous phase was carefully neutralised to approximately pH 7 using 1.0 M NaOH. This neutralisation step ensured efficient transfer of the organic products into the organic phase during extraction. The mixture was subsequently extracted with chloroform (2 × 20 mL). Residual moisture was removed from the combined organic phase using anhydrous magnesium sulfate. After filtration, the solvent was eliminated under vacuum to afford the total residue.

For reactions performed using silicotungstic acid solutions reduced by $6e^-$, persistent emulsions were occasionally observed during phase separation in the separatory funnel, which may have resulted in partial loss of organic material during extraction.

4.2.4 Product Analysis and Determination of Conversion, and Yield

Reaction mixtures and organic residues were analysed by ^{1}H NMR spectroscopy, GC-MS, and FT-IR spectroscopy as described in Section 3.2.3 unless otherwise stated. For GC-MS analysis, samples were dissolved in dichloromethane prior to injection.

^{1}H NMR spectra were recorded in $CDCl_3$ at room temperature. Substrate conversion (%) was determined by integration of diagnostic resonances corresponding to starting material and product signals in the total reaction mixture.

Total yields (%) reported in this chapter correspond to product yields calculated from the mass of organic residue obtained after extraction and solvent removal under reduced pressure, without further chromatographic purification.

In cases where no conversion was detected, starting materials were isolated during work-up, confirmed by ^{1}H NMR spectroscopy, and weighed. Substrate (%) is reported relative to the initial substrate mass.

4.3 Results and Discussion

4.3.1 Hydrogenation of 4-Cyanobenzaldehyde

The reduction of 4-cyanobenzaldehyde was selected as the primary model reaction to evaluate the reactivity of electrochemically reduced silicotungstic acid. This substrate contains both an aldehyde group and a strongly electron withdrawing nitrile substituent, allowing assessment of chemoselectivity under mediated reduction conditions.

The proposed reduction pathway for aryl aldehydes bearing electron withdrawing substituents (such as –CN and –CF_3) is illustrated in Figure 4.2. The process consists of two separate stages. First, silicotungstic acid is electrochemically reduced to generate the 2-electron or 4-electron reduced form. The reduced mediator is then transferred from the electrochemical cell and reacted ex situ with the selected organic substrate. During this second stage, the reduced silicotungstic acid acts as a source of reducing equivalents, allowing reduction of the aldehyde group to the corresponding benzyl alcohol while the mediator is re-oxidised.[2,4]

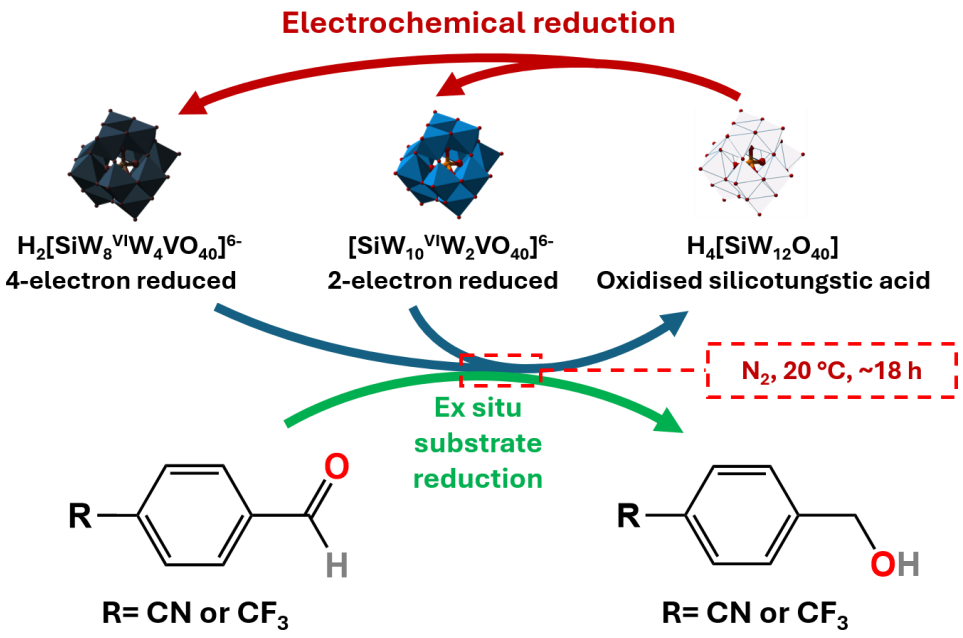


Figure 4.2. Proposed hydrogenation of aryl aldehydes bearing electron withdrawing substituents (–CN and $–CF_3$) mediated by the 2-electron and 4-electron reduced forms of silicotungstic acid.

Reactions were performed using the $2e^-$, $4e^-$, and $6e^-$ reduced forms of silicotungstic acid at defined silicotungstic acid to substrate ratios. Conversion values were determined from ^1H NMR analysis of the total reaction mixtures, while product yields were estimated gravimetrically based on the mass change of the reaction mixture relative to the theoretical product mass.

For the 2-electron reduced form, increasing the mediator loading from a 1:1 to a 10:1 ratio significantly improved substrate conversion, rising from 12% to 49%, with the product yield increasing from 9% to 43%. However, further increasing the ratio to 20:1 did not enhance performance, affording 37% conversion and 31% yield. These results suggest that increasing the availability of reducing equivalents improves reaction efficiency up to an optimal mediator loading, beyond which additional mediator does not provide further benefit. This behaviour may reflect limitations in effective electron transfer or competing processes that reduce the efficiency of electron utilisation at higher mediator concentrations.

Under identical 10:1 conditions, the 4-electron reduced form exhibited markedly higher activity, achieving 88% substrate conversion and 81% product yield (Table 4.1). These results indicate that

increased electron storage within the mediator significantly enhances the reducing capability of the system while maintaining controlled and selective reactivity. The reduction of the aldehyde is proposed to proceed through transfer of reducing equivalents from the reduced silicotungstic acid mediator to the carbonyl functionality. Upon reaction with the substrate, the reduced mediator acts as a source of electrons and protons, facilitating conversion of the aldehyde group to the corresponding benzyl alcohol while the mediator is re-oxidised. The higher activity of the 4-electron reduced form compared with the 2-electron reduced form is consistent with its greater capacity to store and subsequently transfer reducing equivalents. The retention of the nitrile functionality indicates preferential reduction of the aldehyde group under these conditions.

The selective conversion of 4-cyanobenzaldehyde to 4-(hydroxymethyl)benzonitrile was confirmed by ^{1}H NMR spectroscopy (Figure 4.3). Comparison of the reaction spectra with the starting material shows a decrease in the aldehyde proton resonance at approximately 9.9 ppm and the appearance of a new benzylic CH_2 signal at approximately 4.6 ppm, consistent with formation of the corresponding benzyl alcohol. The aromatic region (7.4–7.8 ppm) remained largely unchanged, suggesting retention of the nitrile substituent.

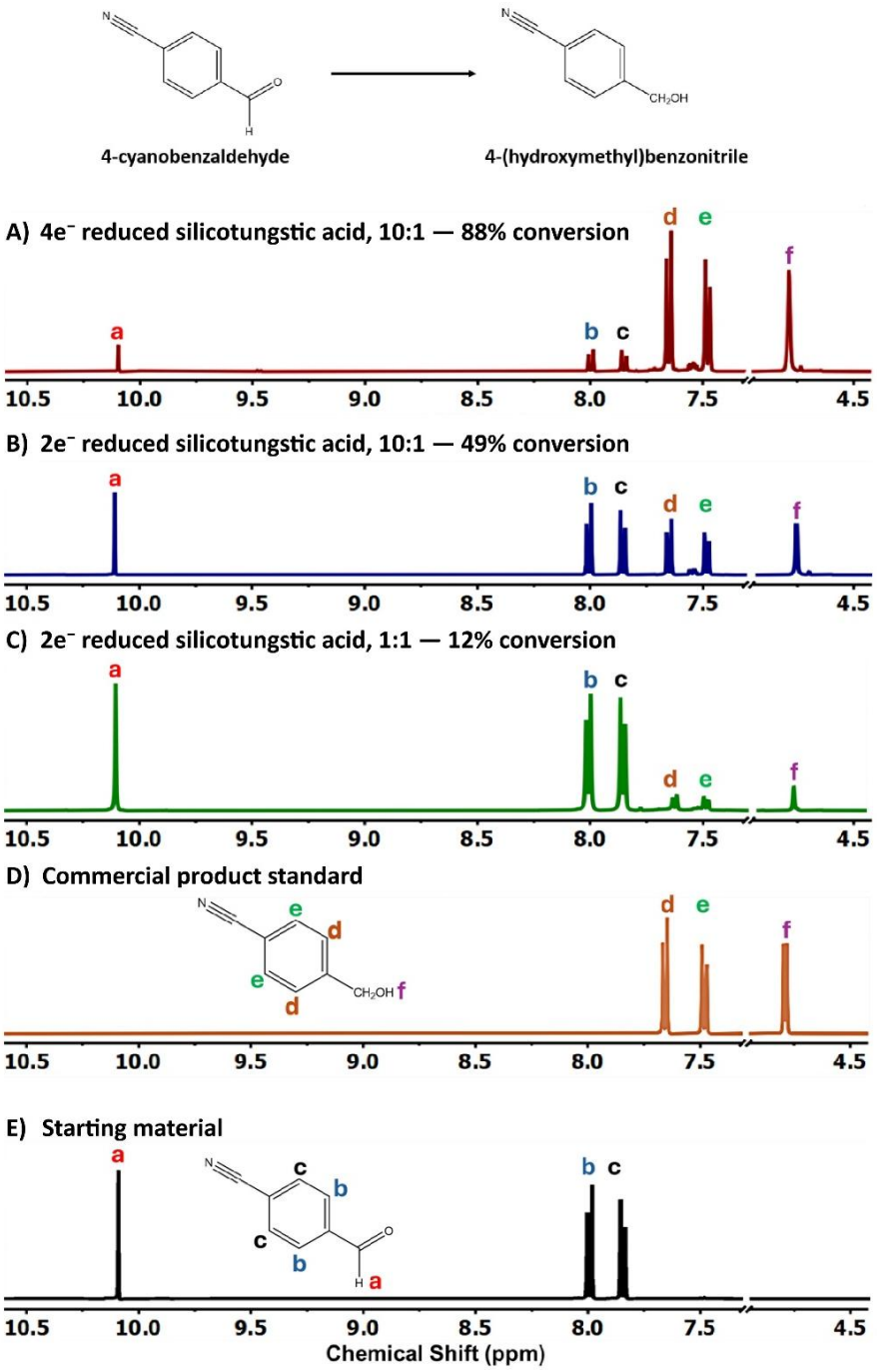


Figure 4.3. Stacked ^{1}H NMR spectra ($CDCl_3$, 400 MHz) showing the conversion of 4-cyanobenzaldehyde to 4-(hydroxymethyl)benzonitrile under different reduction conditions: (A) reaction mixture obtained using 4-electron reduced silicotungstic acid at a 10:1 silicotungstic acid to substrate ratio (88% conversion), (B) reaction mixture obtained using 2-electron reduced silicotungstic acid at a 10:1 ratio (49% conversion), (C) reaction mixture obtained using 2-electron reduced silicotungstic acid at a 1:1 ratio (12% conversion), (D) commercial standard of 4-(hydroxymethyl)benzonitrile, and (E) starting material, 4-cyanobenzaldehyde.

Further confirmation was obtained by GC-MS analysis (Figure 4.4). The chromatogram of the reaction mixture displayed peaks corresponding to both the starting material and 4-(hydroxymethyl)benzonitrile. The retention time and mass spectrum of the product peak matched those of the commercial standard, confirming successful reduction of the aldehyde functionality.

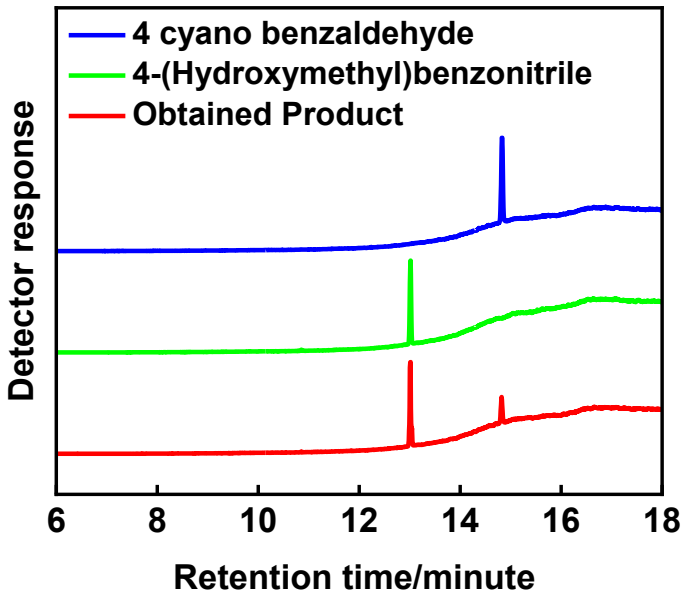


Figure 4.4. Stacked GC-MS chromatograms of 4-cyanobenzaldehyde, commercial 4-(hydroxymethyl)benzonitrile, and the reaction mixture obtained using 4-electron reduced silicotungstic acid (10:1 ratio).

FT-IR spectroscopy provided additional support for selective functional group transformation (Figure 4.5). In the starting material, a strong aldehyde C=O stretching band was observed at approximately 1700 cm^{-1}. This band disappeared in the reduced product, while a broad O–H stretching band appeared in the 3200-3500 cm^{-1} region, consistent with formation of the corresponding alcohol. Importantly, the nitrile stretching band (~2220 cm^{-1}) remained unchanged, confirming preservation of the –CN group during reduction.

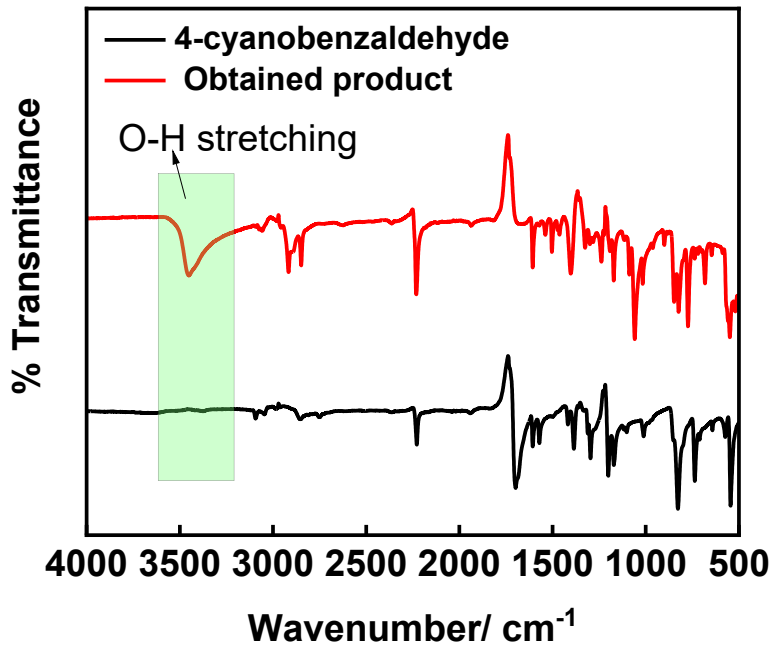


Figure 4.5. FT-IR spectra of 4-cyanobenzaldehyde and the corresponding product obtained after reduction with 4-electron reduced silicotungstic acid.

Increasing the degree of reduction to the 6-electron form, generated galvanostatically at −100 mA and −200 mA, resulted in high substrate conversion (87% and 93%, respectively). However, the corresponding product yields were significantly lower (both ~38%). The discrepancy between NMR conversion and calculated product yield indicates that although the substrate is largely consumed, the selectivity towards formation of the desired benzyl alcohol decreases under these more strongly reducing conditions. This behaviour may reflect the occurrence of competing reduction pathways when highly reduced mediator species are present. Additionally, persistent emulsions were observed during extraction of reactions involving the 6-electron reduced form, which may have contributed to inaccuracies in yield estimation during work-up. It is also possible that further reduction of the nitrile group to more polar species, such as amines, occurred under these strongly reducing conditions, potentially increasing the partitioning of products into the aqueous phase. However, the aqueous and emulsion phases were not analysed in detail, and this possibility cannot be confirmed.

Although the 6-electron reduced form afforded higher substrate conversions (87–93%), the substantially lower product yields (~38%) indicate poorer overall performance compared with the 4-electron reduced form. Therefore, the 4-electron reduced form of silicotungstic acid provides the optimal balance between substrate conversion, product yield, and selectivity towards the desired benzyl alcohol under the conditions investigated.

Table 4.1. Reduction of 4-cyanobenzaldehyde with different silicotungstic acid levels and loadings.

Reduced STA Form	Electrochemical Method	Silicotungstic acid:Substrate Ratio	Conversion (%)	Total Yield (%)	Product Yield (%)	Substrate (%)
Oxidised STA	Potentiostatic (−0.36 V)	10:1	0	0	0	>98
Reduced STA by $2e^-$	Potentiostatic (−0.36 V)	1:1	12.28	73.09	8.85	64.24
Reduced STA by $2e^-$	Potentiostatic (−0.36 V)	10:1	48.71	89.27	43.15	46.12
Reduced STA by $2e^-$	Potentiostatic (−0.36 V)	20:1	36.90	84.28	30.80	53.47
Reduced STA by $4e^-$	Potentiostatic (−0.36 V)	10:1	87.87	92.63	81.24	11.38
Reduced STA by $6e^-$	Galvanostatic (−100 mA)	10:1	86.62	43.61	37.52	6.08
Reduced STA by $6e^-$	Galvanostatic (−200 mA)	10:1	92.49	41.22	38.08	3.13

4.3.2 Hydrogenation of 4-(Trifluoromethyl)benzaldehyde

To further examine the scope of the mediated reduction system, 4-(trifluoromethyl)benzaldehyde was investigated under identical conditions using the 4-electron reduced form of silicotungstic acid at a 10:1 silicotungstic acid to substrate ratio. This substrate contains a strongly electron withdrawing $–CF_3$ group, allowing comparison with 4-cyanobenzaldehyde and assessment of substituent effects on reactivity.

Under these conditions, a substrate conversion of 39% was observed, with a corresponding product yield of 23 %. These values are significantly lower than those obtained for 4-cyanobenzaldehyde under the same conditions (88% conversion and 81% yield), indicating reduced reactivity of the trifluoromethyl substituted substrate.

The lower reactivity of 4-(trifluoromethyl)benzaldehyde compared with 4-cyanobenzaldehyde suggests that the nature of the electron withdrawing substituent influences the efficiency of the mediated reduction. Although both –CN and $–CF_3$ are strongly electron withdrawing groups, they affect the aromatic system differently. The –CN group can withdraw electron density through both inductive and resonance effects, whereas the $–CF_3$ group acts mainly through an inductive effect. These differences may influence the reduction behaviour of the carbonyl group and its interaction with the reduced silicotungstic acid mediator. However, the exact reason for the difference in reactivity cannot be determined from the present experiments.

Formation of 4-(trifluoromethyl)benzyl alcohol was confirmed by ^{1}H NMR spectroscopy (Figure 4.6). The aldehyde proton signal at approximately 10.1 ppm in the starting material was significantly reduced in the reaction mixture, while a new benzylic CH_2 resonance appeared at approximately 4.7 ppm, consistent with alcohol formation. The aromatic region remained consistent with the expected substitution pattern. Comparison with a commercial sample of 4-(trifluoromethyl)benzyl alcohol confirmed the identity of the product.

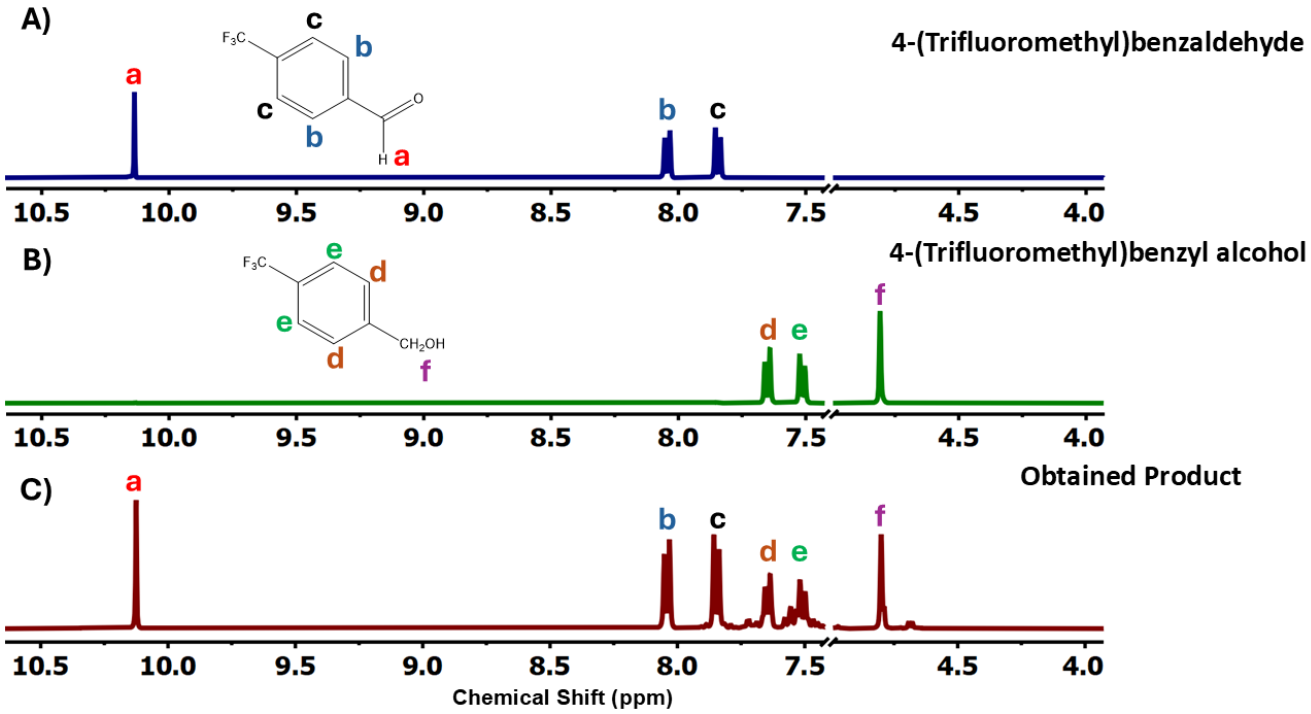


Figure 4.6. Stacked ^{1}H NMR spectra ($CDCl_3$, 400 MHz) of (A) 4-(trifluoromethyl)benzaldehyde (starting material), (B) commercial 4-(trifluoromethyl)benzyl alcohol, and (C) the reaction mixture obtained using 4-electron reduced silicotungstic acid (10:1 ratio).

Further confirmation was obtained by GC-MS analysis (Figure 4.7). The chromatogram of the reaction mixture displayed peaks corresponding to both the starting material and the reduced product. The retention time and mass spectrum of the product peak matched those of the commercial 4-(trifluoromethyl)benzyl alcohol standard, confirming successful reduction of the aldehyde functionality.

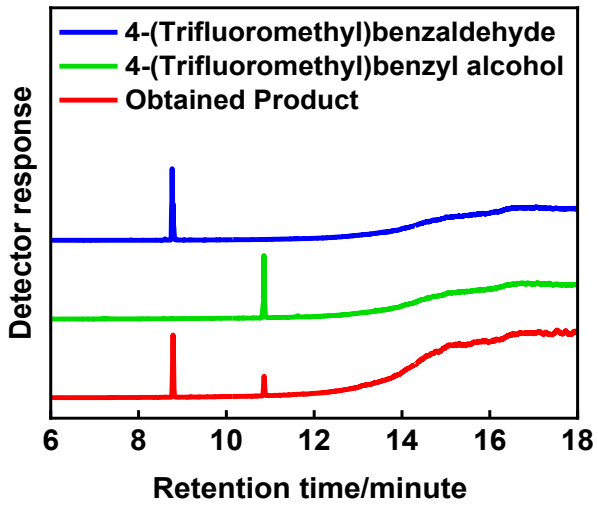


Figure 4.7. Stacked GC-MS chromatograms of (A) 4-(trifluoromethyl)benzaldehyde, (B) commercial 4-(trifluoromethyl)benzyl alcohol, and (C) the reaction mixture obtained using 4-electron reduced silicotungstic acid (10:1 ratio).

FT-IR spectroscopy provided additional supporting evidence for the reduction (Figure 4.8). In the starting material, a characteristic aldehyde C=O stretching band was observed at approximately 1700 cm^{-1}, consistent with reported values for aromatic aldehydes. In the spectrum recorded after reaction, this band was markedly reduced and no longer clearly distinguishable as a defined absorption, indicating consumption of the aldehyde functionality. In the higher wavenumber region (3200-3500 cm^{-1}), no distinct O–H stretching band was clearly resolved. Benzyl alcohol derivatives typically display O–H stretching absorptions near ~3300 cm^{-1} (for example, 3327 reported for 3-(trifluoromethyl)benzyl alcohol, neat). Given the moderate conversion (~40%) and the attenuated total reflectance (ATR) concentration employed, the O–H absorption corresponding to the alcohol product is expected to be relatively weak and may therefore not appear as a prominent feature in the spectrum. Importantly, the characteristic $–CF_3$ stretching vibrations, observed as strong absorption at approximately 1250 and 1150 cm^{-1}, remained unchanged after reaction, confirming that the trifluoromethyl substituent was preserved during the reduction process.

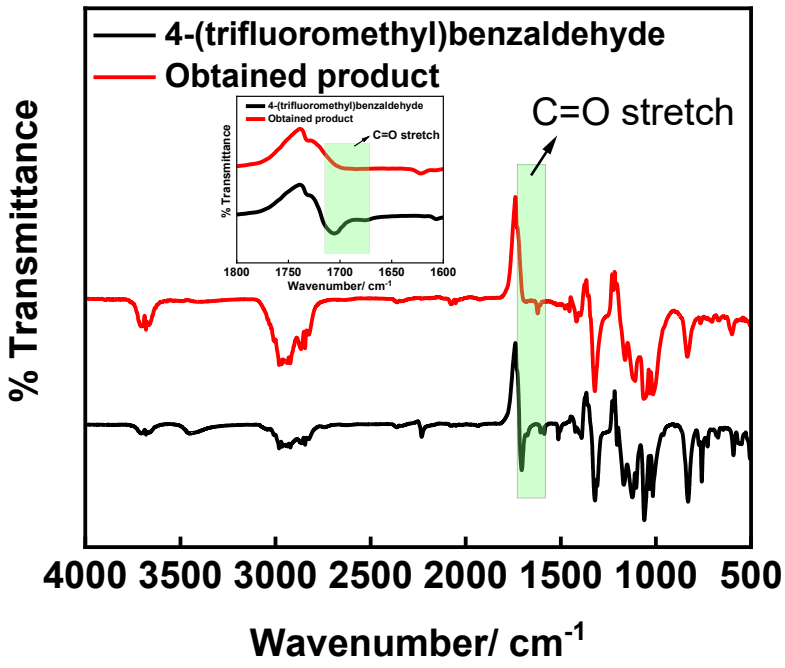


Figure 4.8. FT-IR spectra of 4-(trifluoromethyl)benzaldehyde and the corresponding product obtained after reduction with 4-electron reduced silicotungstic acid.

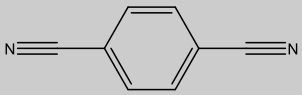
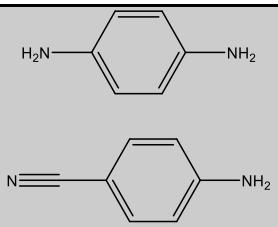
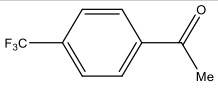
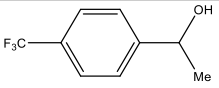
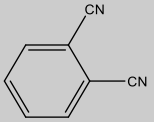
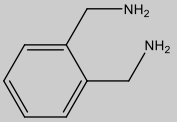
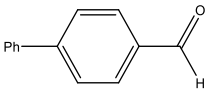
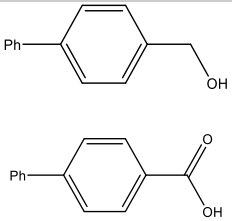
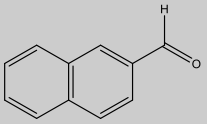
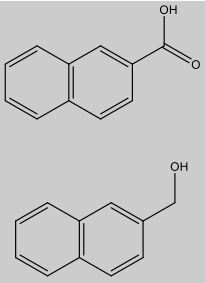
Overall, these results demonstrate that the 4-electron reduced form of silicotungstic acid is capable of reducing electron deficient aromatic aldehydes. However, the electronic nature of the substituent clearly influences the reaction efficiency. Compared to the nitrile-substituted analogue, the trifluoromethyl-substituted substrate exhibits lower conversion and yield under identical conditions, highlighting the importance of electronic effects in governing reactivity within the mediated reduction system.

4.3.3 Substrate Scope and Functional Group Tolerance

To further assess the applicability of the mediated reduction system, a range of additional electron deficient aromatic substrates was examined using the 4-electron reduced form of silicotungstic acid at 10:1 silicotungstic acid to substrate ratio. The selected substrates included aromatic nitriles (1,4-dicyanobenzene and 1,2-dicyanobenzene), a trifluoromethyl substituted ketone (4′-(trifluoromethyl)acetophenone), and sterically more demanding aldehydes such as biphenyl-4-

carboxaldehyde and 2-naphthaldehyde. The results obtained for these substrates are summarised in Table 4.2.

Table 4.2. Reactivity of additional electron-deficient aromatic substrates using 4-electron reduced silicotungstic acid (10:1 mediator to substrate ratio)

Substrate	Initial substrate (g)	Substrate recovered (%)	Substrate Conversion (%)	Product	Product Yield (%)
	0.0644	83.5	-		-
	0.0944	78.2	-		-
	0.0644	88.9	-		-
	0.0911	90.5	-		-
	0.0782	90.8	-		-

Under the reaction conditions employed, these substrates showed little or no observable conversion (<5% by ^{1}H NMR integration). In most cases, the starting material was recovered in high proportion following work up (83-91%), and ^{1}H NMR analysis of the organic residue confirmed the absence of significant product formation. Representative stacked ^{1}H NMR spectra of the starting materials and the corresponding reaction mixtures are provided in Appendix A (Figures A4.1−A4.5), confirming that no new resonances corresponding to reduced products were observed. GC-MS chromatograms further support these observations, with the reaction mixtures displaying only peaks corresponding to the starting materials (Appendix A, Figures A4.6-A4.10). Both 1,4-dicyanobenzene and 1,2-dicyanobenzene exhibited negligible reactivity, consistent with the high thermodynamic stability of aromatic nitriles and their resistance to reduction under mild mediated conditions. Similarly, 4′-(trifluoromethyl)acetophenone showed no measurable conversion, indicating that the ketone functionality was not readily reduced by the 4-electron reduced form of silicotungstic acid under these conditions.

The limited reactivity of these substrates demonstrates that the mediated reduction system displays clear functional group selectivity. While aldehydes were shown to undergo reduction to the corresponding benzyl alcohols, aromatic nitriles and ketones remained largely unaffected. This suggests that, under the experimental conditions employed, the reducing equivalents stored in the 4-electron reduced form of silicotungstic acid were insufficient to achieve measurable reduction of these functional groups. This does not exclude the possibility of their reduction under different reaction conditions or with more strongly reduced forms of the mediator.

Although steric and electronic effects may contribute to the limited reactivity of these substrates, particularly for substrates containing extended aromatic frameworks such as biphenyl-4-carboxaldehyde and 2-naphthaldehyde, solvent effects may also be important. The reactions were performed in an aqueous medium, and the limited aqueous solubility of some organic substrates may restrict their interaction with the dissolved silicotungstic acid mediator and therefore contribute to the low observed conversion. Consequently, the lack of reactivity cannot be attributed solely to electronic or steric effects.

Overall, the results demonstrate that the mediated reduction system exhibits selective reactivity toward specific aldehyde substrates while showing limited activity toward aromatic nitriles, ketones, and sterically demanding carbonyl compounds. These findings define the functional group tolerance of the system and support the suitability of electrochemically reduced silicotungstic acid as a mediator for selective aldehyde to alcohol reduction.

4.4 Conclusions

This chapter investigated the use of electrochemically generated reduced silicotungstic acid as a soluble redox mediator for the indirect reduction of electron deficient aromatic substrates. Building on the redox stability window established in Chapter 3, the $2e^-$, $4e^-$, and $6e^-$ reduced forms of silicotungstic acid were evaluated to determine how the degree of reduction influences reactivity, selectivity, and practical efficiency in organic transformations.

Among the systems studied, the 4-electron reduced form provided the most effective balance between reducing power and control. In the case of 4-cyanobenzaldehyde, high substrate conversion (88%) and yield (81%) were achieved under a 10:1 silicotungstic acid to substrate ratio, with selective transformation of the aldehyde group to the corresponding benzyl alcohol while preserving the nitrile functionality. In contrast, the 2-electron reduced form showed moderate reactivity that improved with increased mediator loading up to a point, while the 6-electron reduced form, although capable of high substrate conversion (>86%), resulted in significantly lower yields of the desired benzyl alcohol (~38–40%) and reduced practical efficiency, suggesting the occurrence of competing side reactions or alternative reduction pathways under these more strongly reducing conditions. These observations are consistent with the onset of competing processes and decreased stability at deeper levels of reduction, as discussed in Chapter 3.

Extension of the study to 4-(trifluoromethyl)benzaldehyde demonstrated that substituent effects significantly influence reaction efficiency. Although reduction to the corresponding benzyl alcohol was confirmed spectroscopically, both conversion (40%) and yield (23%) were lower than for the nitrile substituted analogue under identical conditions. Additional substrates, including aromatic nitriles,

ketones, and sterically demanding aldehydes, showed minimal or no conversion (<5%), with high recovery of starting material (78–91%), indicating clear functional group selectivity within the mediated system.

Overall, the results demonstrate that electrochemically generated reduced silicotungstic acid functions as an effective homogeneous redox mediator for selective aldehyde to alcohol reduction. The degree of mediator reduction plays a central role in determining reactivity, while electronic properties of the substrate strongly influence reaction outcome. These findings establish the practical scope and limitations of the mediated reduction strategy and provide a foundation for the further development of polyoxometalate based redox systems in indirect electrochemical synthesis.

4.5 Appendix

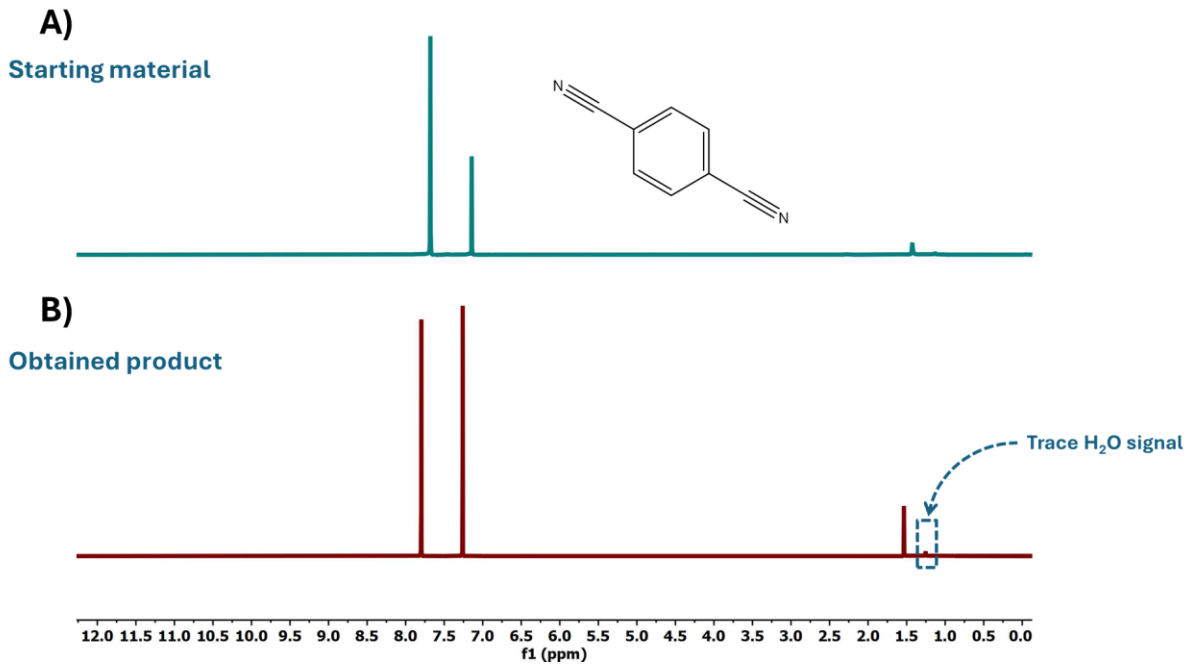


Figure A4.1. Stacked ^{1}H NMR spectra ($CDCl_3$, 400 MHz) of (A) 1,4-dicyanobenzene (starting material) and (B) the reaction mixture obtained after treatment with the 4-electron reduced form of silicotungstic acid (10:1 ratio), showing no observable conversion.

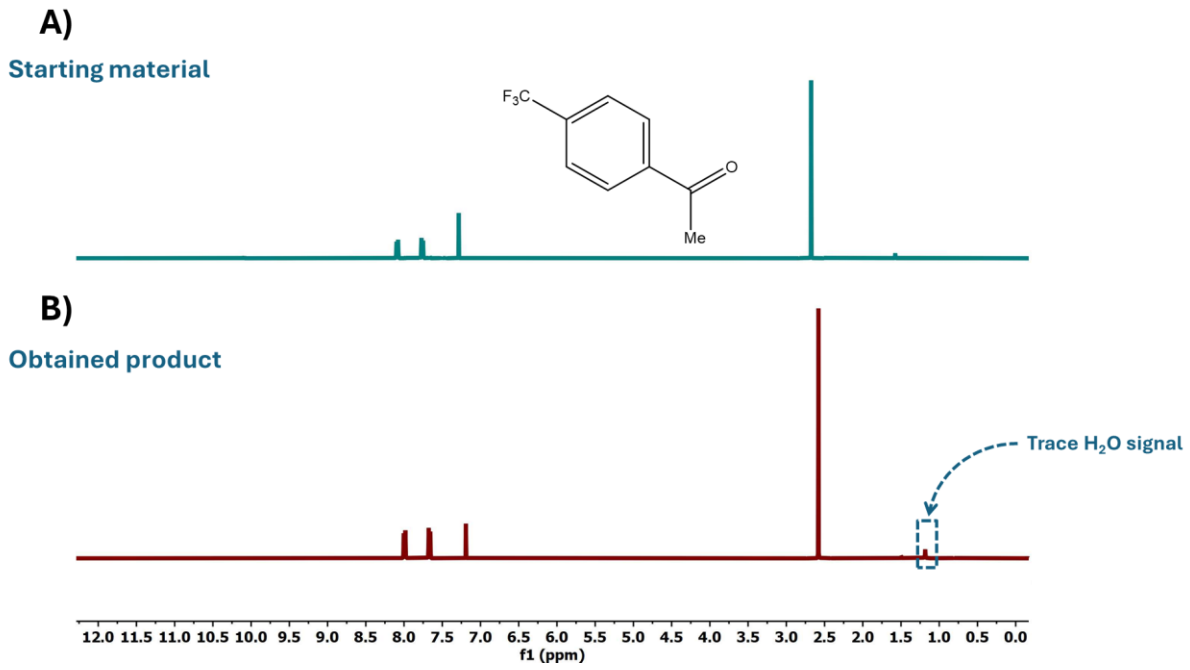


Figure A4.2. Stacked ^{1}H NMR spectra ($CDCl_3$, 400 MHz) of (A) 4'-(trifluoromethyl)acetophenone (starting material) and (B) the reaction mixture obtained after treatment with the 4-electron reduced form of silicotungstic acid (10:1 ratio), showing no observable conversion.

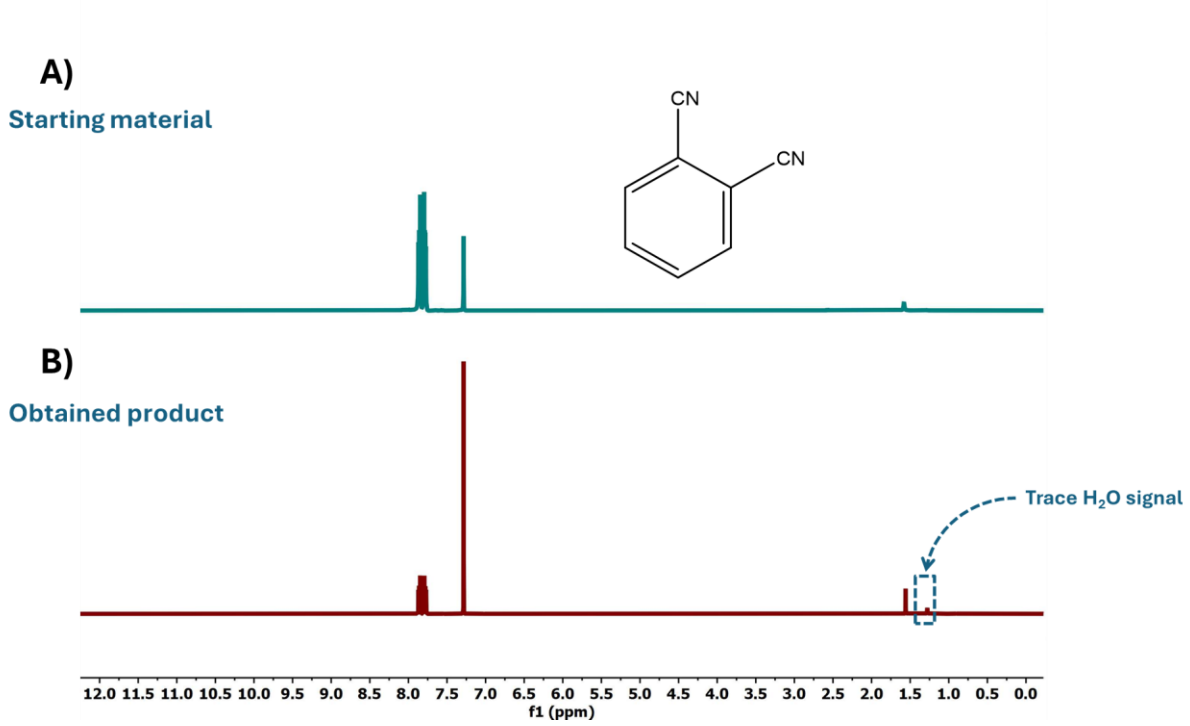


Figure A4.3. Stacked ^{1}H NMR spectra ($CDCl_3$, 400 MHz) of (A) 1,2-dicyanobenzene (starting material) and (B) the reaction mixture obtained after treatment with the 4-electron reduced form of silicotungstic acid (10:1 ratio), showing no observable conversion.

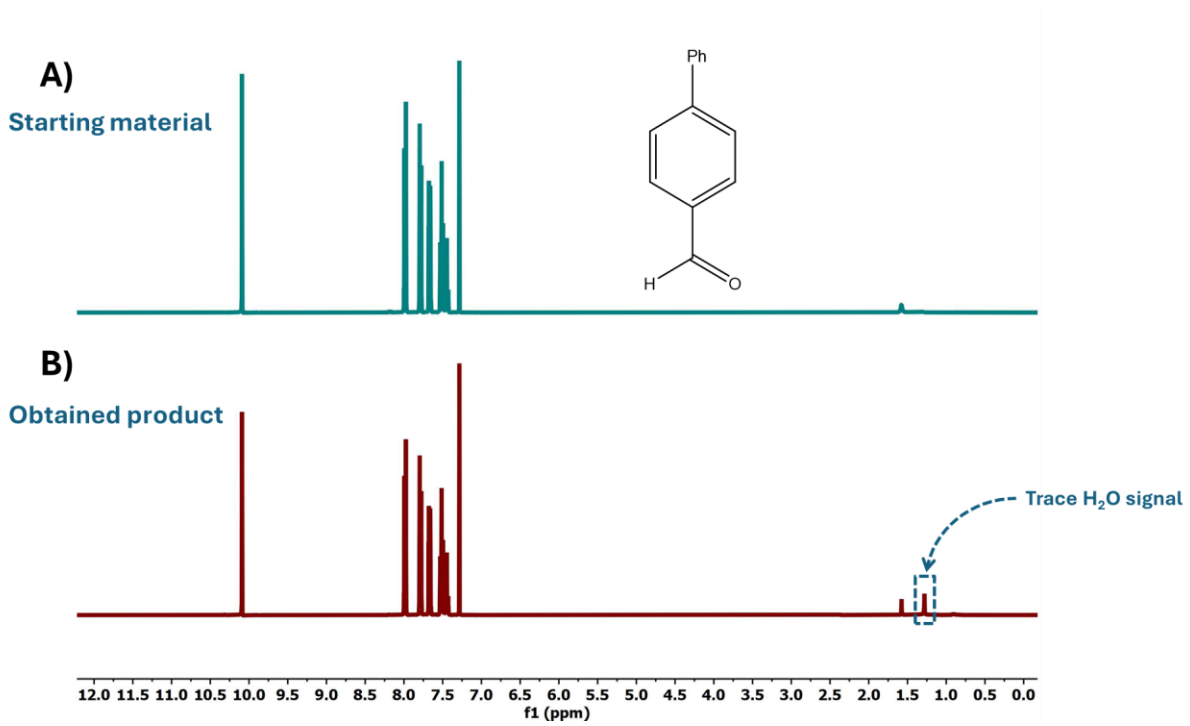


Figure A4.4. Stacked ^{1}H NMR spectra ($CDCl_3$, 400 MHz) of (A) biphenyl-4-carboxaldehyde (starting material) and (B) the reaction mixture obtained after treatment with the 4-electron reduced form of silicotungstic acid (10:1 ratio), showing no observable conversion.

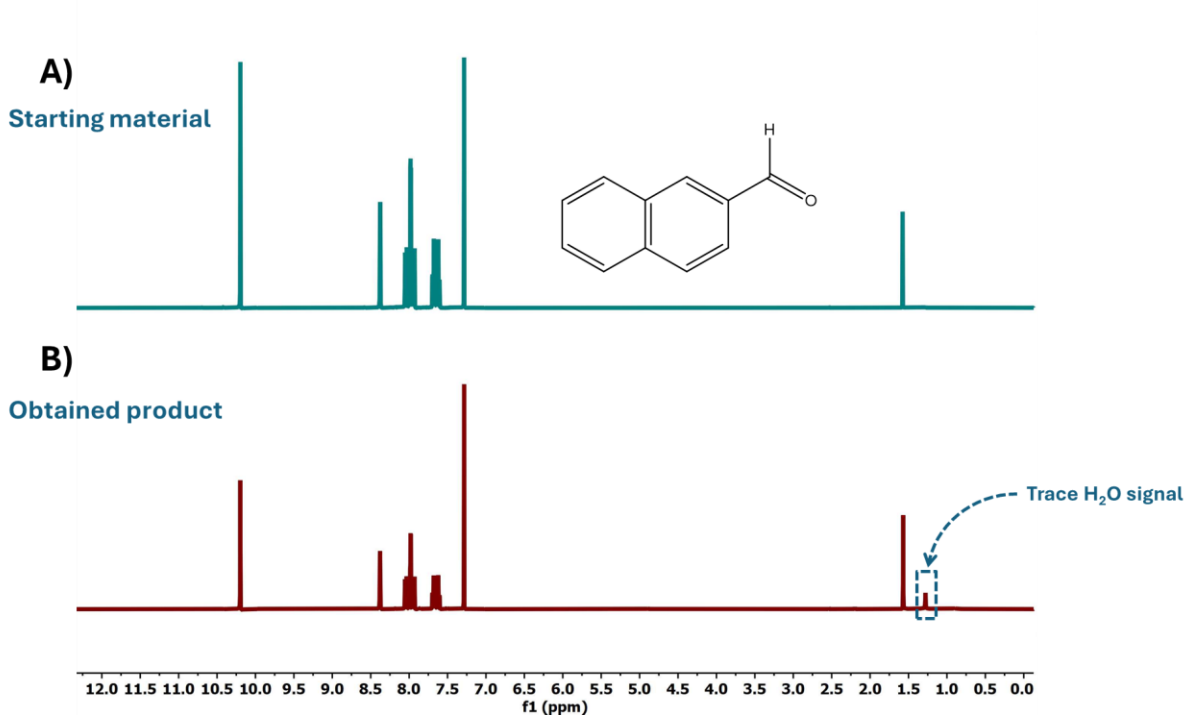


Figure A4.5. Stacked ^{1}H NMR spectra ($CDCl_3$, 400 MHz) of (A) 2-naphthaldehyde (starting material) and (B) the reaction mixture obtained after treatment with the 4-electron reduced form of silicotungstic acid (10:1 ratio), showing no observable conversion.

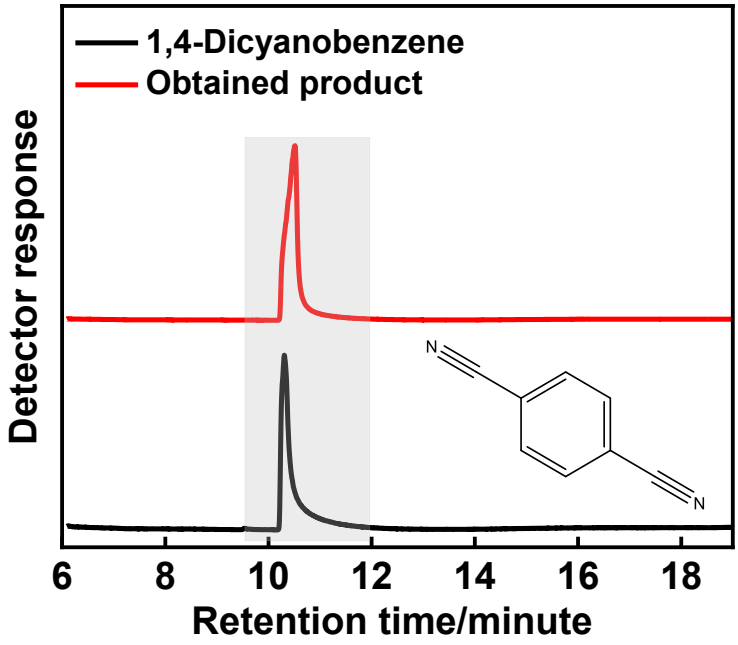


Figure A4.6. Stacked GC-MS chromatograms of (A) 1,4-dicyanobenzene (starting material) and (B) the reaction mixture obtained after treatment with the 4-electron reduced form of silicotungstic acid (10:1 ratio), confirming the absence of new product peaks.

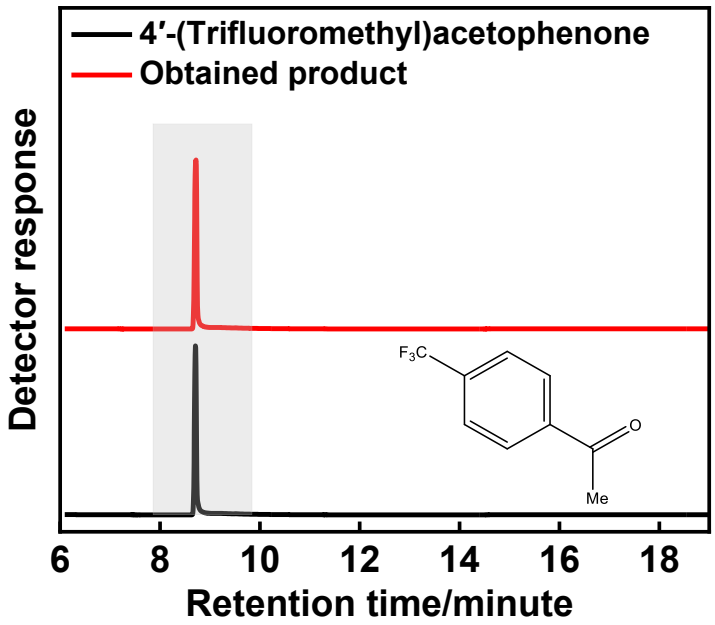


Figure A4.7. Stacked GC-MS chromatograms of (A) 4'-(trifluoromethyl)acetophenone (starting material) and (B) the reaction mixture obtained after treatment with the 4-electron reduced form of silicotungstic acid (10:1 ratio), confirming the absence of new product peaks.

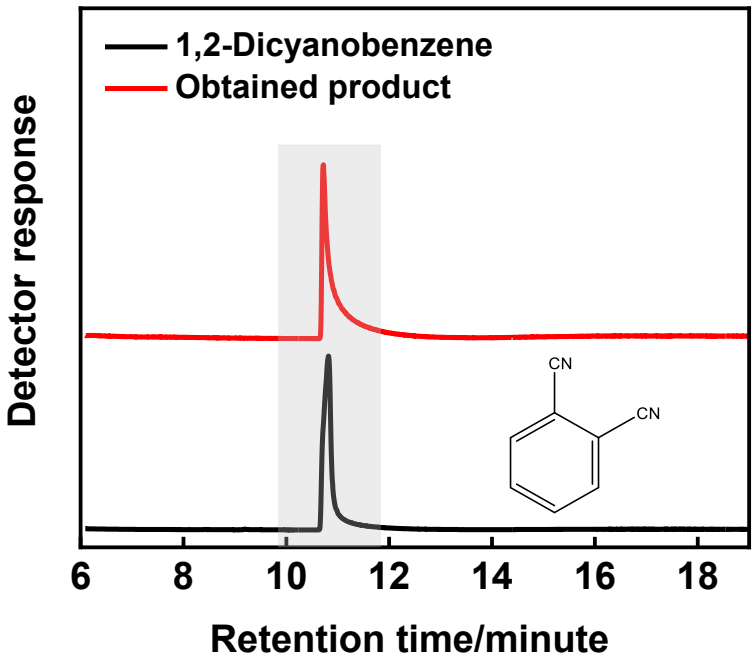


Figure A4.8. Stacked GC-MS chromatograms of (A) 1,2-dicyanobenzene (starting material) and (B) the reaction mixture obtained after treatment with the 4-electron reduced form of silicotungstic acid (10:1 ratio), confirming the absence of new product peaks.

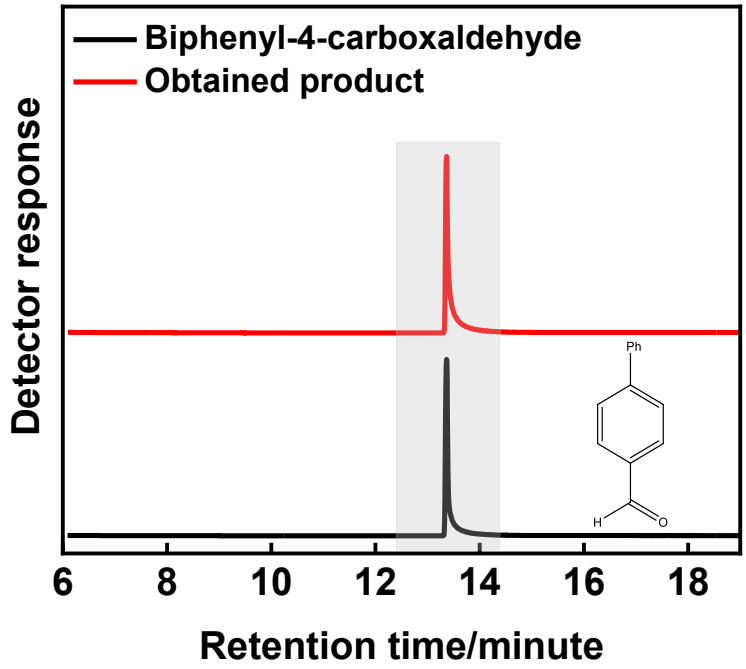


Figure A4.9. Stacked GC-MS chromatograms of (A) biphenyl-4-carboxaldehyde (starting material) and (B) the reaction mixture obtained after treatment with the 4-electron reduced form of silicotungstic acid (10:1 ratio), confirming the absence of new product peaks.

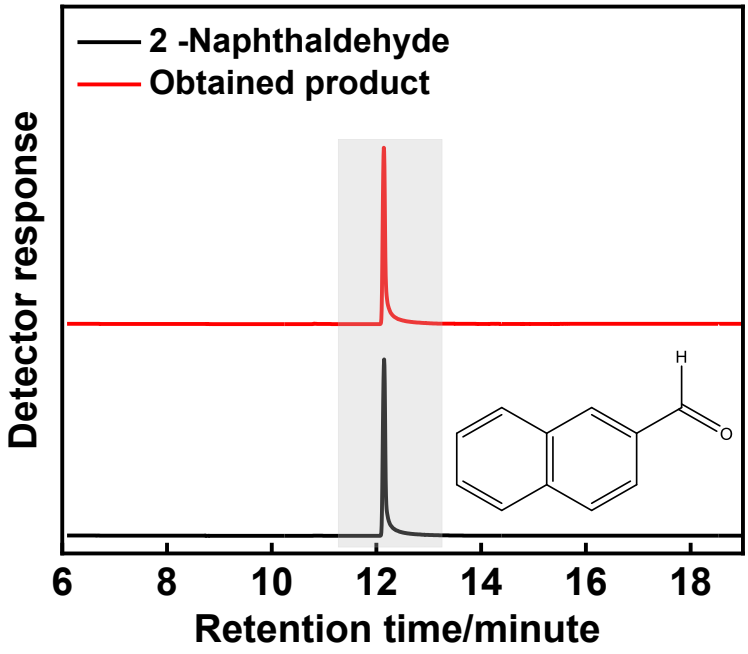


Figure A4.10. Stacked GC-MS chromatograms of (A) 2-naphthaldehyde (starting material) and (B) the reaction mixture obtained after treatment with the 4-electron reduced form of silicotungstic acid (10:1 ratio), confirming the absence of new product peaks.

4.6 References

1 C. Boskovic, M. Sadek, R. T. C. Brownlee, A. M. Bond and A. G. Wedd, *J. Chem. Soc., Dalton Trans.*, 2001, 187–196.

2 S. P. E. Smith and J. B. Christian, *Electrochim. Acta*, 2008, **53**, 2994–3001.

3 J. P. Launay, *J. Inorg. Nucl. Chem.*, 1976, **38**, 807–816.

4 C. Falaise, *Eur. J. Inorg. Chem.*, 2025, 28, e202400827.

5 B. Keïta and L. Nadjo, *J. Electroanal. Chem. Interfacial Electrochem.*, 1985, **191**, 441–448.

6 B. Keita and L. Nadjo, *J. Electroanal. Chem. Interfacial Electrochem.*, 1987, **217**, 287–304.

7 A. D. Stergiou, D. H. Broadhurst and M. D. Symes, *ACS Org. Inorg. Au*, 2023, **3**, 51–58.

8 L. MacDonald, B. Rausch, M. D. Symes and L. Cronin, *Chem. Commun.*, 2018, **54**, 1093–1096.

9 S. Dong, X. Xi and M. Tian, *J. Electroanal. Chem.*, 1995, **385**, 227–233.

Chapter 5: Electrochemical Investigation of Polyoxometalate Mediators for Carbon Monoxide Reduction

Synopsis

This chapter explores the feasibility of using electrochemically reduced polyoxometalates as mediators for the chemical reduction of carbon monoxide. Phosphomolybdic acid and silicotungstic acid were chosen because they are capable of undergoing multiple electron-transfer processes in acidic aqueous solutions. In the first step, the mediators were electrochemically reduced and subsequently exposed to carbon monoxide in a separate reaction stage to determine whether the electrons stored in the reduced species could be transferred to CO. Phosphomolybdic acid was reduced to a 4-electron form, whereas silicotungstic acid was reduced to both 4-electron and 6-electron forms. The resulting reduced solutions were then reacted with carbon monoxide by bubbling CO through the electrolyte. Further experiments were conducted with a gold catalyst present to examine whether interactions with a catalytic surface could promote the activation and subsequent reduction of CO. Under the conditions tested, no CO reduction products were detected by GC and ^{1}H NMR analysis. These observations indicate that while polyoxometalates can serve as multi-electron redox reservoirs, their reduced forms alone are not capable of activating or reducing carbon monoxide under the conditions investigated. Importantly, the presence of a gold catalyst did not lead to any detectable CO reduction products, indicating that gold is not an effective catalytic surface for promoting this transformation in combination with the mediator. The results therefore emphasise that successful CO reduction requires not only electron storage, but also a catalytic system capable of efficiently adsorbing and activating CO prior to electron transfer.

Acknowledgements and Declarations

The work presented in this chapter was carried out by the author under the supervision of Professor Mark Symes. I am grateful to Professor Symes for his valuable input and guidance during the development of this project.

Abstract

The electrochemical reduction of carbon monoxide represents a potential route for the sustainable production of fuels and value-added chemicals. However, the activation of CO remains a significant challenge due to the strength of the C≡O bond. In this chapter, the possibility of using electrochemically reduced polyoxometalates as soluble redox mediators for the reduction of carbon monoxide was investigated. Phosphomolybdic acid and silicotungstic acid were selected as representative Keggin type polyoxometalates capable of undergoing multi-electron redox processes in acidic aqueous media.

Phosphomolybdic acid was reduced potentiostatically at +0.15 V vs NHE. A total charge of 3322 C was passed, corresponding to approximately four electrons per Keggin unit on the basis of charge alone. However, given the relatively positive applied potential, contributions from competing processes cannot be excluded. Silicotungstic acid was reduced to the 4-electron form under potentiostatic conditions and further reduced to 6-electron form using galvanostatic electrolysis.

Following electrochemical reduction, the mediator solutions were transferred to a separate reaction vessel and reacted with carbon monoxide in a non-electrochemical step by bubbling CO through the solution. Additional experiments were performed in the presence of a gold catalyst to assess whether assess whether surface-mediated activation of CO could promote reduction.

Gas-phase products were examined by gas chromatography, and liquid-phase samples were characterised using ^{1}H NMR spectroscopy. No products attributed to carbon monoxide reduction were detected under any of the conditions investigated. Importantly, no reactivity was observed even in the presence of a gold catalyst, indicating that gold does not provide sufficient activation of CO in this system. Instead, the stored electrons are preferentially consumed in competing processes such as proton reduction.

These findings demonstrate that, although polyoxometalates can function as multi-electron redox reservoirs, electron storage alone is insufficient to enable carbon monoxide reduction. The results

suggest that successful mediator based CO reduction likely requires coupling with catalytic systems capable of effectively adsorbing and activating CO prior to electron transfer.

5.1 Introduction

The electrochemical reduction of carbon monoxide (CO) has attracted considerable attention due to its potential role in sustainable chemical synthesis and carbon utilisation strategies.[1,2] CO is widely utilised in industrial chemistry as a C1 feedstock for the production of fuels and a variety of value-added compounds, including hydrocarbons and alcohols. CO is also an important intermediate in electrochemical CO_2 reaction, where its further reduction can lead to multicarbon product.[1–3] However, its reduction remains challenging due to its high thermodynamic stability and the strength of the C≡O bond.[4]

Current approaches to electrochemical CO reduction predominantly rely on metal-based electrocatalysts, where CO interacts with the electrode surface and undergoes subsequent electron- and proton-transfer processes.[1,5,6] The nature of the catalytic surface plays an important role in the adsorption and activation of CO and therefore influences the subsequent reaction pathways. Copper-based catalysts have received particular attention because of their ability to promote further CO reduction and carbon–carbon bond formation.[1,3,7] Despite these advances, these approaches depend strongly on interactions between CO and the catalytic surface.

To address these limitations, mediated electrochemical systems may offer a possible approach, in which a soluble redox mediator is electrochemically reduced and subsequently transfers the stored electrons to the substrate in solution.[8–10]

Polyoxometalates (POMs) are a class of metal oxygen cluster compounds that can undergo reversible multi-electron redox processes while largely maintaining structural integrity.[11,12] Their ability to store multiple electrons within a single molecular framework has led to their investigation as soluble redox mediators in indirect electrochemical reduction systems.[12]

Among the various polyoxometalates, phosphomolybdic acid and silicotungstic acid are well known Keggin type structures that exhibit well defined electrochemical behaviour in acidic aqueous media. These polyoxometalates were selected because of their ability to undergo multi-electron reduction and store multiple electrons, which could potentially be transferred to CO during the subsequent chemical reaction step.[11,13]

However, despite their favourable redox properties, whether reduced polyoxometalates can transfer their stored electrons directly to carbon monoxide remains uncertain. This may be particularly significant for carbon monoxide, where activation of the C≡O bond generally requires interactions with a catalytic metal surface.[5,6]

The hypothesis investigated in this chapter was that electrons stored within electrochemically reduced polyoxometalates could subsequently be transferred to carbon monoxide, thereby enabling its chemical reduction. The rationale for this approach was to use the polyoxometalate as a soluble multi electron redox mediator, separating electrochemical electron storage from the subsequent chemical reduction of carbon monoxide.

In this chapter, the possibility of using electrochemically reduced polyoxometalates as mediators for carbon monoxide reduction was investigated. Phosphomolybdic acid was reduced electrochemically to approximately the 4-electron form, while silicotungstic acid was reduced to the 4-electron and 6-electron forms under the conditions described in Chapter 3. The reduced mediator solutions were subsequently exposed to carbon monoxide in a separate chemical step by bubbling CO through the solution. Additional experiments were performed in the presence of a gold catalyst to examine whether adsorption of CO on a metal surface could facilitate activation of the molecule and promote reduction.[5,6]

The results of these experiments provide insight into the limitations of transferring stored electrons from reduced polyoxometalates to carbon monoxide and highlight the limitations of mediator-based approaches for carbon monoxide reduction under the conditions investigated.

5.2 Experimental

5.2.1 Materials

Phosphomolybdic acid hydrate ($H_3PMo_{12}O_{40}\cdot xH_2O$) was obtained from Tokyo Chemical Industry (TCI) and used as received. Gold gauze (52 mesh, woven from 0.102 mm wire, 99.99%, 50 × 50 mm) and platinum gauze (52 mesh, woven from 0.10 mm wire, 99.9%, 50 × 50 mm) were purchased from Alfa Aesar. Research-grade carbon monoxide gas (N3.7, 99.97%) was supplied by BOC Ltd. and used without further purification.

Silicotungstic acid ($H_4SiW_{12}O_{40}\cdot xH_2O$), supporting electrolytes, Nafion® membranes, and other reagents used for electrochemical experiments were obtained and handled as described in Section 3.2.1. Deionised water was used for all solution preparations. Electrochemical experiments were performed under an inert nitrogen atmosphere in order to minimise oxidation of reduced mediator species.

5.2.2 Electrochemical Generation of Reduced Mediators

Electrochemical reduction of the polyoxometalate mediators was performed using the three-electrode configuration and divided H-cell described previously in Section 3.2.2. A carbon felt working electrode (total geometric dimensions: 2.5 × 4.0 cm^2), platinum mesh counter electrode, and Ag/AgCl reference electrode were employed. All electrolysis experiments were conducted under a nitrogen atmosphere to minimise oxidation of the reduced species.

Phosphomolybdic acid solutions (0.5 M) were reduced electrochemically under potentiostatic control at +0.15 V vs NHE, corresponding to reduction beyond the main reduction waves observed in cyclic voltammetry. Electrolysis was continued until the current decayed to near steady state values.

The progress of electrolysis was monitored by recording both the charge passed and current response as a function of time (Figure 5.1). The charge-time profile (Figure 5.1a) shows an initial linear increase in the magnitude of charge passed over the first ~6 h, corresponding to the primary reduction process.

Beyond this point, the slope of the curve decreases, with a total cathodic charge of approximately 3322 C passed over the complete electrolysis experiment. The continued passage of charge at longer times is likely to include contributions from background or competing processes rather than solely further reduction of the polyoxometalate.

This behaviour is also evident in the current–time profile (Figure 5.1b), where the cathodic current decreases initially but then approaches a relatively constant value after ~6 h, consistent with the cessation of the main reduction process.

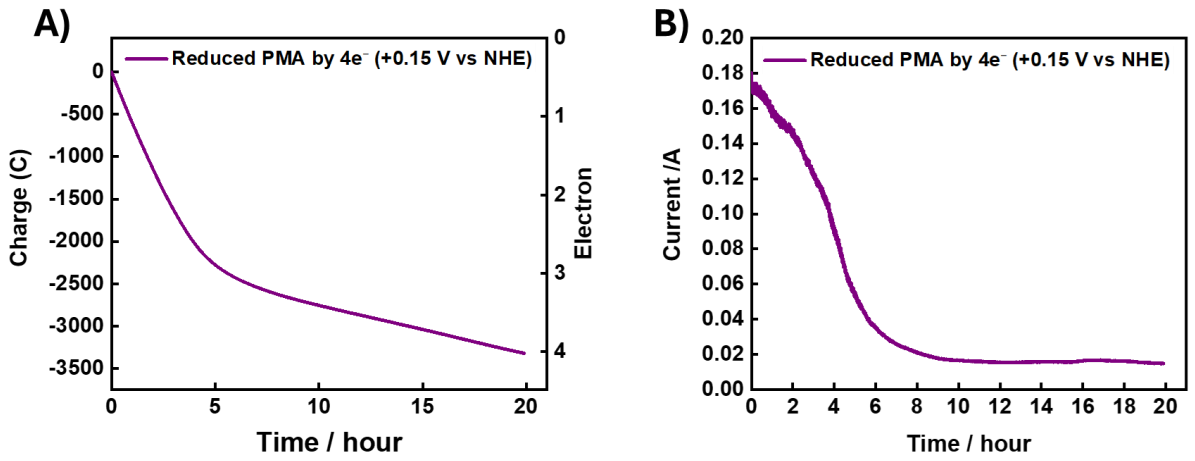


Figure 5.1. A) Charge passed (C vs time) and B) current response (I vs time) recorded during potentiostatic electrolysis of 0.5 M phosphomolybdic acid (PMA) at +0.15 V vs NHE under a nitrogen atmosphere. The decay in current and decrease in the slope of the charge–time profile indicate the cessation of the primary reduction process and the increasing contribution of background processes.

Based on the charge associated with the initial linear region of the charge-time profile (approximately 2000 C) and the concentration of phosphomolybdic acid (0.5 M, 17 mL) this corresponds to a reduction of approximately 2–3 electrons per Keggin unit. This estimate excludes the additional charge passed at longer electrolysis times, which is attributed to background processes rather than further reduction of the polyoxometalate. These observations are consistent with the electrochemical behaviour observed in cyclic voltammetry and indicate that full four-electron reduction is not achieved under these conditions.

Silicotungstic acid solutions (0.5 M) were reduced electrochemically under two different conditions in order to generate mediators with different degrees of reduction. The 4-electron reduced form was prepared potentiostatically at −0.36 V vs NHE following the procedure described in Chapter 3. Deeper reduction to approximately the 6-electron form was achieved under galvanostatic conditions by applying a constant cathodic current of −100 mA until the desired charge had been delivered.

Following electrochemical reduction, the reduced mediator solutions were transferred under a nitrogen atmosphere to a round bottom flask containing approximately 10 mL of the reduced mediator solution for subsequent reaction with carbon monoxide in a separate chemical step.

5.2.3 Reaction of Reduced Mediator with Carbon Monoxide

Following electrochemical reduction, the mediator solutions were exposed to carbon monoxide in a separate chemical step. Carbon monoxide gas was bubbled continuously through the reduced mediator solution for 6 hours at ambient temperature under constant stirring.

Two sets of experiments were performed. In the first set, carbon monoxide was bubbled directly through the reduced mediator solution without the addition of any catalyst. In the second set, a piece of gold gauze was introduced into the reaction flask prior to CO bubbling in order to investigate whether adsorption of CO on a metal surface could facilitate activation of the molecule and promote electron transfer from the reduced mediator.

Headspace gas samples were collected at defined time intervals and analysed by gas chromatography (GC) to detect any gaseous products formed during the reaction. Headspace gas (0.5 mL) was withdrawn using a gas tight syringe and injected directly into the GC instrument for analysis. The reaction solutions were also analysed by ^{1}H NMR spectroscopy to determine whether any liquid-phase reduction products were present.[8]

A schematic overview of the experimental procedure used for the reaction of the reduced polyoxometalate mediators with carbon monoxide and subsequent product analysis is shown in Figure 5.2.

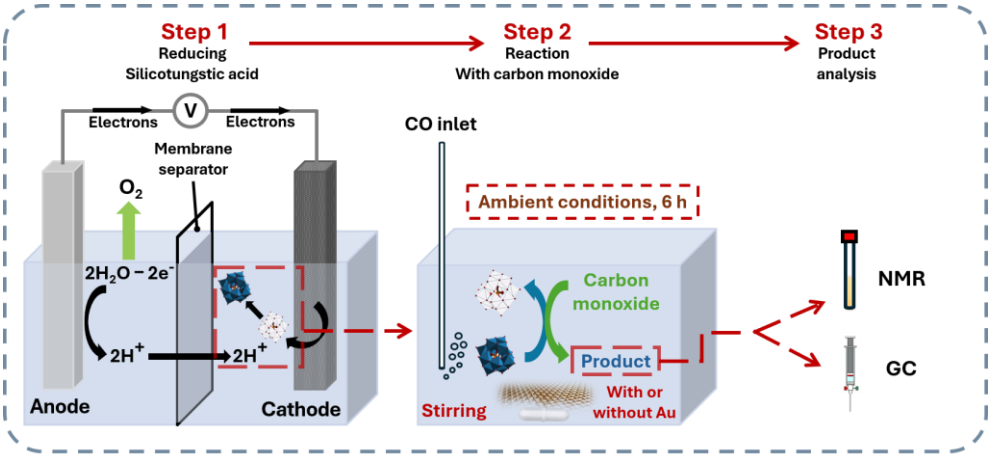


Figure 5.2. Schematic overview of the experimental procedure used to investigate carbon monoxide reduction with electrochemically reduced polyoxometalate mediators. Step 1: electrochemical reduction of the polyoxometalate mediators. Step 2: reaction of the reduced mediator with carbon monoxide by bubbling CO through the solution for 6 h under ambient conditions with constant stirring, either in the absence or presence of Au gauze. Step 3: analysis of the reaction solution and beadspace by ^{1}H NMR spectroscopy and GC, respectively.

5.3 Results and Discussion

5.3.1 Electrochemical behaviour of phosphomolybdic acid

The electrochemical behaviour of phosphomolybdic acid was first examined by cyclic voltammetry in order to determine whether the presence of carbon monoxide influences the redox chemistry of the mediator. Cyclic voltammograms were recorded under different gas atmospheres including air, nitrogen, argon, and carbon monoxide (Figure 5.3). Measurements were conducted using a platinum disc working electrode (geometric area = 0.0314 cm^2), a platinum wire (1 mm diameter) as the counter electrode, and an Ag/AgCl reference electrode in 0.5 M phosphomolybdic acid solution at a scan rate of 100 mV s^{-1}.

The voltammograms exhibit the characteristic reduction waves associated with the stepwise reduction of the Keggin type polyoxometalate framework. Comparison of the voltammograms recorded under different gases shows that the overall electrochemical behaviour of the polyoxometalate remains largely unchanged. In particular, the positions and shapes of the reduction waves are essentially identical regardless of the gas atmosphere.

This observation indicates that carbon monoxide does not significantly interact with the mediator during the electrochemical step, at least on the timescales of the cyclic voltammetry experiment. The absence of any additional catalytic current under CO further suggests that polyoxometalate does not directly promote electrochemical CO reduction under the conditions investigated.

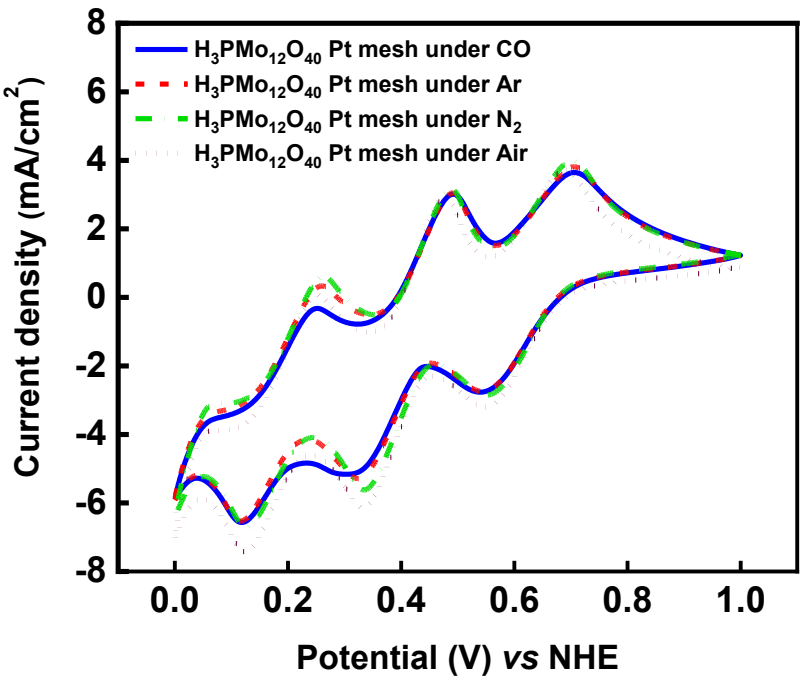


Figure 5.3. Cyclic voltammetry of phosphomolybdic acid (0.5 M) recorded under different gas atmospheres (air, N_2, Ar, and CO). Measurements were conducted using a platinum disc working electrode (geometric area = 0.0314 cm^2), a platinum wire (1 mm diameter) counter electrode, and an Ag/AgCl reference electrode at a scan rate of 100 mV s^{-1}. The voltammograms show similar electrochemical behaviour in all cases, indicating no significant interaction between CO and the mediator under these conditions.

5.3.2 Influence of electrode material

Because the interaction and activation of carbon monoxide can be influenced by the catalytic properties of the electrode surface, cyclic voltammetry measurements were also carried out using different electrode materials. Cyclic voltammograms of the polyoxometalate were recorded using a glassy carbon disc electrode (geometric area = 0.071 cm^2), a platinum disc electrode (geometric area = 0.0314 cm^2), and a gold wire electrodes (0.5 mm diameter, 1.0 cm exposed length, geometric area ≈ 0.157 cm^2) under otherwise identical conditions in the presence of CO (Figure 5.4).

The voltammograms obtained for all three electrodes display the characteristic redox waves associated with the stepwise reduction and oxidation of the phosphomolybdic acid Keggin cluster. The positions of these redox waves are broadly similar for the three electrode materials, indicating that the intrinsic redox behaviour of the polyoxometalate mediator remains largely unchanged.

However, differences in current magnitude are observed, particularly for the gold electrode, which exhibits significantly higher currents compared with the platinum and glassy carbon electrodes. This behaviour may reflect differences in surface properties or electron transfer kinetics at the electrode interface. Despite these variations, no additional features indicative of catalytic CO reduction are observed.[14]

These results indicate that while the electrode surface influences the magnitude of the electrochemical response, the fundamental redox chemistry is governed by the polyoxometalate mediator itself rather than by catalytic effects of the electrode surface.

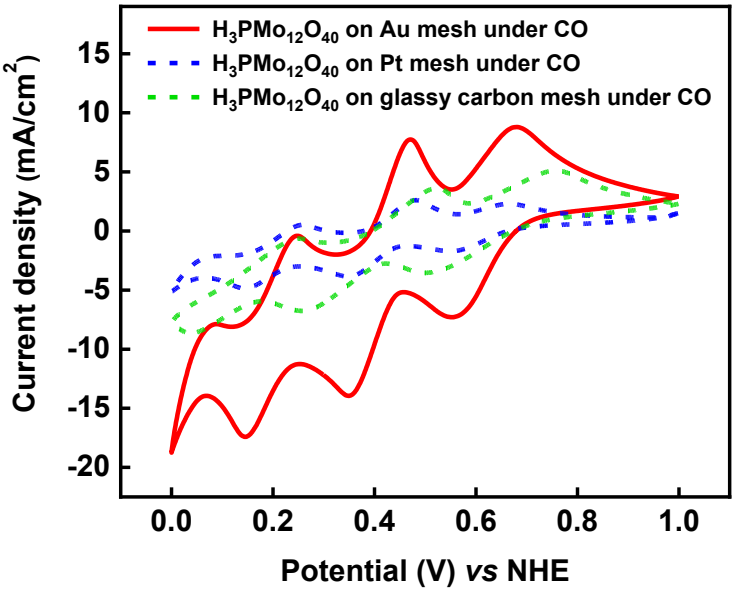


Figure 5.4. Comparison of cyclic voltammograms of 0.5 M phosphomolybdic acid recorded on glassy carbon disc electrode (geometric area = 0.071 cm^2), platinum disc electrode (geometric area = 0.0314 cm^2), and a gold wire electrode (0.5 mm diameter, 1.0 cm exposed length, geometric area ≈ 0.157 cm^2). Measurements were conducted under identical conditions in the presence of CO at a scan rate of 100 m V s^{-1}. Comparable redox features are observed across all electrode materials within the applied potential window.

5.3.3 Reactivity of reduced silicotungstic acid with CO

Following electrochemical generation of reduced mediator species, their ability to transfer stored electrons to carbon monoxide was investigated in a separate chemical step. In these experiments, carbon monoxide was bubbled through the reduced silicotungstic acid solutions, and the headspace gases were analysed by gas chromatography.

Initial experiments were performed using the 4-electron reduced form of silicotungstic acid. Representative gas chromatograms obtained under different conditions are shown in Figure 5.5. Experiments were conducted both in the absence of a catalyst and in the presence of a gold gauze catalyst for varying reaction times.

The chromatograms are dominated by a peak corresponding to carbon monoxide (retention time approximately 9.2 minutes), with no additional peaks corresponding to potential reduction products. The absence of new peaks indicates that no detectable gaseous reduction products were formed during the reaction, even after prolonged exposure to carbon monoxide.

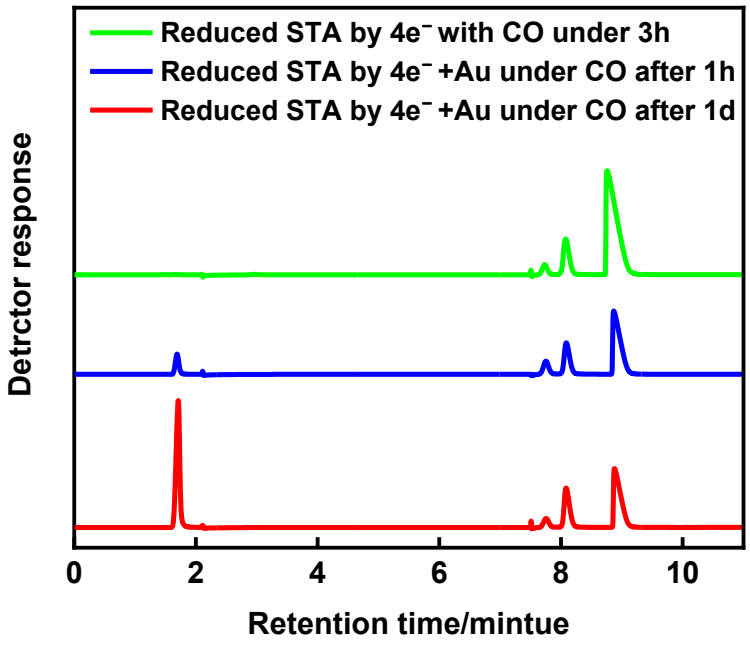


Figure 5.5. Gas chromatography obtained after exposure of 4-electron reduced silicotungstic acid (0.5 M) to CO under different conditions: without Au catalyst after 3 h, with Au catalyst after 1 h, and with Au catalyst after 24 h. The observed peaks correspond to H_2 (approximately 1.76 min), O_2 (approximately 8.10 min), and CO (approximately 9.20 min). No additional peaks corresponding to reduction products were detected.

5.3.4 Effect of deeper reduction of silicotungstic acid

To investigate whether a higher degree of reduction could promote reactivity toward carbon monoxide, similar experiments were performed using a higher reduced form of silicotungstic acid. Gas chromatography comparing reactions of the moderately reduced and more highly reduced species after exposure to CO for 24 hours in the presence of a gold catalyst are shown in Figure 5.6.

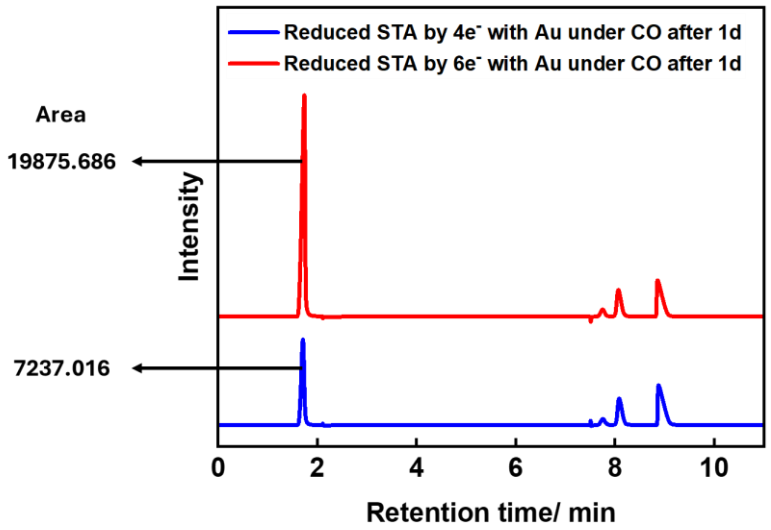


Figure 5.6. Gas chromatography comparing reaction of 4-electron and 6-electron reduced silicotungstic acid after exposure to CO for 24 h in the presence of a gold catalyst.

In both cases, the chromatography are dominated by a peak at approximately 1.76 min retention time, corresponding to hydrogen. The intensity of this peak is significantly greater for the more highly reduced mediator, with the peak area increases from 7237.016 for the 4-electron reduced mediator to 19875.686 for the 6-electron reduced species (approximately 2.75-fold). This increase enhanced to hydrogen evolution under strongly reducing conditions. This behaviour is consistent with the electrochemical results discussed in Chapter 3, where deeper reduction favours competing proton reduction processes.[12,14]

A second peak corresponding to carbon monoxide is observed at approximately 9.20 min, confirming that the majority of CO remains unreacted under the experimental conditions. Potential reduction products such as methane would be expected to appear at a retention time of approximately 8.88 min under the conditions employed; however, no peaks were observed in this region. These results indicate that increasing the degree of reduction does not promote measurable CO reduction but instead enhances competing hydrogen evolution.

5.3.5 Reactivity of reduced phosphomolybdic acid with CO

The reactivity of electrochemically reduced phosphomolybdic acid was also investigated under similar conditions. The extent of reduction was estimated based on the charge passed during electrolysis. However, coulometric confirmation of the exact electron stoichiometry was not performed.

Gas chromatography analysis of the reaction mixtures, both in the absence and presence of a gold catalyst, shows only a peak corresponding to carbon monoxide, with no detectable formation of reduction products (Figure 5.7). These observations are consistent with those obtained for silicotungstic acid and indicate that reduced phosphomolybdic acid does not exhibit measurable reactivity toward carbon monoxide under the conditions investigated.

Minor variations in peak intensity between traces are attributed to differences in sampling and injection conditions rather than chemical changes.

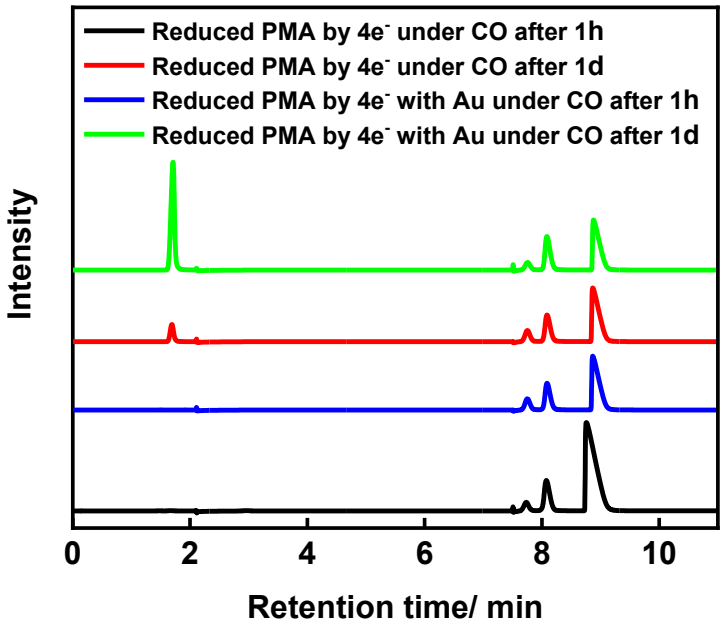


Figure 5.7. Gas chromatography obtained after exposure of 4-electron reduced phosphomolybdic acid (PMA) to CO under different conditions: without Au catalyst after 1 h and 24 h, and with Au catalyst after 1 h and 24 h.

5.3.6 NMR analysis of reaction mixtures

In addition to gas phase analysis, aliquots of the reaction mixtures were analysed by proton nuclear magnetic resonance ^{1}H NMR spectroscopy to detect potential liquid phase reduction products. Representative spectra obtained after exposure of the reduced mediator solution to CO are shown in Figures 5.8-5.10.

The spectra obtained for the 4-electron reduced silicotungstic acid system show no additional resonances compared with the initial solution (Figure 5.8). Similarly, spectra recorded for the 6-electron reduced silicotungstic acid system likewise show no detectable formation of new species (Figure 5.9).

Threse results confirm that no detectable liquid phase products were generated during the experiments.

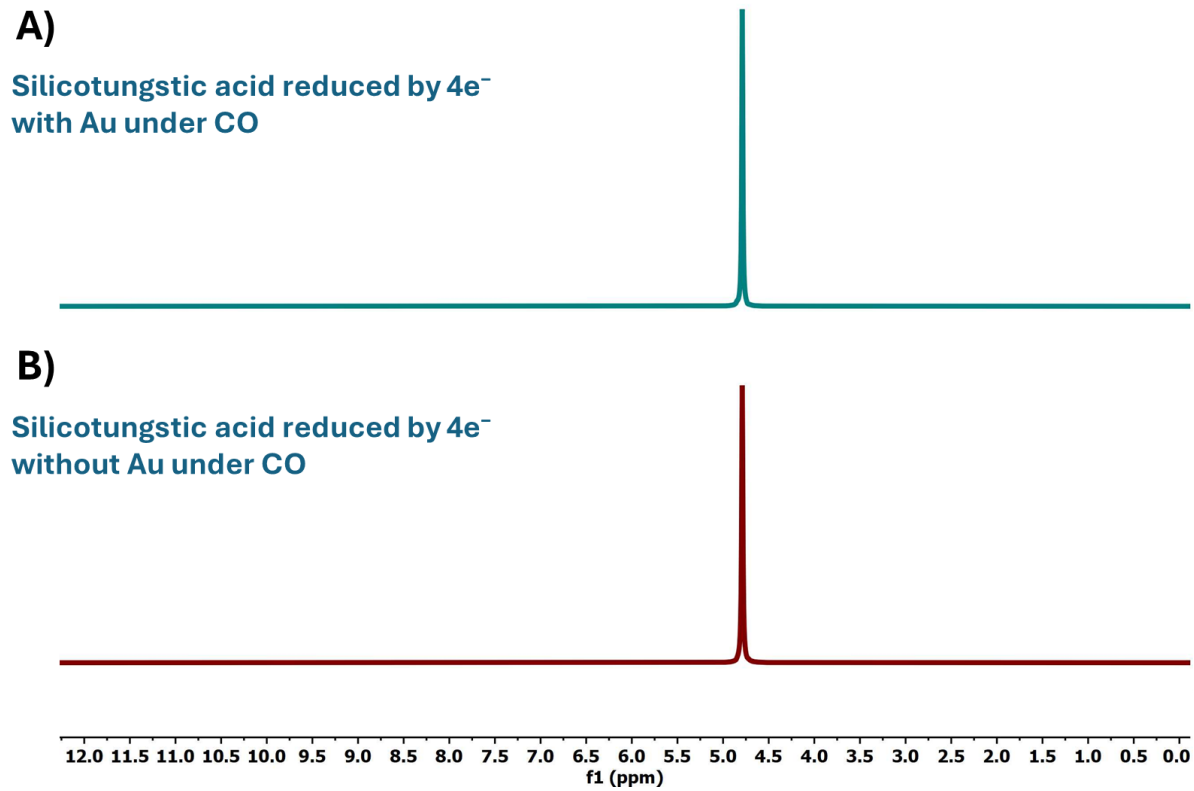


Figure 5.8. ^{1}H NMR spectra of the reaction mixture obtained after exposure of 4-electron reduced silicotungstic acid to CO for 24 h (A) with and (B) without Au catalyst.

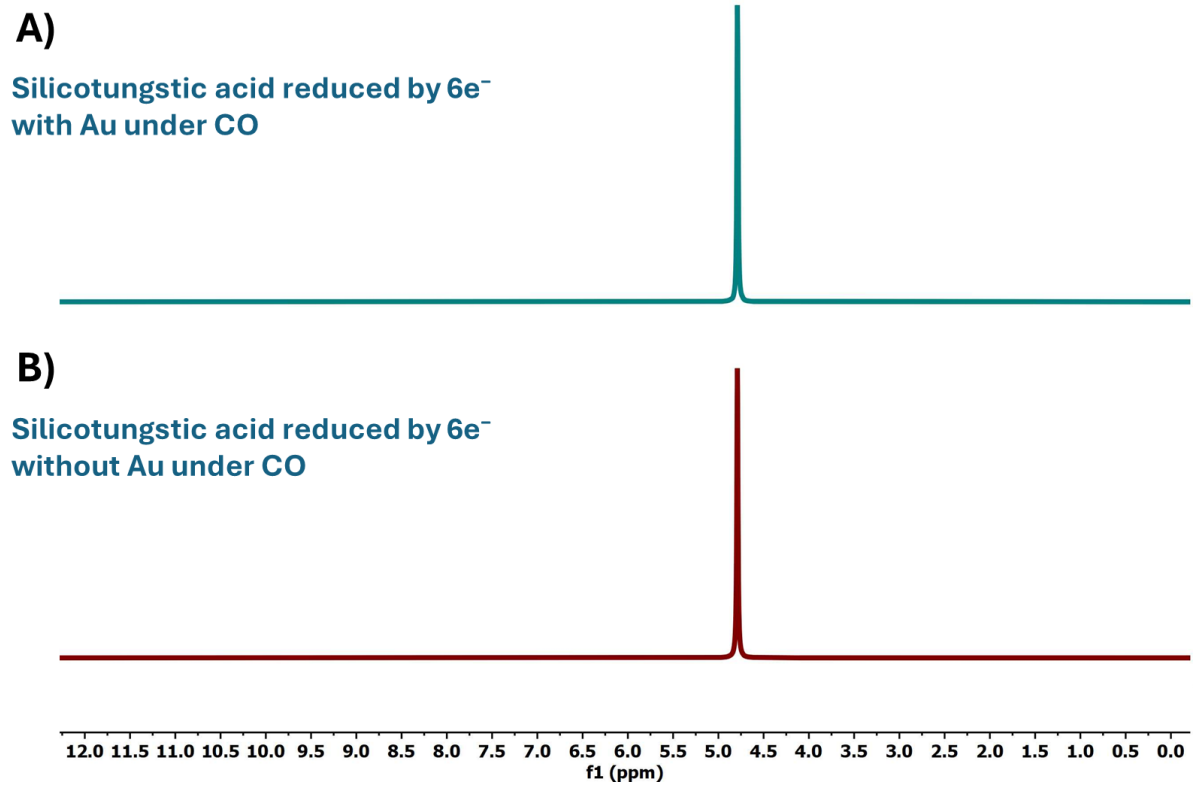


Figure 5.9. ^{1}H NMR spectra of the reaction mixture obtained after exposure of 6-electron reduced silicotungstic acid to CO for 24 h (A) with and (B) without Au catalyst.

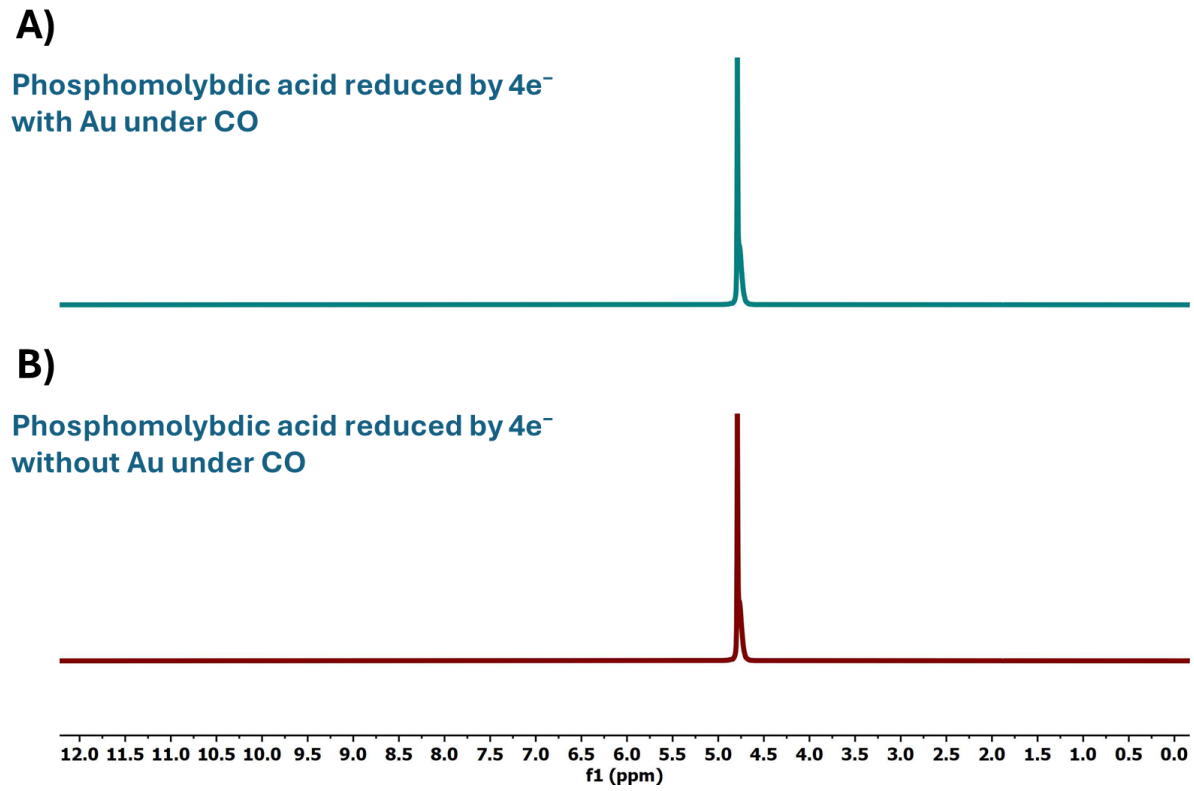


Figure 5.10. ^{1}H NMR spectra of the reaction mixture obtained after exposure of 4-electron reduced phosphomolybdic acid to CO for 24 h (A) with and (B) without Au catalyst.

5.3.7 Implications for CO reduction using polyoxometalate mediators

Overall, the combined GC and NMR analyses indicate that no detectable carbon monoxide reduction occurred under the conditions investigated. Although the polyoxometalate mediators are capable of storing multiple electrons, effective reduction of carbon monoxide requires activation of the strong C≡O bond.[5,6]

Such activation typically occurs through binding of CO to a catalytic metal surface via metal–CO interactions, which facilitate weakening of the bond prior to electron transfer. In contrast, polyoxometalates operate primarily through outer sphere electron transfer and do not provide suitable sites for substrate binding or activation.

The addition of a gold catalyst was intended to promote adsorption and activation of CO. However, no measurable reactivity was observed, indicating that gold is not sufficiently active for CO reduction under the conditions employed. More active metals, such as copper, are known to facilitate CO reduction. However, they were not investigated in this work due to their limited stability in strongly acidic media. Under the acidic conditions used here, copper would be expected to undergo dissolution, preventing its effective use as a catalyst.[5]

These findings highlight an important limitation of mediator based approaches to CO reduction. While polyoxometalates function efficiently as multi-electron redox reservoirs, additional catalyst components capable of activating carbon monoxide are required to achieve efficient reduction.

5.4 Mechanistic Considerations and Limitations

The experimental results presented in Section 5.3 indicate that no detectable reduction of carbon monoxide was observed under the conditions investigated, despite the presence of electrochemically reduced polyoxometalate mediators capable of storing multiple electrons. These observations highlight important mechanistic limitations associated with the use of reduced polyoxometalates as electron-transfer mediators for CO reduction.

A key limitation arises from the difficulty of activating the carbon monoxide molecule. The C≡O bond is exceptionally strong, with a bond dissociation energy of approximately 1076 kJ mol^{-1}, and reduction of CO typically requires prior adsorption of the molecule onto a catalytic metal surface.[15] Such adsorption weakens the C≡O bond and enables subsequent proton coupled electron transfer steps. In the absence of this activation, direct electron transfer from a soluble mediator to CO in solution is kinetically unfavourable.

The polyoxometalates investigated in this study function as soluble redox mediators capable of storing electrons within the metal oxygen framework of the Keggin cluster. While these stored electrons can be transferred to suitable organic substrates, as demonstrated in Chapter 4, the present results indicate that carbon monoxide does not readily accept electrons directly from the reduced mediator species under

the conditions employed. This behaviour is consistent with the absence of any significant changes in the cyclic voltammograms recorded under a carbon monoxide atmosphere and the lack of new products detected by GC and NMR analysis.

Experiments were also performed in the presence of a gold catalyst to investigate whether adsorption of carbon monoxide on a metal surface could promote reduction. However, the presence of gold did not lead to detectable CO reduction products. This observation is consistent with the relatively low catalyst activity of gold for carbon monoxide reduction compared with metals such as copper or nickel.[6]

Furthermore, the results indicate that increasing the degree of reduction of the mediator leads primarily to enhanced hydrogen evolution rather than carbon monoxide conversion. This behaviour reflects competition between proton reduction and substrate reduction under strongly reducing conditions, where proton reduction is kinetically favoured over CO reduction.[5]

Overall, these results indicate that although polyoxometalates are effective multi-electron redox reservoirs, their use as stand alone mediators for carbon monoxide reduction is limited by the absence of a suitable mechanism for CO activation. Future approaches may therefore require hybrid systems in which polyoxometalates function as electron reservoirs coupled with catalytic metal surfaces capable of adsorbing and activating carbon monoxide.

5.5 Conclusions and Future Outlook

This chapter investigated the possibility of using electrochemically reduced polyoxometalates as mediators for the reduction of carbon monoxide. Phosphomolybdic acid and silicotungstic acid were selected as representative Keggin type polyoxometalates due to their ability to undergo multi-electron redox processes in acidic aqueous media. The mediators were first reduced electrochemically and subsequently exposed to carbon monoxide in a separate chemical step in order to evaluate whether the stored electrons could be transferred to CO.

Electrochemical studies showed that phosphomolybdic acid can be reduced under potentiostatic control, with the extent of reduction estimated from the charge passed during electrolysis, although the exact number of electrons transferred could not be independently verified. Silicotungstic acid was also found to access multiple reduced states under conditions described in Chapter 3. However, analysis of the reaction mixture by gas chromatography and ^{1}H NMR spectroscopy showed no detectable formation of products resulting from carbon monoxide reduction, both in the absence and presence of a gold catalyst. These results indicate that the reduced polyoxometalate mediators investigated in this work do not exhibit measurable electron transfer to carbon monoxide under the conditions employed.

The lack of reactivity can be attributed primarily to the difficulty of activating the strong C≡O bond of carbon monoxide. In most catalyst systems, reduction of CO requires adsorption on a catalytic metal surface, which weakens the C≡O bond prior to electron transfer. In contrast, the polyoxometalates studied here act as soluble electron reservoirs and do not provide suitable binding sites for effective CO activation. As a result, the stored electrons remain within the mediator framework rather than being transferred to the substrate.

Future studies may therefore require hybrid systems in which polyoxometalates function as electron reservoirs coupled with catalytic surfaces capable of adsorbing and activating carbon monoxide. Such approaches could potentially combine the advantages of multi-electron storage with effective catalytic activation of small molecules.

5.6 References

1 M. Jouny, G. S. Hutchings and F. Jiao, *Nat. Catal.*, 2019, **2**, 1062–1070.

2 S. Nitopi, E. Bertheussen, S. B. Scott, X. Liu, A. K. Engstfeld, S. Horch, B. Seger, I. E. L. Stephens, K. Chan, C. Hahn, J. K. Nørskov, T. F. Jaramillo and I. Chorkendorff, *Chem. Rev.*, 2019, **119**, 7610–7672.

3 W. Ma, X. He, W. Wang, S. Xie, Q. Zhang and Y. Wang, *Chem. Soc. Rev.*, 2021, **50**, 12897–12914.

4 P. Atkins, J. De Paula and R. Friedman, *Physical chemistry: quanta, matter, and change*, Oxford University Press, 2014.

5 Y. Hori, A. Murata and R. Takahashi, *J. Chem. Soc., Faraday Trans. 1*, 1989, **85**, 2309–2326.

6 K. P. Kuhl, E. R. Cave, D. N. Abram and T. F. Jaramillo, *Energy Environ. Sci.*, 2012, **5**, 7050–7059.

7 Y. Ji, A. Guan and G. Zheng, *Cell Rep. Phys. Sci.*, 2022, **3**, 101072.

8 J.-M. Savéant, *Elements of molecular and biomolecular electrochemistry: an electrochemical approach to electron transfer chemistry*, John Wiley & Sons, 2006.

9 E. Steckhan, *Angew. Chem. Int. Ed. Engl.*, 1986, **25**, 683–701.

10 E. J. Horn, B. R. Rosen and P. S. Baran, *ACS Cent. Sci.*, 2016, **2**, 302–308.

11 M. T. Pope, Y. Jeannin and M. Fournier, *Heteropoly and isopoly oxometalates*, Springer, 1983, vol. 33.

12 M. Sadakane and E. Steckhan, *Chem. Rev.*, 1998, **98**, 219–238.

13 C. L. Hill, *Chem. Rev.*, 1998, **98**, 1–2.

14 A. J. Bard and L. R. Faulkner, *Electrochemical methods: fundamentals and applications*, John Wiley & Sons, Inc., 2001.

15 S. Mehariya, A. Iovine, P. Casella, D. Musmarra, A. Figoli, T. Marino, N. Sharma and A. Molino, in *Lignocellulosic Biomass to Liquid Biofuels*, Elsevier, 2020, pp. 217–248.

Chapter 6: Overall Conclusions and Future Perspectives

Synopsis

This chapter summarises the overall findings of this thesis on polyoxometalates as multi-electron redox mediators in aqueous electrochemical systems. Silicotungstic acid and phosphomolybdic acid were show to undergo controlled multi-electron reduction, with the 2-electron and 4-electron reduced forms exhibiting high reversibility and stability, while deeper reduction leads to hydrogen evolution and structural degradation. The reduced mediators were effective in transferring electrons to activated organic substrates, particularly for the selective reduction of electron deficient aromatic aldehydes, with 4-electron reduced form providing the optimal balance between reducing power and selectivity. In contrast, no reactivity was observed toward carbon monoxide, highlighting the limitation of these systems in the absence of substrate activation. Overall, the results demonstrate that polyoxometalates function as efficient multi-electron redox reservoirs for activated substrates but are limited for reduction of chemically inert molecules.

Chapter 6

6.1 Overall Conclusions

This thesis investigated the electrochemical behaviour and reactivity of polyoxometalates as multi-electron redox mediators in aqueous acidic media, with particular focus on silicotungstic acid and phosphomolybdic acid.

Chapter 1 introduced the fundamental chemistry of polyoxometalates and reviewed their application as redox mediators in electrochemical and catalytic systems, with emphasis on their multi-electron transfer capability and relevance to organic and small molecule reduction.

Chapter 2 outlined the experimental and analytical techniques employed throughout this work, including electrochemical methods and spectroscopic and structural characterisation, which enabled reliable evaluation of mediator behaviour and reactivity.

Chapter 3 established that silicotungstic acid undergoes controlled multi-electron reduction, with the 2-electron and 4-electron reduced forms exhibiting high electrochemical reversibility, structural stability, and efficient charge recovery. In contrast, deeper reduction leads to increased hydrogen evolution, structural degradation, and diminished reversibility, defining a clear practical limit for electron storage.

Building on these findings, Chapter 4 demonstrated that electrochemically reduced silicotungstic acid can function as an effective mediator for indirect organic reduction. In particular, selective conversion of electron deficient aromatic aldehydes to the corresponding alcohols was achieved, with the 4-electron reduced form providing the optimal balance between reducing power and selectivity.

In Chapter 5, the scope of mediator based reduction was extended to carbon monoxide. Despite the use of multi-electron reduced polyoxometalates and the presence of a gold catalyst, no detectable CO reduction products were observed. These results demonstrate that electron storage alone is insufficient for the reduction of chemically inert molecules such as carbon monoxide.

Taken together, the findings of this thesis show that polyoxometalates are effective multi-electron redox reservoirs capable of mediating electron transfer to activated organic substrates, but show limitations in systems where effective substrate activation is required prior to reduction.

6.2 Mechanistic Insights

The findings of this thesis provide important insight into the mechanistic factors governing mediated electrochemical reduction.

For organic substances, the successful reactivity observed in Chapter 4 demonstrates that electrochemically reduced polyoxometalates can transfer reducing equivalents to suitable electrophilic functional groups in solution. This behaviour was effective for activated substrates such as electron deficient aldehydes, which underwent reduction under mild conditions with high selectivity.

In contrast, the absence of reactivity toward carbon monoxide observed in Chapter 5 highlights a fundamental limitation of this mechanism. Carbon monoxide is a chemically inert molecule characterised by a strong C≡O bond, and its reduction typically requires prior adsorption onto a catalytic surface to weaken the bond and enable proton coupled electron transfer.[1]

Because the polyoxometalates investigated in this work do not provide suitable binding or activation sites, electron transfer to carbon monoxide in solution is kinetically unfavourable.[2] Under strongly reducing conditions, the stored electrons are instead consumed by competing processes such as proton reduction, leading to hydrogen evolution.

These observations demonstrate that effective mediated reduction requires not only sufficient reducing power, but also an appropriate mechanism for substrate activation. The distinction between outer sphere electron transfer and catalytic activation therefore represents a key factor in determining reactivity.

6.3 Limitations of the Mediator Based Approach

The results presented in this thesis identify several limitations associated with the use of polyoxometalates as stand alone redox mediators.

First, although multi-electron storage is achievable, practical operation is restricted to a limited reduction window. The 2-electron and 4-electron reduced forms exhibit high reversibility and stability, whereas deeper reduction leads to competing hydrogen evolution, incomplete charge recovery, and structural degradation.

Second, the mediated system shows limited reactivity toward substrates that require more effective activation prior to reduction. This limitation is particularly evident for carbon monoxide, which did not undergo detectable reduction under the conditions investigated.

Third, increasing the degree of reduction does not necessarily enhance reactivity. More highly reduced species tend to favour competing side reactions, particularly proton reduction, rather than productive substrate transformation.

Finally, the scope of the mediated system is restricted to activated organic substrates. More stable functional groups, such as aromatic nitriles and ketones, show little or no reactivity under the conditions investigated.

These limitations define the conditions under which polyoxometalates can be effectively applied as redox mediators and highlight the importance of coupling electron transfer with substrate activation.

6.4 Future Perspectives

The findings of this work suggest several directions for the development of more effective mediated electrochemical systems.

One promising approach involves the design of hybrid systems combining polyoxometalates with catalytic metal surfaces. In such systems, the polyoxometalate could function as a multi-electron

reservoir, while the metal surface provides active sites for adsorption and activation of the substrate. This strategy may enable efficient reduction of small molecules such as carbon monoxide.

Another potential direction is the incorporation of polyoxometalates into gas diffusion electrode architectures.[3] Immobilisation of the mediator within a catalytic layer could enhance integration between gaseous substrates, the electrode surface, and the redox active species, thereby improving mass transport and reaction kinetics. This approach could be particularly relevant for carbon monoxide reduction, where the limited interaction between dissolved polyoxometalate mediators and CO may contribute to the lack of detectable reactivity observed in this work. Bringing the mediator, gaseous substrate, and catalytic surface into closer proximity could therefore provide a more favourable environment for coupled substrate activation and electron transfer.

Chemical modification of the polyoxometalate framework also represents a promising strategy. Functionalisation of the Keggin structure may introduce coordination sites capable of interacting more effectively with small molecules, potentially enabling inner sphere electron transfer pathways.

In addition, the use of alternative catalytic materials may improve reactivity. Metals such as copper, which exhibit higher activity for carbon monoxide and carbon dioxide reduction, could be explored in combination with polyoxometalate mediators.[1]

Together, these approaches aim to integrate efficient electron storage with effective catalytic activation, addressing the key limitation identified in this work.

6.5 Final Remarks

This thesis demonstrates that electrochemically reduced polyoxometalates are effective multi-electron redox mediators for selective organic transformations, while also highlighting fundamental limitations in their application to the reduction of chemically inert molecules.

The work established that the 2-electron and 4-electrons reduced forms of silicotungstic acid represent the most stable and functionally relevant redox states under aqueous conditions. Within this regime, efficient and selective electron transfer to activated organic substrates can be achieved.

6.6 References

1 Y. Hori, in *Modern Aspects of Electrochemistry*, eds. C. G. Vayenas, R. E. White and M. E. Gamboa-Aldeco, Springer, New York, 2008, vol. **42**, pp. 89–189.

2 M. T. Pope, *Heteropoly and isopoly oxometalates*, Springer, Berlin, 1983, vol. **8**.

3 X. Liu, P. Schlexer, J. Xiao, Y. Ji, L. Wang, R. B. Sandberg, M. Tang, K. S. Brown, H. Peng, S. Ringe, C. Hahn, T. F. Jaramillo, J. K. Nørskov and K. Chan, *Nat. Commun.*, 2019, **10**, 32.